Relationship between Textile Irregularities and Pre-Mature Rupture of Polyester Vascular Graft Knitted Fabric

By

MOHAMMAD SAYEEDUL ISLAM

A Thesis submitted to the Faculty of Graduate Studies of

The University of Manitoba

in partial fulfillment of the requirements of the degree of

MASTER OF SCIENCE

Department of Biosystems Engineering

University of Manitoba

Winnipeg

Abstract

Polyethylene terephthalate (PET), commonly known as polyester, has been used as an artificial graft material since 1952 because of its bio-inertness and durability nature. However, over the years numerous deaths have been recorded due to the premature rupture of polyester grafts caused by graft tearing. In the current study, has been conducted to determine the role of material irregularities in the premature rupture of polyester graft.

Thickness, diameter, breaking strength, and tearing strength of apparel grade polyester and Double Velour Polyester Vascular Graft Knitted Fabric (***DVPVGKF***) were measured to find irregularities. The irregularities in both apparel fabric and ***DVPVGKF*** were very high. For ***DVPVGKF***, the breaking strength lies between 45.8 N to 55.5 N (SD: 4.09), however, probability analysis showed that this breaking strength variation alone cannot be responsible for the 25% graft failure as reported in the recent medical literature. Variation in tearing strength data and scanning electron microscopy (SEM) micrographs of virgin and hydrolysed ***DVPVGKF*** reveal that the manufacturing irregularities (cracks, holes) in the material are responsible for lower tearing strength. Further, these irregularities originated in the 'weaker region' of polyester and produced the angled transverse cracks.

The study suggests that the regulatory body for Medical Devices (Health Canada) should specify a minimum standard specification of 4400 kPa for tearing strength of virgin polyester material which is twice the amount of post implantation pulsatile pressure (PIPP).

Acknowledgements

Studying in master's program at the Department of Biosystems Engineering, University of Manitoba has been a great experience for me. I would like to take the opportunity to express my gratitude to my supervisor Dr. Mashiur Rahman, Department of Biosystems Engineering for his support, guidance and valuable advice. It would have not been possible for me to complete my research without his continuous support and patience throughout my Master's program. It was a great honour to work under his supervision. I am also thankful to my committee members Dr. Tammi Feltham, Adjunct Professor, Department of Biosystems Engineering and Dr. Marolo Alfaro, Professor in the Department of Civil Engineering for their valuable suggestions and advices. I am truly grateful to Mrs. Mary Pelton for her genuine work on editing this thesis. I would also like to thank Dr. Ravinder Sidhu for his support to get SEM images and Md. Rabiul Islam Khan for helping me doing lab works. I am also grateful to all the fellow lab members for their generous support. I gratefully acknowledge the support of Nygard International where I work full time as Product Manager in the Fabric department. Finally, I extend my heartiest gratitude to my parents and wife for their constant support and encouragement.

Table of Contents

List of Tables

List of Figures

Chapter 1 Introduction

1.1 Vascular Grafts

Synthetic vascular prostheses are commonly known as vascular grafts or artificial arteries. A vascular graft is a sophisticated specialized artificial organ [(*Figure 1.1(a*), (b)] which is used as a substitute artery to redirect blood flow to a specific part of body when the natural artery is blocked or diseased. Vascular grafts must be very strong and durable, non-thrombogenic, biocompatible, resistant to sterilization, resistant to bacteria, excellently suturable, comfortable, easy - to - handle, nonfraying, and inert. In order to withstand the continuous pulsatile blood flow, vascular grafts also need to be fatigue resistant, wear and tear resistant, and flexible. The surface of the grafts need to be smooth to prevent graft abrasion (Santos et al., 2012). Textile materials for vascular implants began in 1952 when diseased aortic vessels of dogs were replaced with woven Vinyon-N (a polyvinylchloride) tubes by Voorhees and his team (Voorhees, Alfred, & Blakemore, 1952). In 1954, a seamless vascular graft was introduced and successful clinical trials were performed. Different types of synthetic materials (for example, Nylon, Teflon®, Dacron®, Orlon®), and constructions (for example, woven, knitted, braided) in various diameters (6–20 mm) were used in those trials (Harris, Shumacker, Siderys, Moore, & Grice, 1955). As a result of the successful trials, vascular grafts became commercially available in 1957, and from 1957 to 1970, synthetic vascular grafts started coming to the market. In 1975, about 80000-100000 vein grafts were implanted in USA for revascularization of segmented coronary-artery occlusion (Baird & Abbott, 1976).

Figure 1.1(a). Woven vascular graft fabric.

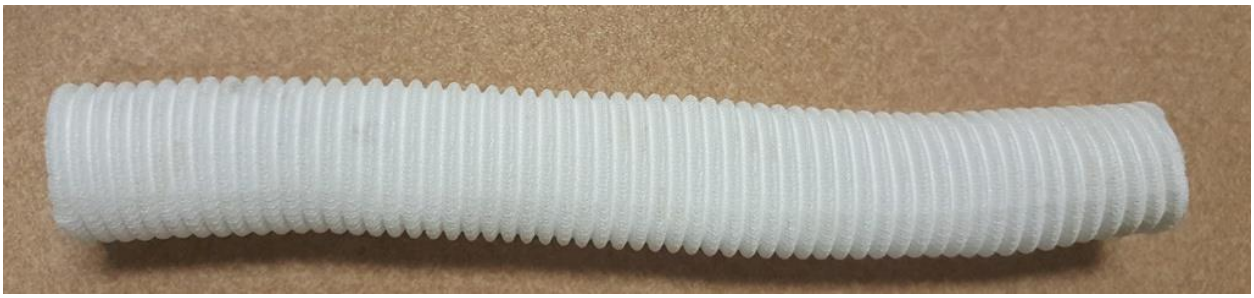

Figure 1.1(b). Knitted vascular graft fabric.

1.2 Requirements of a Vascular Graft

Vascular grafts are expected to be biologically inert, stable, active and almost completely non-thrombogenic in the human body throughout the patient's lifetime. The following requirements for a vascular graft are set by the Society of Vascular Surgery (Creech et al., 1957) .

a) No physical modification by exposure to tissue fluids
b) Inert to chemicals
c) Inert in respect to foreign body effect
d) Non-carcinogenic
e) Non-allergenic
f) Stable under continuous mechanical stress
g) Easy to fabricate at a low cost
h) Easy to sterilize adequately
i) Immediately available

j) Biocompatible with nonthrombogenic surfaces

k) Low infectability

l) Durable, strong, and long life expected once implanted

m) Proven highly patent.

1.3 Fibres Used in Vascular Graft

Various synthetic polymers such as expanded polytetrafluoroethylene (ePTFE), polyethylene terephthalate (PET) and polyurethane are used for designing vascular grafts as they are easy to handle and the mechanical properties are easily altered to obtain higher strength, modulus and low elongation (Ravi & Chaikof, 2010). Out of all these synthetic polymers, PET (polyethylene terephthalate or polyester) is most commonly used for making grafts. Among all polyesters, Dacron fibres from DuPont de Nemours and Company, Inc. obtained the first licence from the Food and Drug Administration (FDA) (Riepe et al., 1997). Dacron is used in about 95% of bypass grafts for arteries having a minimum diameter of 10 mm which includes aorto-femoral and extra-anatomical grafts. Initially, Dacron grafts were a simple weft knitted structure. Over the years, numerous improvements have been made including seamless and bifurcated grafts (Samuel E et al., 1997). In 1967, velour construction was used for the internal surface of Dacron grafts, and in 1978 an external double velour graft was introduced (D'Sa, et al., 1980). Usually these velour grafts have a soft inner surface, a better preclotting and healing tendency, are easy to suture and do not fray (D'Sa Barros et al., 1980).

1.3.1 Poly (ethylene terephthalate) or PET

The foundation of polyesters was laid by Carothers and his team, especially Hill, in DuPont's Wilmington laboratories at the beginning of the 1930s (Carothers & Hill, 1932). Carothers and Hill produced low melting and hydrolytically sensitive polyesters from propylene glycol and hexadecanedicarboxylic acid, m.p. 75°C, w-hydroxydecanoic acid, m.p. 65°C, and w-hydroxypentadecanoic acid, m.p. 95°C (Ludewig & Roth, 1971). In the early 1940s, Whinfield and Dickson (1947) in the United Kingdom and Schlack (Ludewig & Roth, 1971) in Germany used terephthalic acid to develop polyesters with higher melting points (Whinfield & Dickson, 1947).

Poly (ethylene terephthalate) or PET (*Figure 1.2*) was first produced commercially by ICI and DuPont and has become the most important man-made fibre in apparel and non-apparel applications. Poly (ethylene terephthalate) is generally made from either terephthalic acid or dimethyl terephthalate together with ethylene glycol.

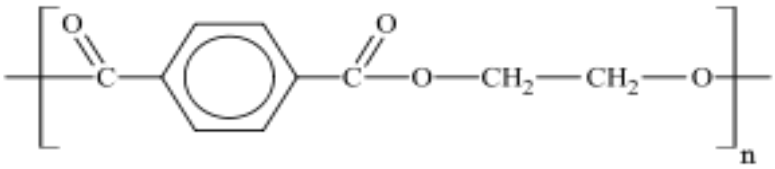

Figure 1.2. Chemical Structure of Poly (ethylene terephthalate).

Currently, polyester fibres dominate the world's synthetic fibre industry with the largest volume of synthetics (about 40 million tons in 2015) and far outweigh use of nylons, rayon and acrylic fibres. Examples of some other commercially used polyester fibres are: poly(1,4-bishydroxymethylcyclohexane terephthalate) from Eastman Kodak (Kodel II) and Bayer, poly(tetramethylene terephthalate), poly(ethylene oxybenzoate) from Unitika (A-Tell) and

polyglycollide for medical uses (biodegradable sutures) from American Cyanamid (Dexon) (Hughes et al., 1976).

1.3.2 Advantages and Disadvantages of Polyester (PET)

Advantages of PET

Polyesters (PET) have some advantages: they are inexpensive (easy to produce), have a desirable range of physical properties (lustre, length, diameter), are strong (low to high tenacity), lightweight (low density of 1.38 g/cc), soft and pliable, easy to handle and to suture (Damme, Deprez, Creemers, & Lime, 2005). Further, polyesters are wrinkle-resistant, have very good wash-wear properties and can be produced as both continuous filament yarn and staple fibre. Due to their wide range of properties, polyester fibres are used in different applications, such as healthcare textiles, outdoor wear, sportswear, carpets, tire cords, car seat belts, filter cloths, and sailcloth.

PET vascular grafts, both woven and knitted, have been used in the human body for implantation for more than 60 years (Riepe et al., 1997). PET is widely used in different implantable medical applications, such as artificial tendons, artificial ligaments, vascular grafts (*Figure 1.1*), artificial kidneys, aortofemoral (joining the abdominal aorta and the femoral arteries) grafts, heart valve sewing cuffs and annuloplasty rings used in heart valve repair surgeries (Joseph et al., 2009). The applications of PET fibres in different healthcare applications with fabric constructions are shown in Table 1.1(a) and (b). The different fabric constructions for medical applications (vascular graft) are discussed in Section 1.4.

Table 1.1(a)

Usage of PET in non-implantable and implantable materials (Rigby, Anand, & Horrocks, 1997)

Non-Implantable Materials		Implantable Materials	
Fabric Structure	Application	Fabric Structure	Application
Woven, nonwoven	Orthopaedic bandages	Woven, braided	Artificial tendon
Woven, nonwoven, knitted	Plasters	Braided	Artificial ligament
		Woven , knitted	Vascular graft, heart valves

Table 1.1(b)

Usage of PET in extracorporeal devices and healthcare-hygiene products materials (Rigby, Anand, & Horrocks, 1997)

Extracorporeal Devices		Healthcare-Hygiene Products	
Application	Function	Application	Function
Artificial kidney	Remove waste products from patients' blood	Woven, nonwoven	Surgical gowns, surgical drapes, cloths
		Nonwoven	Surgical masks
		Knitted	Surgical hosiery, blankets

Disadvantages of PET

The major disadvantage of polyester is hydrolysis, particularly in an alkaline media. Alkaline hydrolysis occurs when a hydroxide ion attacks the electron-deficient carbonyl carbons of the polyester (*Figure 1.2*) to form an intermediate anion. Further reaction breaks the macromolecular chain and produces –COOH and O^- - CH_2-CH_2- groups (McIntyre, 1993). It is

known that the rate of alkaline hydrolysis increases if the fibre contains any cracks or other manufacturing defects (Zeronians & Collins, 1989).

1.3.3 Manufacturing of PET - Melt Spinning Process

Polyester is produced through melt spinning which is the most economical fibre forming process. Polymer pellets are fed into one end of the extruder. With the help of screws, the pellets are carried into a barrel where heat and shear are applied to soften the polymer. The screw helps to deliver the molten polymer to a spinneret, which has up to 1000 ‘shaped holes’ that create the fibre cross-section, as high pressure forces the molten polymer through the shaped holes, whereupon the extrudate is stretched and solidified. Molecular orientation is achieved by taking up the fibre as much as 100 times faster that it is extruded (Warner, 1995). The fibres are then solidified by cooling with flowing air and subsequently drawn or stretched to further increase the molecular alignment in the axial direction (*Figures 1.3 and 1.4*). During the spinning process, various chemicals can be added depending on the end uses (flame retardant, antistatic, dye ability) of the fibres.

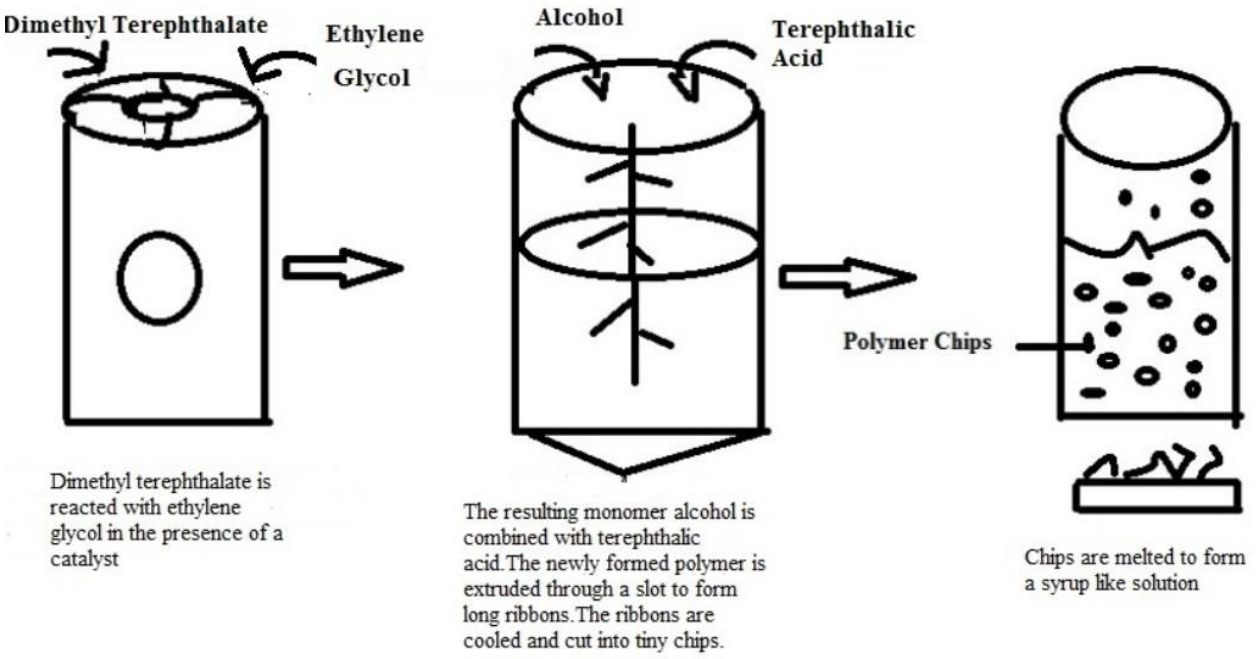

Figure 1.3. Melt spinning procedures – reaction and polymerization bath.

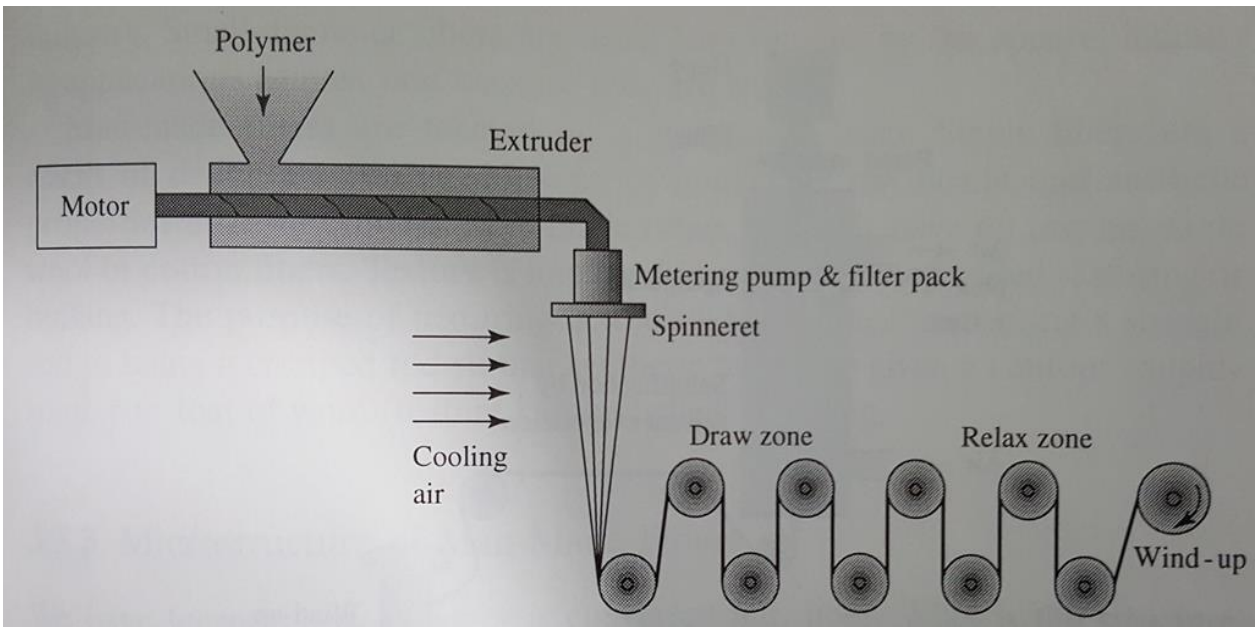

Figure 1.4. Melt spinning procedure - Schematic diagram of filament formation (Warner, 1995).
[Used with permission]

1.3.4 Production of High Tenacity PET Yarn for Medical Applications

The mechanical properties of yarn used in the apparel industry are not same as yarn used for industrial applications, including the medical industry, for example prosthetic grafts (Table 1.2). Yarn used in prosthetic grafts needs to be of high tenacity, have high strength, toughness, and modulus, low extension at break and high chemical resistance. Graft materials need to have higher strength and the molecular weight, which is determined by using intrinsic viscosity (IV), needs to be high. The higher the tenacity, the higher the intrinsic viscosity required to make stronger yarn. For example, apparel grade polyester with tenacity of 2.0-2.5g/d will have IV of 0.60-0.70 g/dl; whereas, high tenacity polyester yarn (8.0-10.0 g/d) will have intrinsic viscosity of about 0.9 to 1.2 dl/g. If the tenacity is even more, 16-20.0g/d, the intrinsic viscosity will be 2.6dl/g. (Falkai, 1996).

The manufacturing process (which includes drawing and heat treatment) of polyester yarn used in vascular grafts is more complex as it needs to have high tenacity, low elongation, higher orientation of the molecules and crystallinity of fibre. Polyester filament spinning machines have a large number of godets and yarns receive some pre-orientation in the first pair (Figure 1.4) which helps to run smoothly for later pairs of rollers (Falkai, 1996). High orientation and high crystallinity (ordered regions) are needed in the structure to increase strength and modulus; whereas, higher amorphous regions (disordered or weak regions) increase elongation and absorbency, but reduce strength (Hearle & Greer, 1970). The implication of crystalline and amorphous regions on the pre-mature rupture of polyester graft is given in Chapter 5, (*Figure 4.42*).

Table 1.2

*Different Mechanical Properties of Apparel and Industrial Grade PET including Medical Grade.*Trevira High Tenacity, Type 703 (Rahman, 2012)*

Polyester Type	**Breaking Tenacity (g/d)**	**Tensile Strength (psi)**	**Breaking Elongation (%)**	**Stiffness (g/d)**	**Toughness (g/d)**	**Intrinsic Viscosity (dl/g)**
Apparel Grade Polyester	2.0-2.5	33,000-42,000	18-60	7-31	0.28-1.5	0.6-0.7
Medical Grade Polyester	7.2-8.2	118,000-140,000	*7-10	54-77	0.35-0.55	0.90-1.0

1.4 Different Constructions of Vascular Grafts

Fabric for vascular grafts can be woven, knitted, braided or non-woven (Rigby et al., 1997) as shown in Tables 1.1(a) and (b). The specific type of fabric construction used depends on the location in the human body, the graft diameter (which varies from 6mm to 10 mm), the material, fibre structure, manufacturing process, shape and size. A woven graft is made by the interlacing of warp and weft yarn and can be woven in plain, twill, or satin design (*Figure 1.5*), and may be produced as a seamless tube on shuttle looms (Pourdeyhimi & Wagner, 1986). Usually, a woven graft is dimensionally stable, has high tensile strength but low tearing strength, and shows minimal tendency to fatigue (Collier & Epps, 1999). However, compared to knit vascular grafts, the performance of woven tubular grafts materials is not satisfactory due to its lack of stretch, poor suturability, healing characteristics, and tendency to fray at the cut edge (D'Sa, et al., 1980).

Knitted grafts can be warp or weft knitted. Due to the interlooping of yarns (*Figure 1.6*) and having loops in an upward direction on the fabric surface, knitted grafts have more available surface area which helps in developing tissue (Ravi & Chaikof, 2010). Weft knitted velour grafts having a filamentous surface are very popular as they are easier to handle and suture and do not run. But single jersey weft knitted grafts need to be pre-clotted (closing the interstitial pores with patient's blood) due to the porous structure. To avoid preclotting, vascular grafts normally contain bovine collagen, albumin, or gelatin (Ravi & Chaikof, 2010). Locknit and reverse locknit are the most popular warp knitted vascular graft constructions, produced in low-stitch-density. They are dimensionally very stable, especially in the course direction (horizontal direction).

For the manufacture of a non-woven graft, biocompatible polymeric materials are extruded through an orifice in the presence of electrostatic charges, producing elongated non-woven or extruded grafts. Electrostatic charges help to gather all the broken fibres during spinning and create sufficient interfibre bonding and expected pore sizes (*Figure 1.7*). The details of fibre spinning for non-woven vascular grafts are given elsewhere (O'Mahony, 2011).

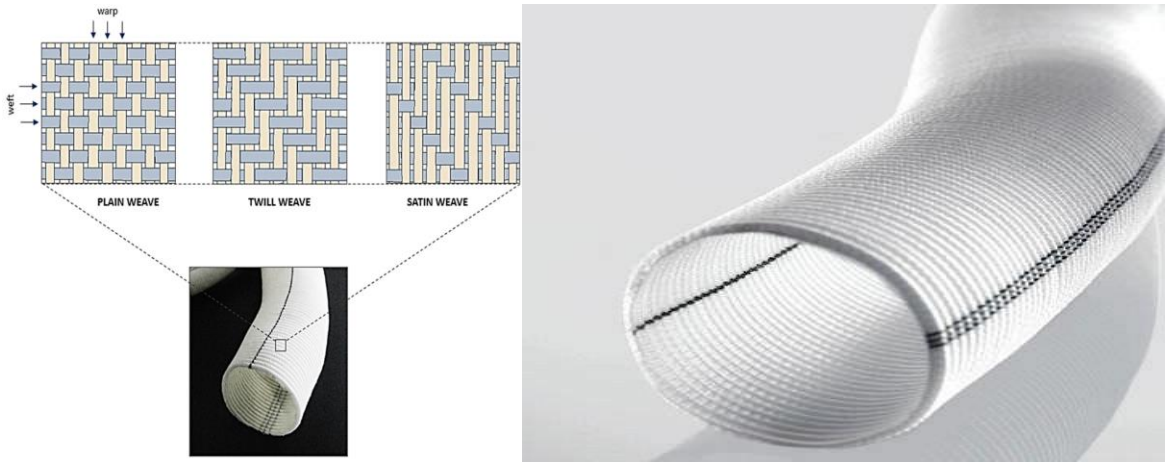

Figure 1.5. Polyester vascular prosthesis woven graft (Singh, Wong, & Wang, 2015). [Used with permission]

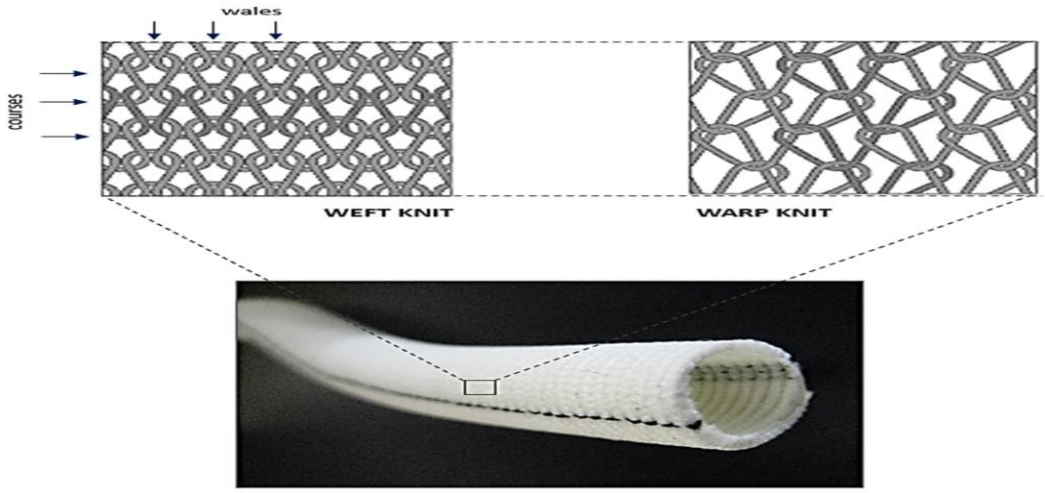

Figure 1.6. Polyester vascular prosthesis knitted graft (Singh, Wong, & Wang, 2015). [Used with permission]

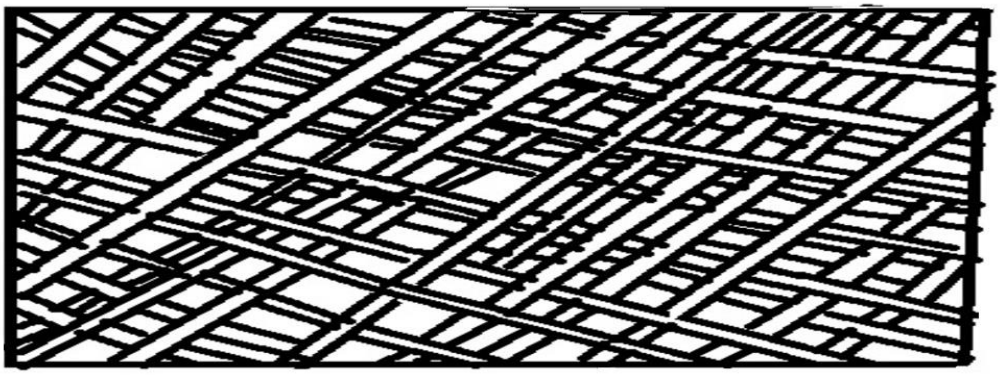

Figure 1.7. Extruded (non-woven) vascular graft.

1.4.1 Failures in Dacron

In general, a PET graft is defined as ruptured when the fibre is damaged (holes or tears), or is broken (split) or frayed after implantation. Ruptures also include fibre separation, fragmentation with bleeding and false aneurysm, which is a localized, blood-filled dilation of a blood vessel caused by disease or weakening of the materials. Polyester is susceptible to acid and alkali as discussed in Section 1.3.2. It has been reported that polyester degrades faster due to the formation of cracks when the fibre is treated in chemical environments under stressing conditions (Rahman & East, 2006, 2009).

Various cases of polyester graft failures have been reported in the literature, although numerous cases of pre-mature rupture have not been published due to the fear of litigation (Yashar et al., 1978). It is very hard to find how many patients have died from graft failure due to the lack of follow-up and autopsies not being performed. Grafts made from Ivalon (PVA), Orlon (Nylon) and Teflon (PTFE) were discarded as potential graft fabrics due to dilation and loss in mechanical properties (Berger & Sauvage, 1981). Although PET fabrics have been used in the medical fields for a long time, the material still has some drawbacks that include pre-mature rupture and infection due to hydrolysis, as discussed in Section 1.3.2, and low structural retention vessel walls.

Of the over 400,000 coronary artery bypass procedures performed in the USA each year, premature eruption of the prosthetic graft accounts for almost 25% of failures within 12 to 18 months after surgery (Singh & Wang, 2015). Table 1.3 shows some selected cases of premature polyester graft failures with failure time, textile structure, defects in the ruptured graft and patient's outcome. The cases of aortic Dacron (polyester) graft ruptures identified between 1970 and 1996 included 10 knitted Dacron, 6 woven grafts and two unspecified Dacron grafts (Rahman & East, 2009). The FDA also published details of graft failure (Riepe et al., 1997).

Analysis of Table 1.3 reveals that both knitted and woven grafts failed prematurely. The main causes of failures are: fabric tear (within materials and suture tear during implantation), fabric dilation (high creep), and manufacturing faults in the materials (cracks both longitudinal and transverse, holes). The results of these faults are the loss of graft fabric strength (Table 1.3).

After tear fault, dilation is another common reason for vascular graft failure. Dilation starts immediately in the postoperative period; and the rate increases slowly over time to nearly double

the graft diameter. As a result, the graft becomes weak and causes pseudoaneurysms (Schroeder et al., 2009). Degradation due to dilation is related to various factors, mainly the design of the vascular graft structure, alterations of the prosthesis during manufacturing or implantation, physiochemical change when exposed to the chronic foreign body inflammatory reaction, and pulsatile stress (Chakfe et al., 2001).

Infections related to implant surgery is another big complication which may cause complete graft failure. About 1-3.0% grafts are infected and among them 50% of these infections were early infections and Methicillin-Resistant Staphylococcus Aureus (MRSA) was the most prevalent pathogen (Amorim et al., 2014).

Grafts are manufactured in different dimensions ranging between <6 to 20 mm. The main cause of graft failure in small-diameter grafts (<6mm in diameter) is associated with loss of patency (which is the reduction in size of the available lumen-inner space of any tubular organ) and blockage (occlusion). For medium to large diameter grafts (6 to 20 mm), the four most significant complications reported were (a) structural defects and suture line failure (tear, cracks), (b) dilation, and (c) bleeding and infection (Pourdeyhimi & Wagner, 1986).

In summary, in vivo premature rupture is caused by tear (manufacturing flaws or errors during production) or fabrication flaws, fabric dilation, intraoperative damage to the graft, incorrect storage conditions, improper handling in surgery, material fatiguing and biodegradation, and direct damage from puncture or external trauma (Van Damme et al., 2005; Wilson, Krug, Mueller, & Wilson, 1997). Further, surgical removal of blood clot (thrombosis) from blood

vessel (thrombectomy) and flexion (bending) with body movements after implantation has significant effects on the deformation of polyester grafts. Examples of ruptured polyester filaments are shown in *Figures 1.8 - 1.10*.

Table 1.3

Data of Dacron Graft Failure (Rahman & East, 2009; Pourdeyhimi & Wagner, 1986)

Operation/ Location	**Interval to Graft Failure (Years)**	**Type of graft**	**Defect/ Causes of Failure**	**Outcome**
Aortobifemoral	2	Knitted Dacron	Aortic tear, graft dilation and 3cm rent	Hematuria, death
Lliofemoral	2	Unspecified	Inguinal tear, developed 2 cm slit	Replaced, alive
Aortobifemoral	3.5	Woven	Bifurcation tear, 1 cm tear along the guide line	Replaced, alive
Aortic tube	10	Knitted (thin wall)	Aortic rupture, 96.9% loss in tensile strength	Death
Aortobifemoral	5	Knitted Dacron	Bifurcation tear surface cracks	Death
Aortobifemoral	8	Woven	Inguinal tear, holes, disintegration, split,	Replaced, alive
Aortobifemoral	8	Tetoran woven	Aorti-ureter, cracks	Hematuria, death
Aortoiliac/ femoral	6	Cooley double velour (knitted)	Right femoral aneurysm, broken graft fibers	Replaced, alive
Aortobifemoral	5	Cooley double velour (knitted)	Inguinal tear	Replaced, alive
Aorto right femoral	7	Knitted double velour	Right femoral aneurysm, manufacturing faults	Replaced, alive
Aortobifemoral	7	Unspecified	Left femoral aneurysm, structural deficiencies	Replaced, alive
Aorta-femoralsa	5	Woven Dacron	Suture tear (polyester)	Death
Aortafemoral	10	Knitted Dacron	Suture tear	Anastomosis disruption
Aortafemoral	3	Woven Dacron	Suture tear	Anastomic false aneurysm
Aortafemoral	1	Dacron (unspecified)	Suture tear	Anastomic false aneurysm
Aortailiac	4 Months	Knitted Dacron	Suture tear	3 deaths
Aorta-aorta	2 and 9	Knitted Dacron	Suture tear	Death
Femoropopliteal	2 to 4	Knitted Dacron	Suture tear	Amputation
Aoritc Bifurcation	8	Woven	Large longitudinal and transverse splits	Replaced, Alive

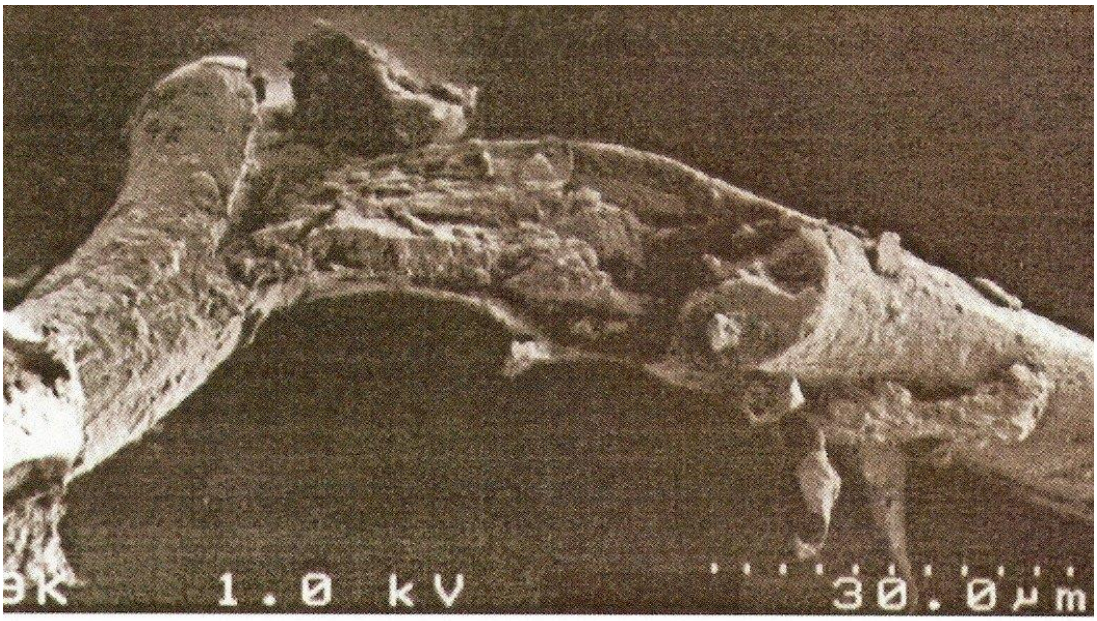

Figure 1.8. A 13-Year-Old PET Vascular Graft Showing a Fracture in the Centre and the Relatively Smooth Surface of the Filament on the Right Side (Riepe et al., 1997, p.544).
[Used with permission]

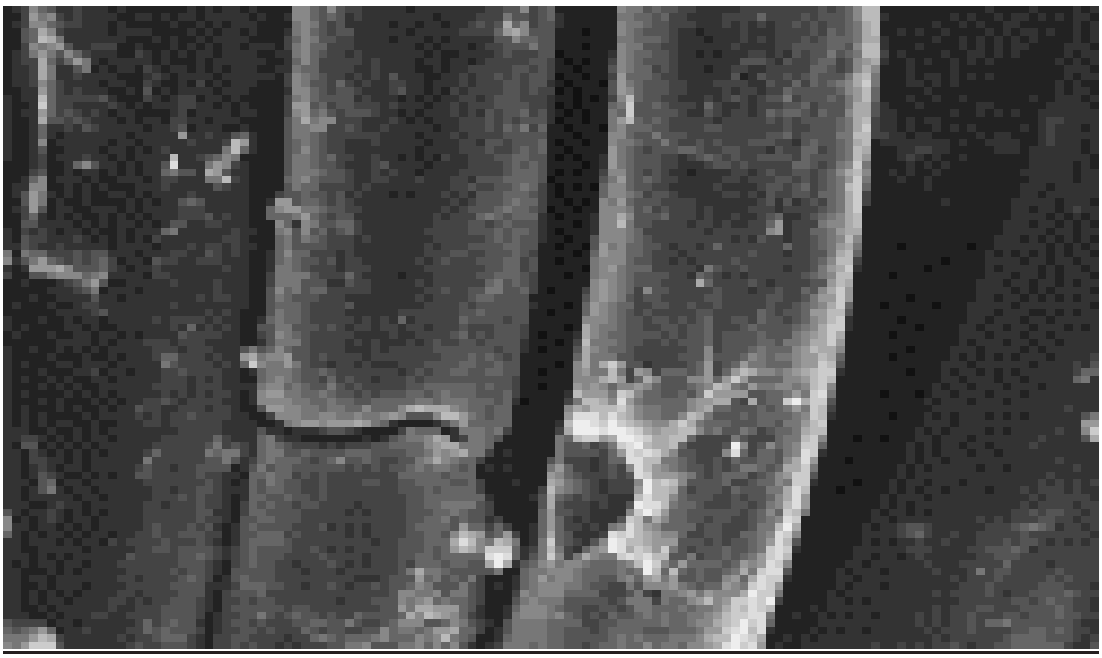

Figure 1.9. Cracks and holes in the explanted graft (Rahman, 2012, p.111).
[Used with permission]

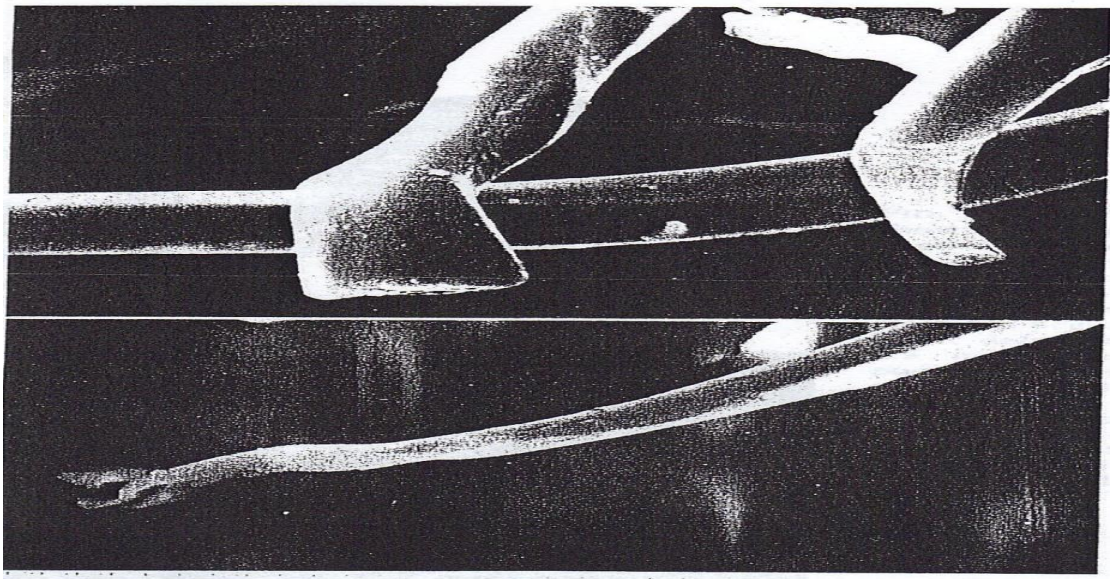

Figure 1.10. Broken, abruptly ruptured thinned out polyester filament. (Rahman, 2012, p.111). [Used with permission]

1.5 Work from Literature

The work regarding the premature rupture of polyester graft can be divided into two groups:

(a) *in vivo* and

(b) in vitro

No in vivo work could be found in humans; very limited work is available using an animal model. However, numerous analyses on the in vivo ruptured explanted polyester graft were carried out, as shown in Table 1.3, Section 1.4.1. These explanted grafts show tear, cracks, holes and splits as shown in *Figures 1.8-1.10*. Further, the detailed analysis of explanted ruptured polyester grafts showed both transverse and longitudinal cracks of various dimensions (Berger & Sauvage, 1981; Yashar et al., 1978). In the animal model, a Dacron (polyester) graft lost 10% of its strength after 100 days in canine subcutaneous tissue (Edwards, 1978).

No in vitro work could be found that completely simulated the actual physiological conditions of hydrolysis (alkaline pH), temperature and pulsatile pressure. However, researchers have attempted numerous in vitro tests using high pH conditions, high stress or high temperature to examine the degradation of polyester grafts. It is reported that 16 - 20% dilation occurred when three different knitted polyester grafts were exposed to dynamic pressure of 120/80mm Hg for 42 days at 37°C (Stollwerck et al., 2011). Although this dilation is comparable with the reported in vivo dilation and the pulsatile pressure and temperature were similar to in vivo, the researchers did not treat the polyester grafts with the physiological fluids, or any fluid of pH 7.4. However, this work suggests that in vivo results can be obtained in laboratory test conditions.

Rahman and East (2006, 2009) used accelerated physiological conditions of higher (pH = 13) and stressing condition of 246 kPa (2000g) at 40°C to obtain degradation in a reasonable time period. The surface cracks in both directions that the authors reported are similar to the transverse and longitudinal cracks found in vivo (Berger & Sauvage, 1981; Yashar et al., 1978). However, the major drawbacks of this work are that the applied load and the alkali concentration are much higher than that of the physiological conditions. Further, physiological stress on graft materials can be continuous or intermittent. An Anterior Cruciate Ligament (ACL) graft, for example, experiences constant stress (Conner et al., 2008). On the other hand, all vein grafts are subjected to arterial pressure pulse (Baird & Abbott, 1976). Dacron heart valve prostheses, even with lower stiffness, may have filament damage or rupture through repeated cycling of a regular pulse rate. Moreover, textile materials contain residual stresses generated during various stages of textile processing: spinning, winding, high speed warping, weaving, knitting, and wet processing treatments. Grafts made from the poly(carbonate) urethanes are produced using a low

temperature cast coagulation method to minimize the stress during production and minimize stress cracking during use. However, these grafts have still produced stress-cracks in vivo due to hydrolytic degradation (Salacinski et al., 2002). White and Hann (1992) reported that residual stress in the textile was responsible for the formation of cracks and deterioration in mechanical properties through chemical degradation.

Finally, both *in vivo* and in vitro studies on different causes of premature rupture of polyester grafts were studied. However, the role of tears and holes on the graft strength of the explanted woven and knitted polyester grafts as shown in *Figures 1.11-1.23* has not been studied.

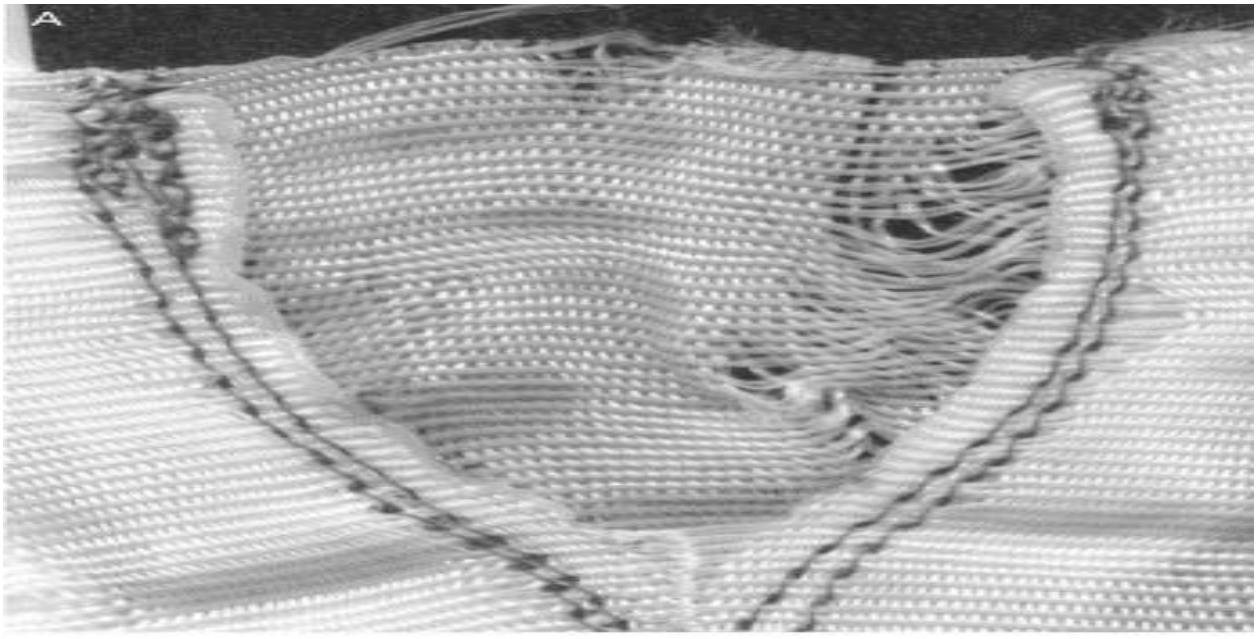

Figure 1.11. Macroscopic view of shifting of warp yarns at the level of suture in woven stentor endoprostheses (Chakfe et al., 2004, p. 36).
[Used with permission]

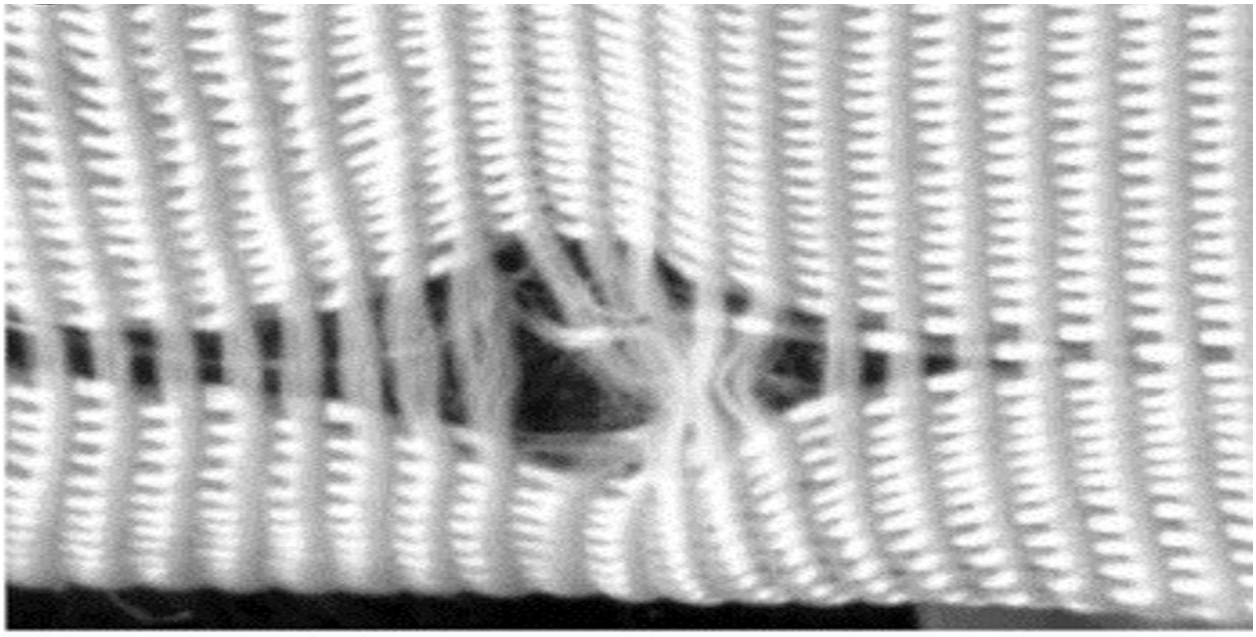

Figure 1.12. Macroscopic view of shifting of warp yarns in woven stentor endoprostheses, probably related to the protrusion of a stent (Chakfe et al., 2004, p. 36).
[Used with permission]

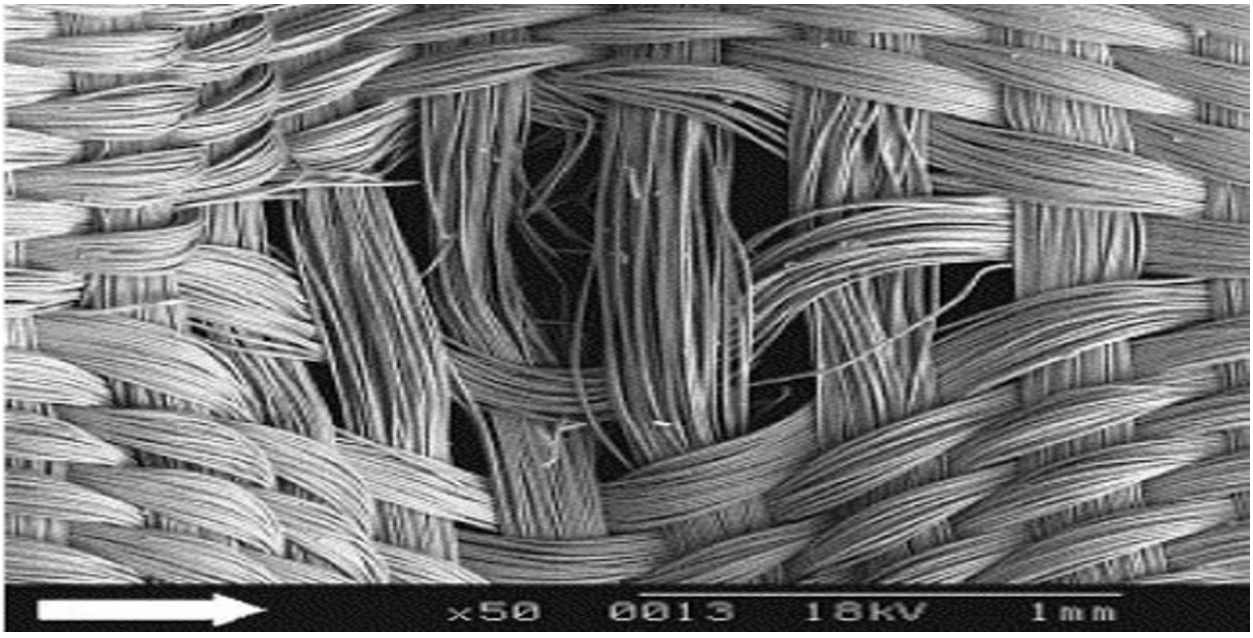

Figure 1.13. SEM Image (Original Magnification: x 50): No major lesion of the filaments at the level of a shifting of the warp yarns in woven structure (Chakfe et al., 2004, p. 36).
[Used with permission]

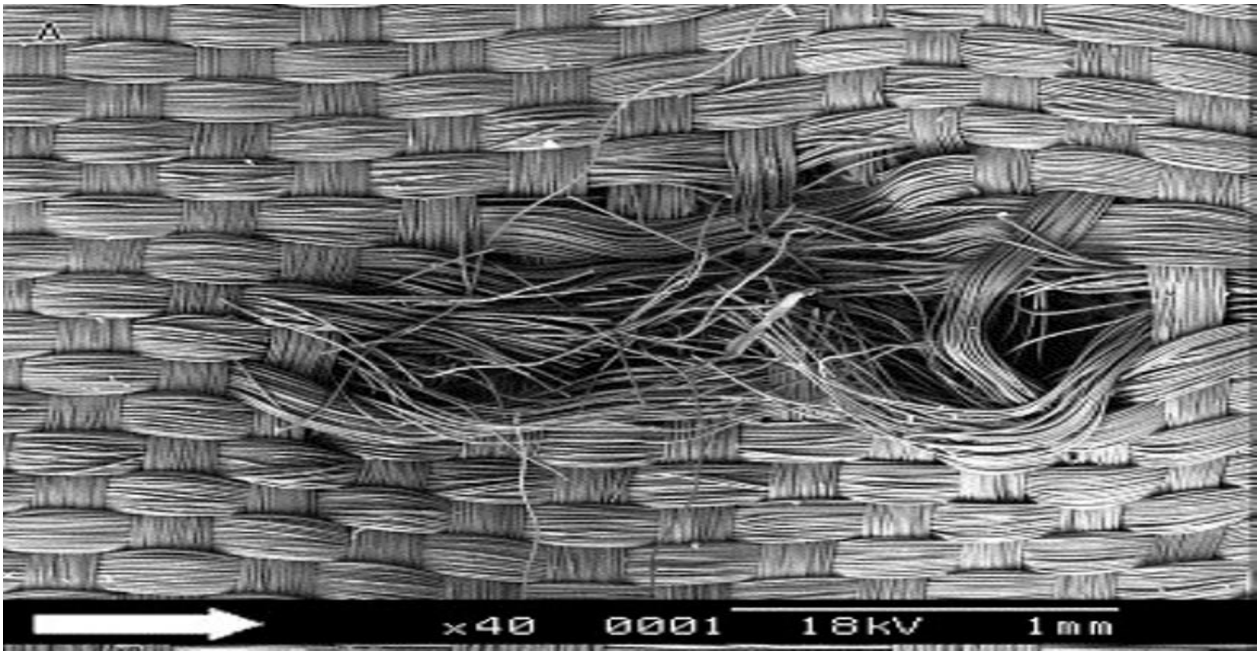

Figure 1.14. SEM image (original magnification: x 40) of the ruptures of filaments on the crinkled warp yarns on the external side of the textile in Vanguard Endoprothesis (arrow: warp direction) (Chakfe et al., 2004, p. 37).
[Used with permission]

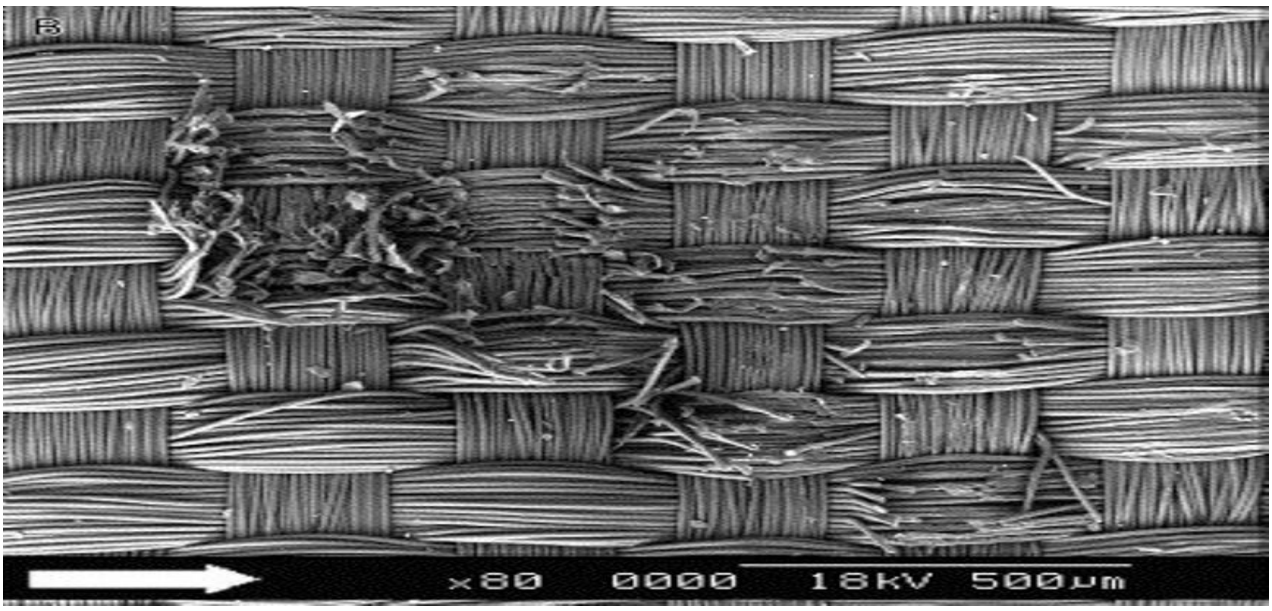

Figure 1.15. SEM image (original magnification: x 80) of the ruptures of filaments on the crinkled warp yarns on the external side of the textile in vanguard Endoprothesis (Chakfe et al., 2004, p. 37).
[Used with permission]

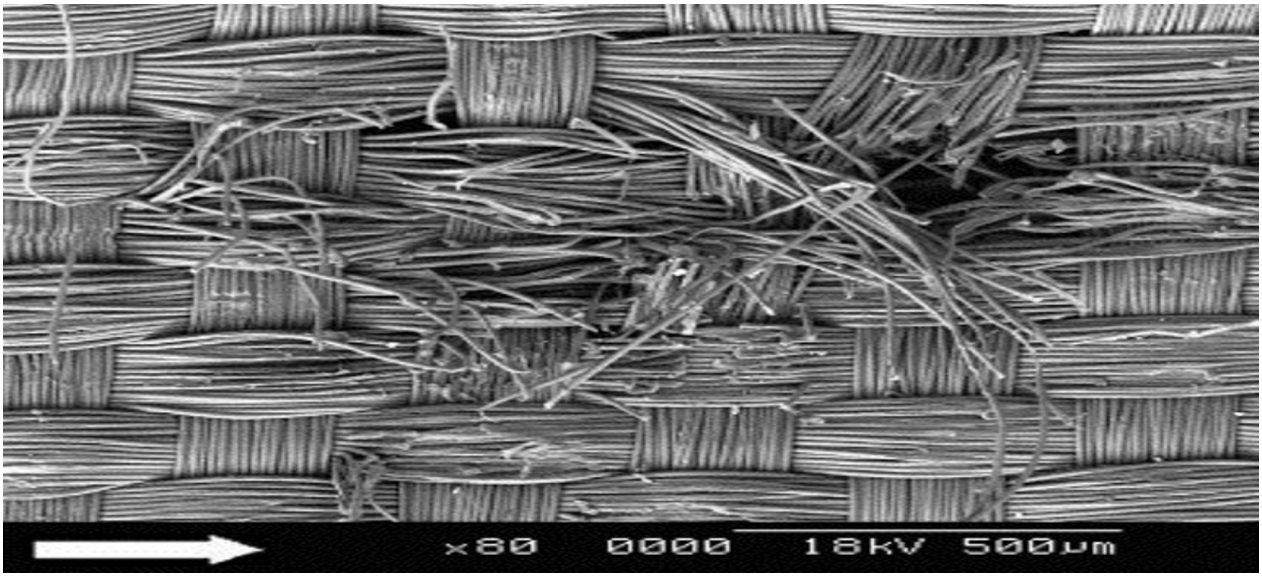

Figure 1.16. SEM Image (Original Magnification: x 80): of the ruptures of flaments on the crinkled warp yarns on the external side of the textile in Vanguard Endoprothesis (arrow: warp direction) (Chakfe et al., 2004, p. 37).
[Used with permission]

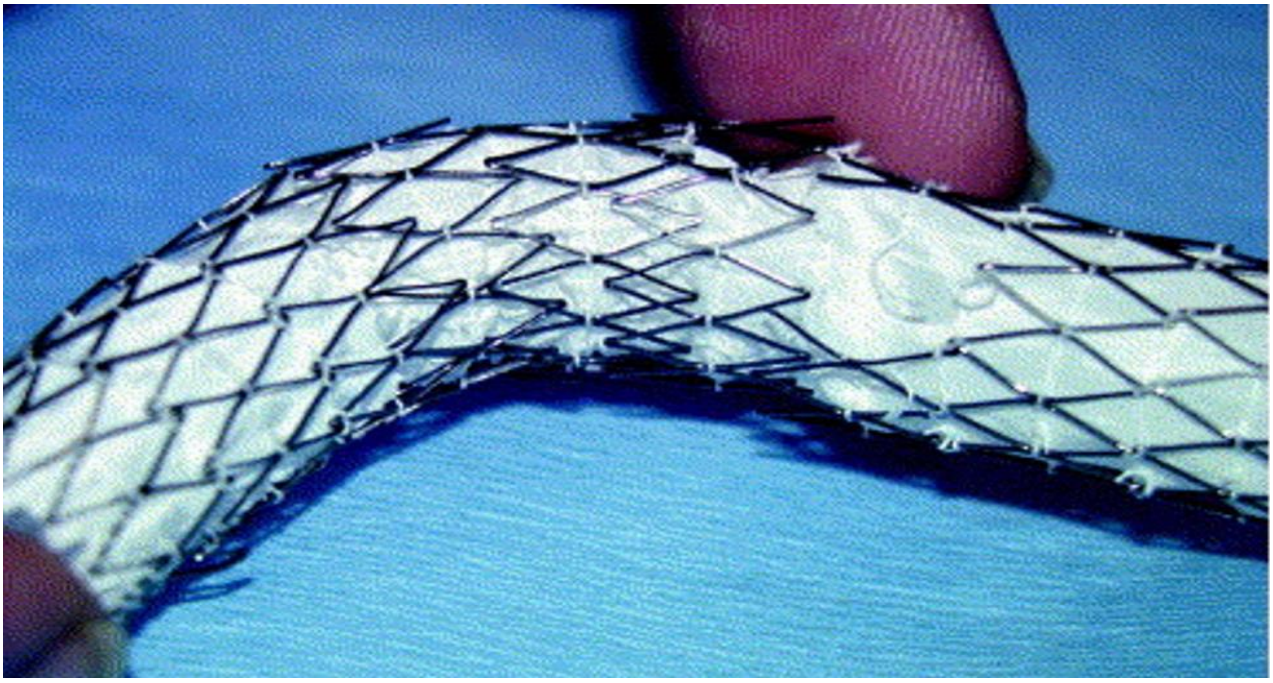

Figure 1.17. Macroscopic view of ruptured stents and ligatures in AneurX Endoprostheses (Chakfe et al., 2004, p. 38).
[Used with permission]

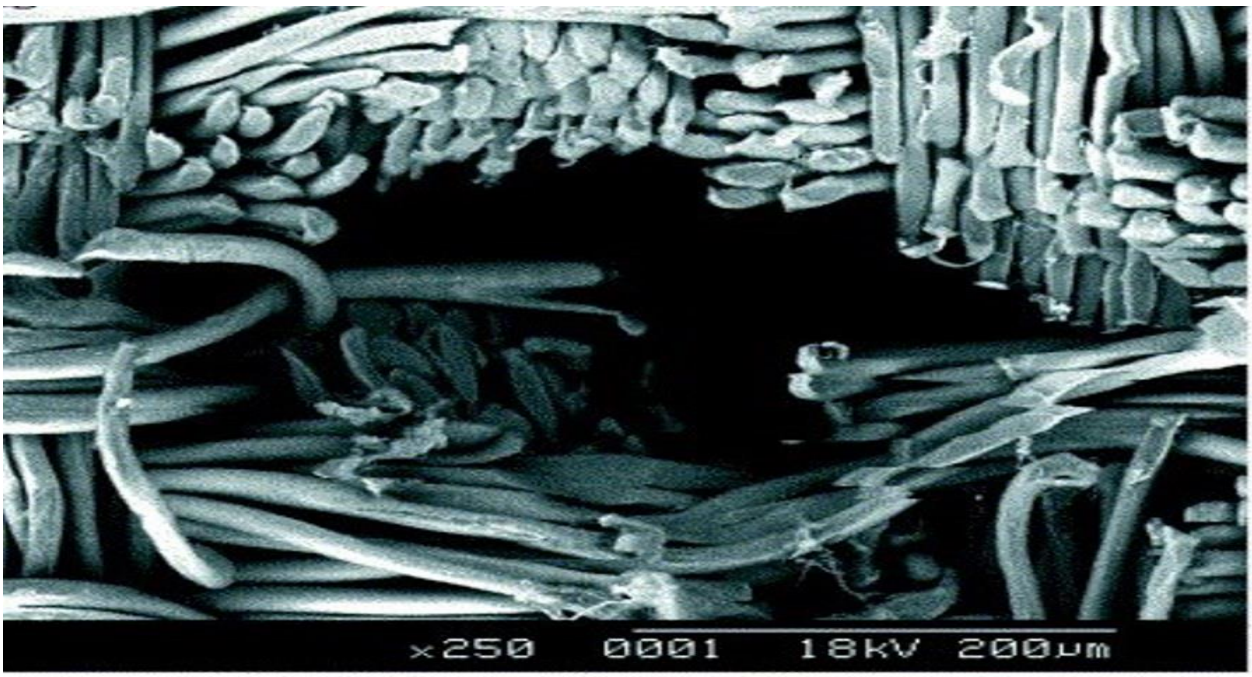

Figure 1.18. SEM Image (Original Magnification: x 250): Hole with degradation of the filaments related to the contact with the stent of the AneurX Endoprostheses. (Chakfe et al., 2004, p. 38).
[Used with permission]

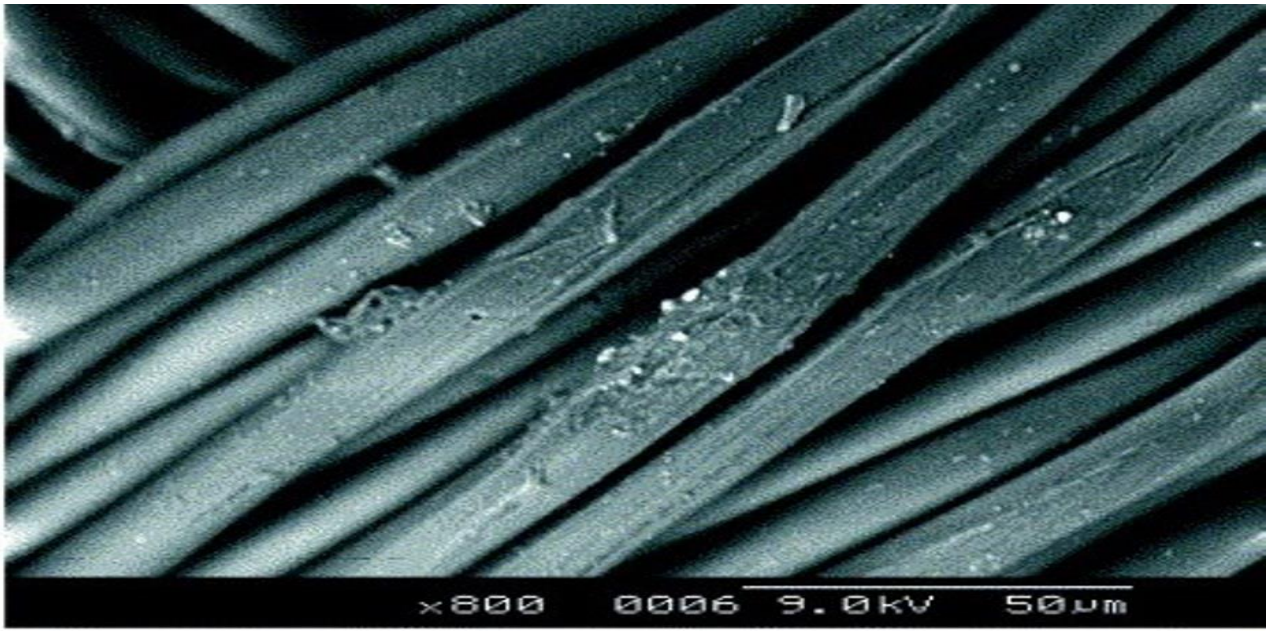

Figure 1.19. SEM Image (original magnification: x 800): Filaments erosions at the contact between the metallic structure of the stents and the textile in AneurX Endoprostheses (Chakfe et al., 2004, p. 38).
[Used with permission]

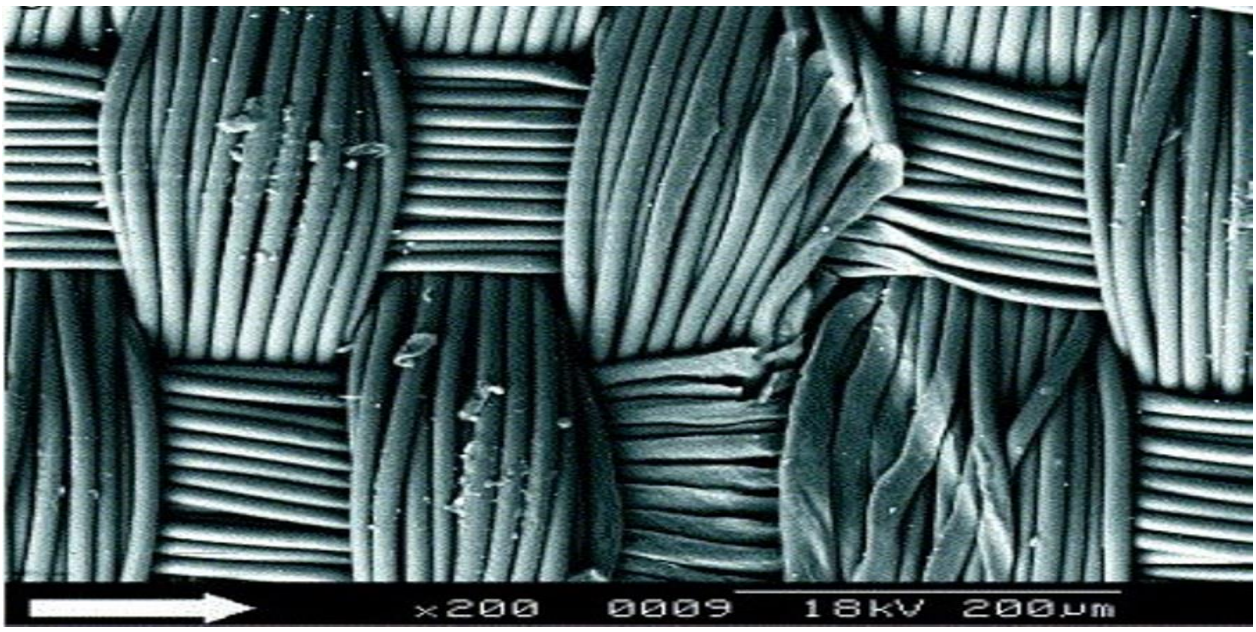

Figure 1.20. SEM image (Original Magnification: x 200): Lesions created by the stents on the external side of the textile in AneurX Endoprostheses (arrow: warp direction) (Chakfe et al., 2004, p. 38).
[Used with permission]

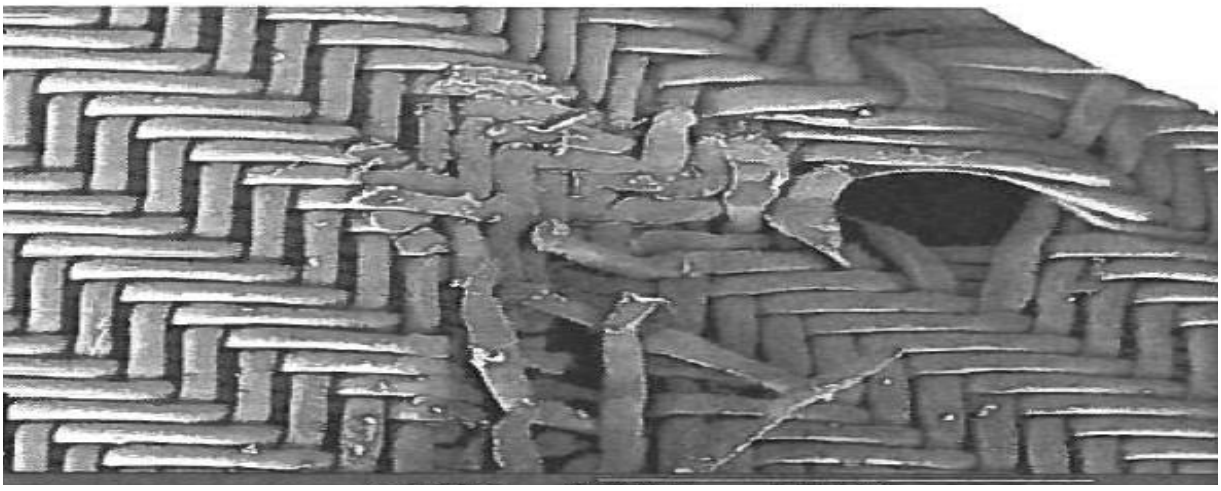

Figure 1.21. SEM image (Original Magnification: x 200) of the puncture of filaments when inserting the braided ligature into Talent Endoprostheses (Chakfe et al., 2004, p. 40).
[Used with permission]

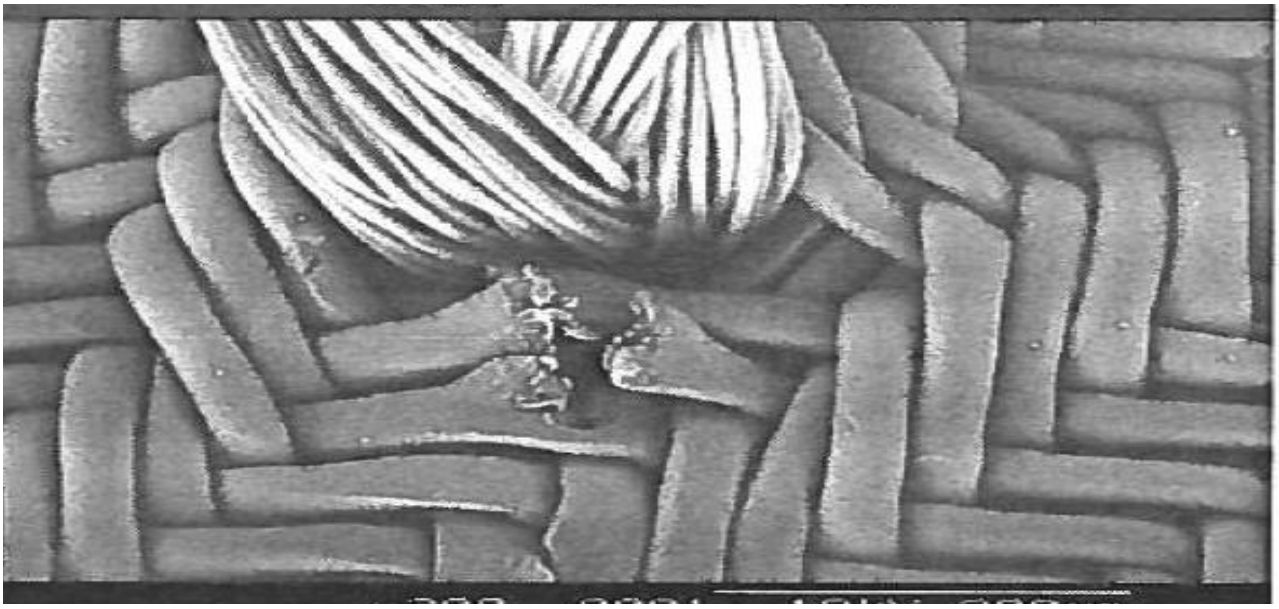

Figure 1.22. SEM Image (original magnification: x 100) of the hole developed at the contact of the stent in Talent Endoprostheses (Chakfe et al., 2004, p. 40).
[Used with permission]

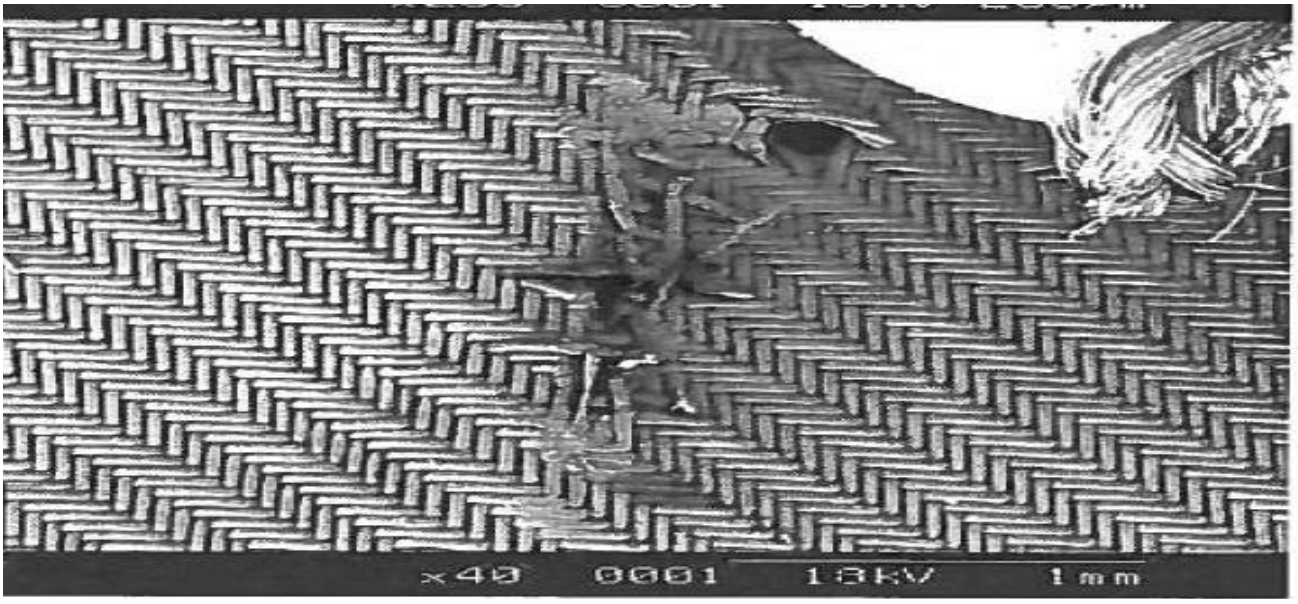

Figure 1.23. SEM Image (original magnification: x 50) of the hole - Signs of wear filaments in Talent Endoprostheses (Chakfe et al., 2004, p. 40).
[Used with permission]

1.6 Objective of the Current Research

The literature review and analysis reveals that the main reason for polyester graft failures is tearing, and the failure could occur as early as right after implantation (Joseph et al., 2009; Miyake, Sakagoshi, & Kitabayashi, 2016) or later, up to 10 years (Table 1.3). Further, complete fragmentation of graft made from other polymers, for example, nylon aortoiliac prosthesis was observed after 14 years due to loss of tensile strength (Yaw et. al., 1974). The reason behind this inconsistency may be the irregularities of polyester materials that are used to make the graft. Criteria of materials are expected to be regular in every aspect, for example thickness, count, breaking and tearing strength. One can expect a consistent and long lasting Dacron graft when material characteristics are even and regular. Any irregularities or unevenness will cause mechanical failure and inconsistency. No work could be found that relates material irregularity with material tearing strength. ***Therefore, the main objective of this research is to find out irregularities in polyester material which may cause premature rupture.***

Chapter 2 Materials and Methods

2.1 Introduction

In this study, the behaviour of polyester graft materials was investigated under different experimental conditions. At the preliminary experiments (Chapter 3), yarn from regular grade polyester woven fabric (Dacron) was used (*Figure 2.1*). This type of polyester is currently used for making apparel articles, furnishing fabrics (bed sheet, bed covers, curtains and so forth) and other industrial applications. There are similarities of this fabric to the Dacron woven polyester prosthetic graft fabric used for human implantation (Wilson et al., 1997). Further, the interlacement diagrams of the vascular graft woven fabrics and Dacron fabric are similar to that shown in Figures 2.2 (plain, 1/1) and twill (2/1 - irregular). The breaking load, extension at break and time to break of the yarn sample were observed in blank (without any liquid medium), water (pH=7) and alkali (pH=12.6) under different fractional loads (60%, 70%, 80%, 90% and 98%) was investigated during the preliminary investigation. Yarn irregularity (diameter) was investigated in order to find the relationship between breaking load under different fractional loads and irregularities (thin/thick places).

At the second stage of experiments (Chapter 4), double velour polyester vascular graft knitted fabric (***DVPVGKF***) was used. At first, thickness and yarn diameter of vascular graft fabric were measured to check the variation in the yarn. Then, breaking load under 2 different fractional loads (80% and 90%) and tearing strength of ***DVPVGKF*** was determined for the virgin and hydrolysed samples of 7%, 16.5% and 25% weight losses.

2.2 Materials

2.2.1 Dacron Polyester Woven Fabric

One hundred percent Dacron polyester double ply spun yarn (Z-twist) plain woven fabric type 64 (Lot 1669, style 763) – semi dull, was obtained from TESTFABRICS INC. A picture of the Dacron fabric used in this study is shown in *Figure 2.1.* For yarn testing (for example, tex, dia), yarn from the weft direction (cross-wise) of this fabric was pulled out as weft yarn is generally weaker and more irregular than warp yarn (yarn in vertical direction).

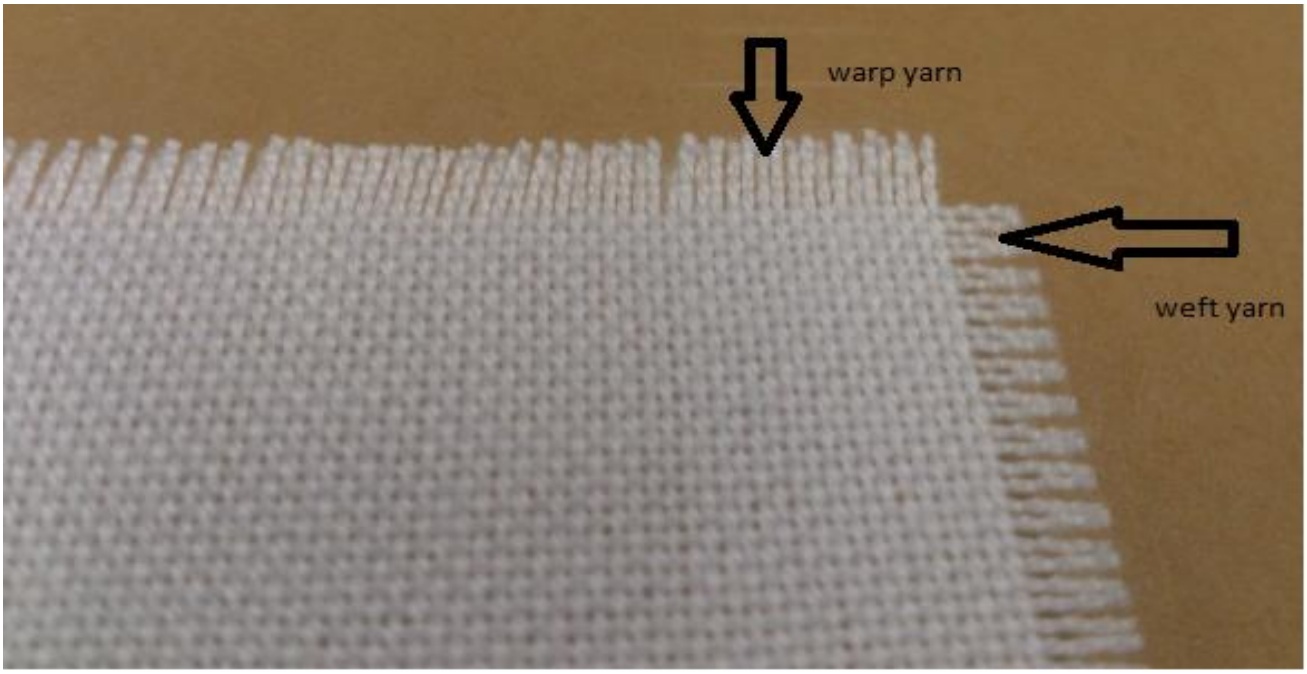

Figure 2.1. 100% Dacron woven fabric (Plain, 1/1).

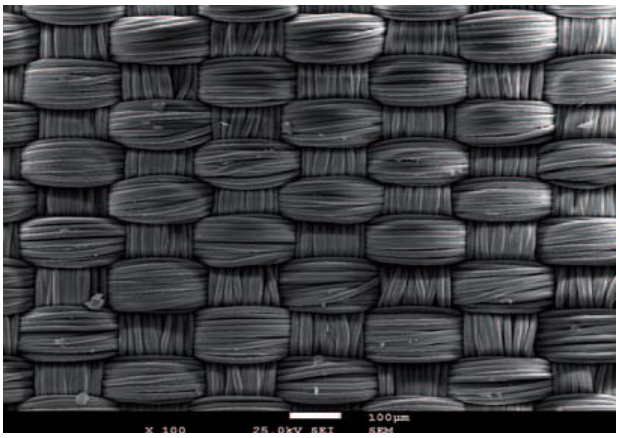

Figure 2.2. SEM of an endovascular prosthesis woven fabric (plain)

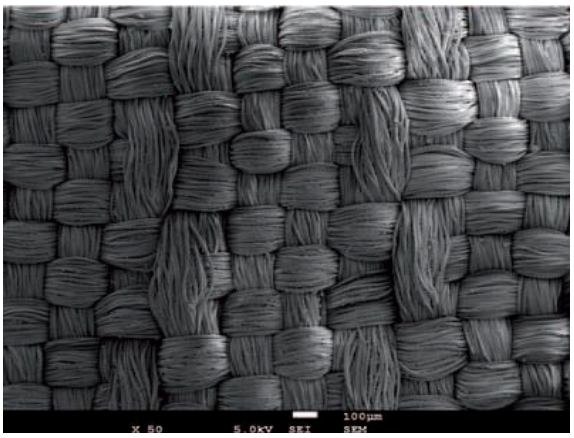

Figure 2.3. SEM of an endovascular prosthesis woven fabric (twill)

(Santos, Figueiredo, Rocha, & Tavares, 2012, p. 335)
[Used with permission]

2.2.2 Double Velour Polyester Vascular Graft Knitted Fabric (*DVPVGKF*)

Double Velour Polyester Vascular Graft Knitted Fabric (***DVPVGKF***) size-6″x6″, lot-HUWJ1970 was bought from Bard group (Bard Peripheral Vascular), Tempe, Arizona, USA. The fabric is shown in *Figure 2.4*; however, the detailed structure of the knitted fabric has not been disclosed by the manufacturer.

Figure 2.4. Double velour polyester vascular graft knitted fabric (***DVPVGKF***).

2.2.3 NaOH Solution

NaOH (analytical grade) pellets were obtained from Sigma-Aldrich. A 1% solution of NaOH was prepared using tap water and the prepared solution (2600 ml) was transferred to Bio-bath (*Figure 2.5*) and heated to raise the temperature to 37°C (*Figure 2.6*).

2.3 Test Procedures

2.3.1 Conditioning of Samples

To standardize the results, fabric samples were conditioned at 65% relative humidity (RH) and 21°C temperature for at least 24 hours before any measurements were taken, in accordance to the test method ASTM D 1776.

2.3.2 Breaking Load Measurement

To measure the breaking load, Instron Universal Tester, Model 5965 was used. The Instron is equipped with BioPuls-bath and heating device (*Figures 2.5* and *2.6*). In order to conduct the rupture test for yarn from woven fabric, in blank medium, in water (pH=7) and in alkaline conditions (pH = 12.6) under different fractional loading conditions, yarns (35 inches long) from the weft direction of the fabric were pulled out. The breaking load and elongation of the yarn were determined using a gauge length of 3 inches and at a speed of 20 mm/minute. The load cell selected was 500N for this entire study. The breaking load of the virgin yarn was used to conduct the test under different fractional loading conditions.

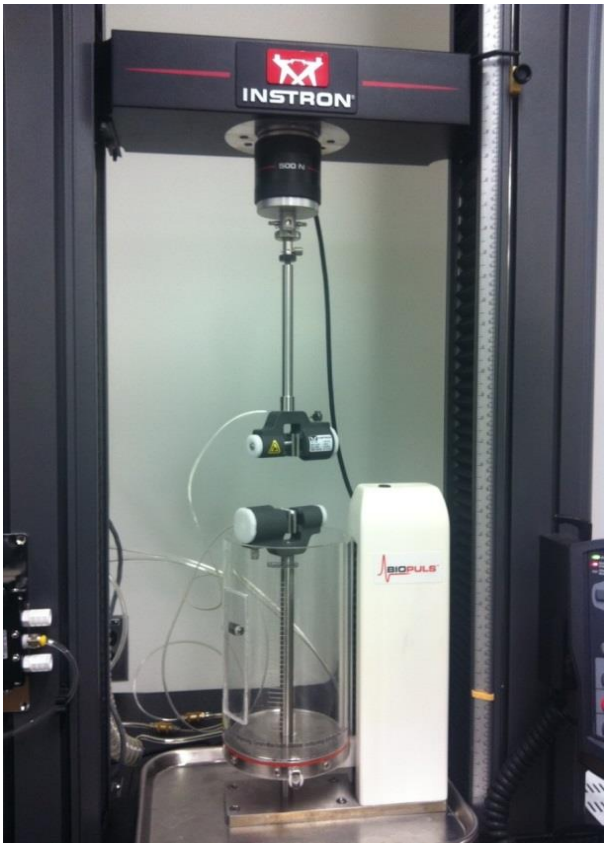

*Figure 2.5.*INSTRON (Model: 5965) Universal tester with biobath (Bio-Puls).

Figure 2.6. Bio bath heating device.

Yarn sample preparation for test

In order to conduct the breaking load test, weft yarn (35 inches) from woven fabric was removed and prepared 7 samples from each yarn by cutting to make 5 inch sample length [*Figure 2.6 (a)*]. The test was conducted in blank medium (no water or alkali; Figure 2.13(a) is similar to the blank yarn test), in water (pH=7) and in alkaline conditions (pH = 12.6) under different fractional loading conditions. The breaking load and elongation of the yarn was determined with a gauge length of 3 inches and at a speed of 20 mm/minute. The load cell selected was 500N for this entire study. The breaking load of the virgin yarn was used to calculate the fractional holding loads, which is given in the next section (Section 2.3.3).

2.3.3 Establishing Holding Load

Different holding loads (98%, 90%, 80%, 70%, and 60%) were used based on the original breaking load of the same sample (35 inch long). The steps in setting up the parameters in Bluehill software for testing the sample under specified loads are given in Appendix A.

Holding load parameters

The holding loads with sample ID are given in Table 2.1

Establishing hold time

Different holding times were used in order to establish a breaking point for a specific holding load. The holding time for different samples with sample ID are given in Table 2.1

2.3.4 Test Procedures in Water and Alkali

The samples were tested in water and alkali in a Biopuls-bath attached to Instron 5965 *(Figures 2.7, 2.8 and 2.9)* under different holding loads and holding times. The Biopuls-bath was filled with distilled water (2600 ml) and then the sample was placed between the two grips. Before testing, the Biopuls-bath was lifted in such a way that the samples (3 inch) stayed under water (*Figure 2.7*). The water temperature of the Bio-bath was raised to 37°C using Cyber Therm (Part-SPM6-OLFT-INSI, Sr. No: 09103) which is similar to physiological temperature. Before each test, the sample was pre-heated for 5 minutes.

For each test, the breaking load and extension of a yarn of 3 inches long, which was pulled from the weft (35 inches long), was measured. The use of the same yarn was necessary in order to avoid variations in the yarn for measuring breaking load at different fractional loads and holding times. This original breaking load was used for calculating holding loads, such as 80%, 70% and 60% of the original breaking load. Table 2.1 shows the sample ID, holding loads and fractional load.

Table 2.1

Sample ID for preliminary study (results given in Chapter 3)

Sample ID	Holding time	Fractional load	Temperature (°C)
A1-1 (control sample)	N/A	N/A	21 (standard conditioned temp.)
A1-2 (blank)	[a]5 min	80%	21 (standard conditioned temp.)
A1-3 (water)	[b]5 min	80%	37
A2-1(control sample)	N/A	N/A	21(standard conditioned temp.)
A2-2 (water)	60 min	60%	37
A2-3 (water)	60 min	70%	37
A2-4 (1% NaOH)	60 min	70%	37
A2-5 (1% NaOH)	60 min	80%	37
A2-6 (water)	24 hours	80%	37
A3-1 (control sample)	N/A	N/A	21 (standard conditioned temp.)
A3-2 (water)	[c]72 hour	80%	37
A3-3 (control sample)	N/A	N/A	21 (standard conditioned temp.)
A3-4 (water)	[d]72 hours	80%	37
A4-1 (control)	N/A	N/A	21
A4-2 (blank)	[e]1 hour	98%	21
A4-3 (control)	N/A	N/A	21
A4-4 (blank)	[f]1 hour	90%	21
A5-1 (control)	N/A	N/A	21
A5-2 (blank)	[g]1 hour	90%	21
A5-3 (blank)	60 minute	80%	21(standard conditioned temp.)

[a]sample broke after 3.06 mins ; [b]sample broke after 0.68 mins; [c]sample broke after 1.08 mins; [d]machine ran 72 hours, however, the computer was frozen after 36 hours; [e]sample broke after 0.84 minutes; [f]sample broke after 2.62 minutes; [g]sample broke after 1.92 minutes.

Figure 2.7. Yarn in water during testing in Instron.

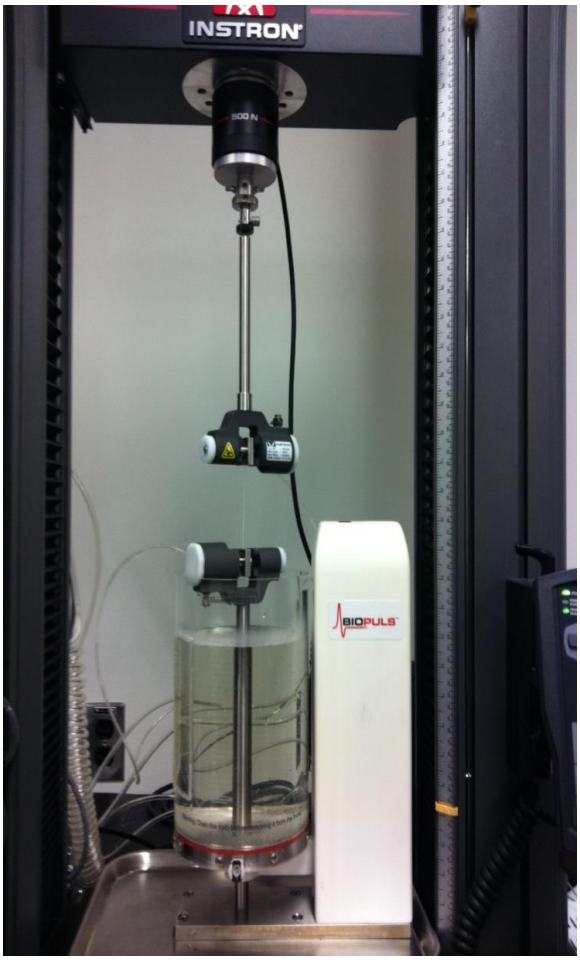

Figure 2.8. Yarn in NaOH before lifting the Biopuls-bath.

Figure 2.9. Yarn in NaOH after lifting the bath.

2.3.5 Determination of Yarn Irregularity

The variations in diameter of the virgin yarns was measured using Bioquant Life Science Image Analysis System (BIOQUANT Image Analysis Corporation-USA) shown in *Figure 2.10*. The system includes two main parts: a microscope and a camera to view the magnified sample on a computer system and to obtain the diameter along the length of the yarn. For the diameter determination, glass slides were prepared using glycerin. A magnification of 4X was used to measure the thick and thin places. The measuring protocol using Bioquant is shown in *Figure 2.11*.

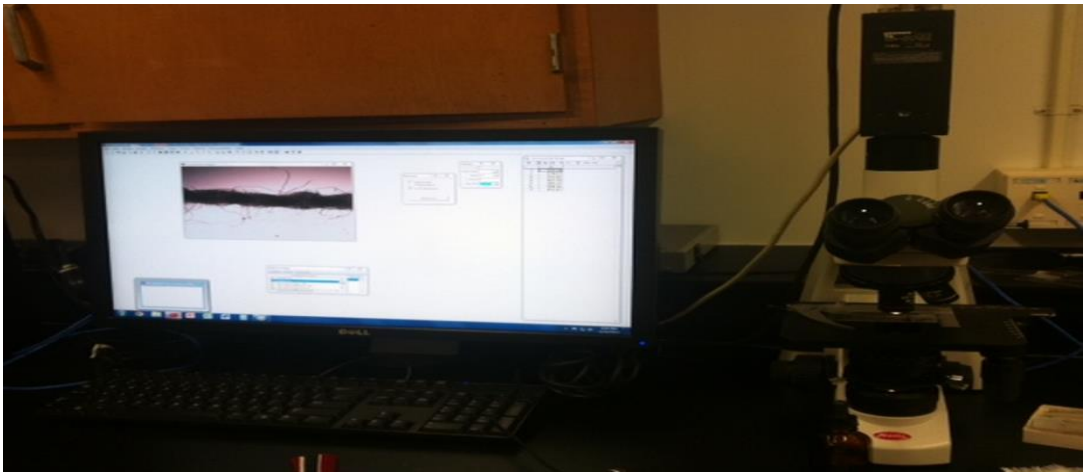

Figure 2.10. Bioquant life science systems – diameter measurement system.

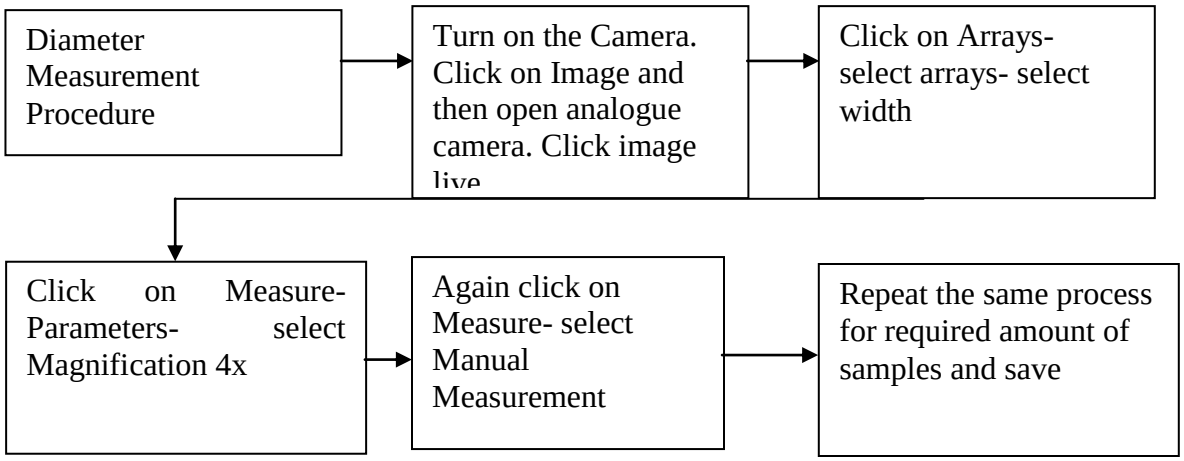

Figure 2.11. Protocol of measuring width in BioQuant life science image analysis.

2.4 Test Procedures for *DVPVGKF* (results given in Chapter 4)

2.4.1 Filament Number and Determination of Yarn Linear Density (Tex)

Number of filaments in a single yarn and diameter of each filament were measured using Bioquant Life Science Image Analysis System (BIOQUANT Image Analysis Corporation-USA) software (*Figures 2.10-2.11*) .Yarn linear density (tex) was calculated using the formula given in Section 4.3.1.

2.4.2 Thickness Measurement

Before testing, all fabrics were conditioned at 20^0 C and 65% relative humidity for at least 48 hours according to ASTM D 1776. Two fabric samples were randomly chosen from six samples that were obtained from the vascular graft manufacturer, Bard Peripheral Vascular (USA). The thickness at 10 different spots on each fabric swatch was taken using Low Pressure Thickness Gage, Model CSI-49 (*Figure 2.12*).

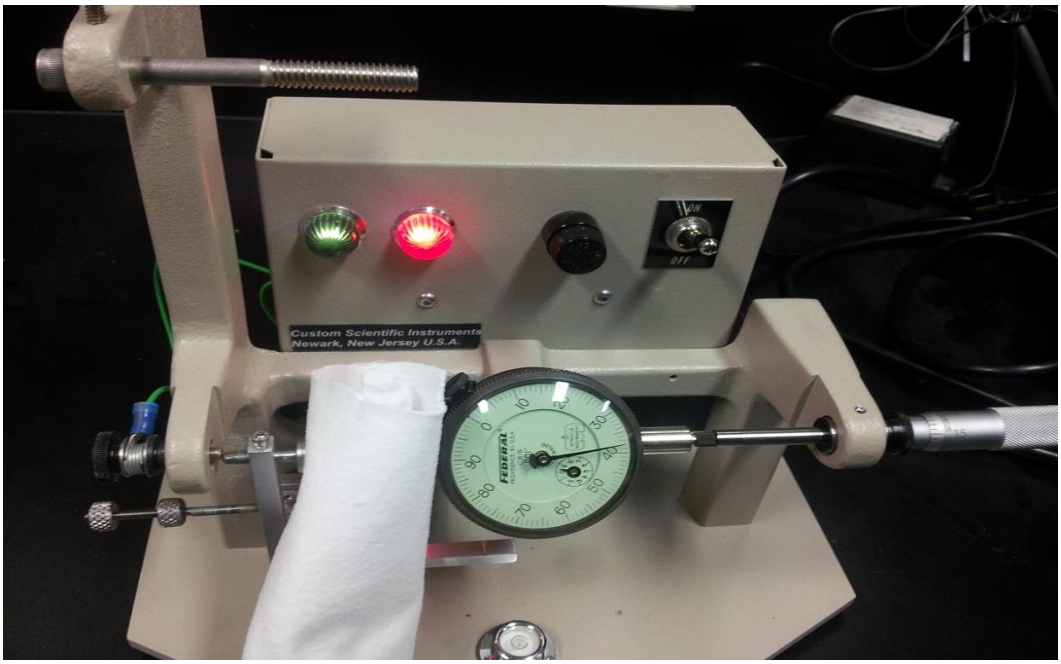

Figure 2.12. Fabric Thickness Tester.

2.4.3 Fabric Breaking Load and Holding Load Measurement

Instron Universal Tester, Model 5965 [*Figure 2.13(a*)] was used to measure the breaking load. Sample length of 3 inches and width of 0.5 inch were cut from the fabric swatch. Each sample was tested with a gauge length of 1″ and 500N load cell. At first, the breaking load was determined on the control sample and then different holding loads were calculated based on the

breaking load of virgin sample. The sample was kept under holding conditions to examine if the samples can survive the pre-set duration (Table 2.2).

2.4.4 Establishing Holding Load, Holding Load Parameters and Hold Time

Establishing Holding Load

The two different holding loads (90% and 80%) used were calculated based on the original breaking load of the same sample. The steps in setting up the parameters in Bluehill software for testing the sample under specified load are given in Appendix D.

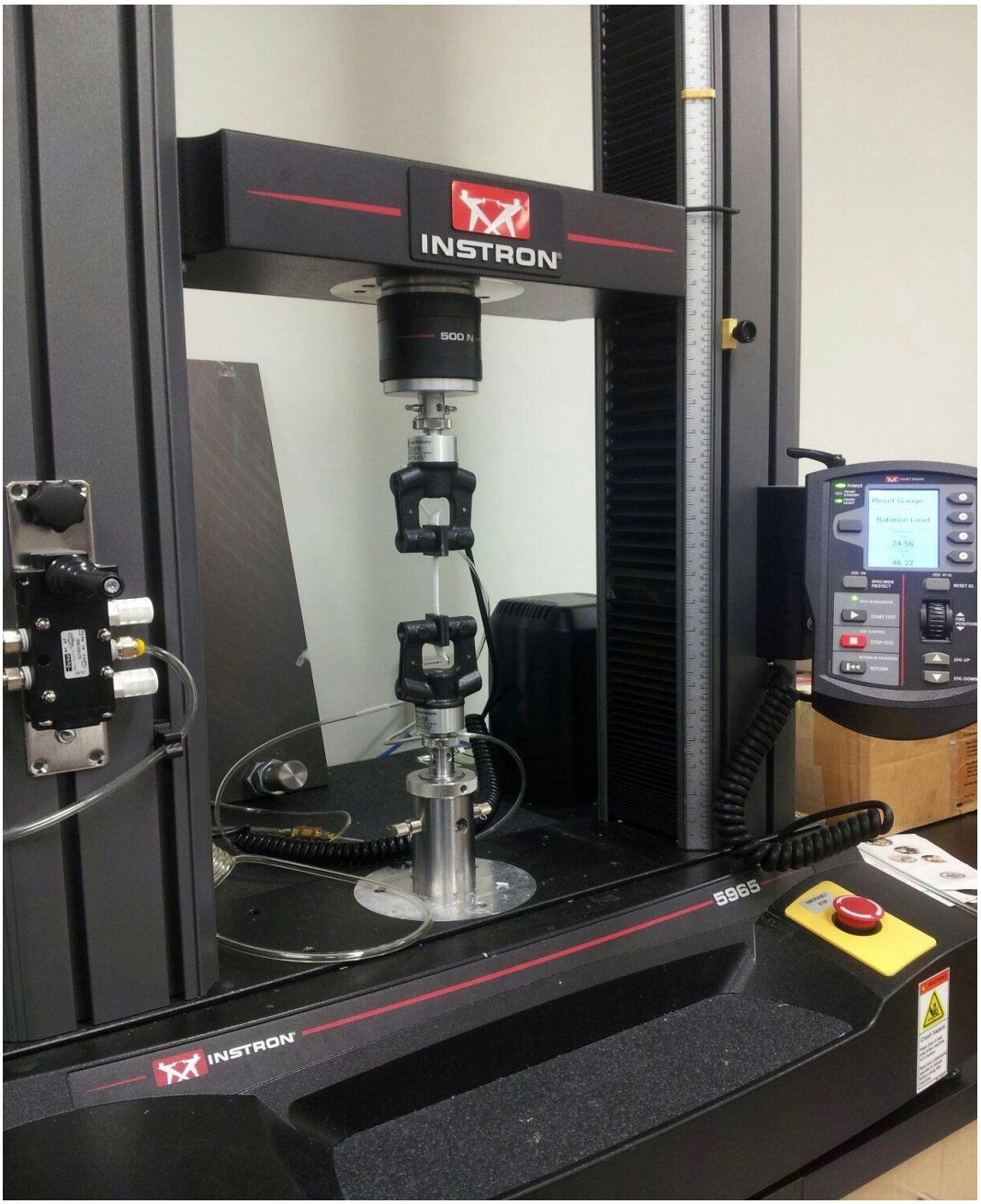

Figure 2.13(a). Fabric breaking strength measurement in Instron.

Holding Load Parameters

The holding loads with sample ID are given in Table 2.2

Establishing Hold Time

Different holding times were used in order to establish a breaking point for a specific holding load. The holding time for different samples with sample ID are given in Table 2.2

Table 2.2

Sample identification

Sample ID	Holding time	Fractional Load
B1(control sample)	N/A	N/A
B2(control sample)	N/A	N/A
B3(control sample)	N/A	N/A
B4	60 min	90%
B5	24 hour	90%
B6	48 hour	80%

2.4.5 Tearing Strength of Virgin and Hydrolysed *DVPVGKF*

Before measuring tearing strength, the graft samples were hydrolysed to mimic the in vivo alkaline condition.

2.4.5.1Hydrolysis Procedure with Different Holding Loads

Hydrolysis was carried out by treating the sample (size: 75mm x 40mm) with 10% NaOH at 60°C for 1 hr (Sample H1), 2hr (Sample H2), and 5 hr (Sample H3) in an Atlas Launder-o-meter.

2.4.5.2Weight Loss Measurement

The weight loss (%) was calculated by taking the weight of the untreated and treated samples using the formula given below:

Weight loss (%) = [(W1-W2) X100]/W1

W1 = weight of the untreated sample

W2 = weight of hydrolysed sample

2.4.5.3 Tearing Strength Measurement

2.4.5.3.1Instron Strength Tester

Instron Universal Tester, Model 5965 was used to measure the tearing strength (*Figures 2.14 and 2.15*). Test procedure was followed according to the *ASTM D2261 -13 Standard Test Method for Tearing Strength of Fabrics by the Tongue (Single Rip) Procedure (Constant-Rate-of-Extension);* sample length of 75mm and 40mm width was taken. Sample was cut 35mm long at the centre. Distance between the two jaws was set as 25.4mm and speed was 30mm/min [*Figure 2.13 (b)*].

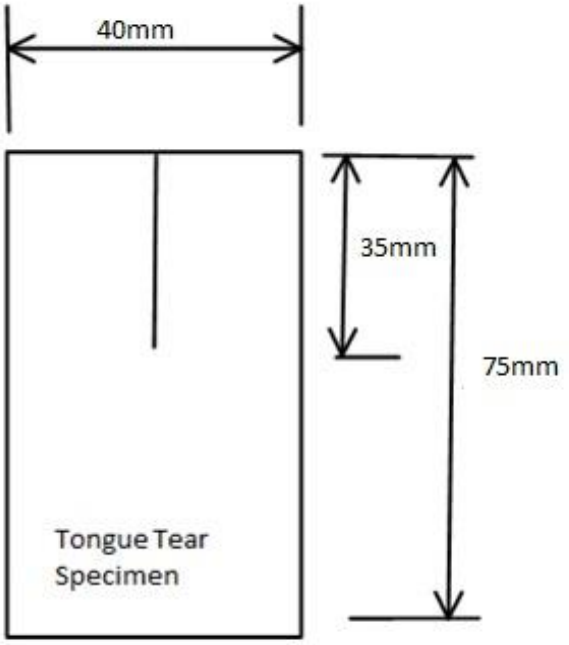

Figure 2.13 (b). Schematic diagram of tongue tearing test specimen.

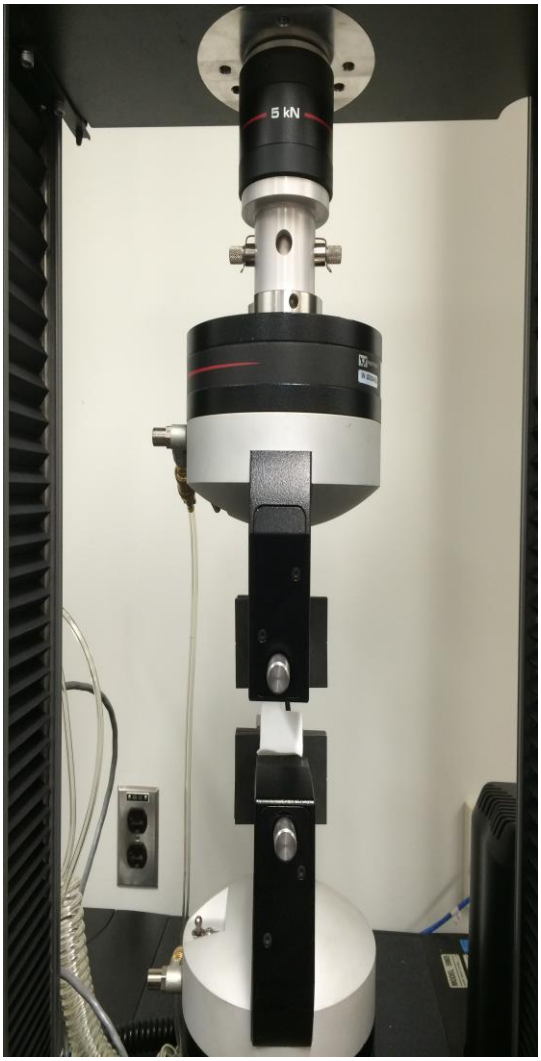

Figure 2.14. Tearing strength measurement at the beginning of the test in Instron.

Figure 2.15. Tearing strength measurement at breaking point in Instron.

2.4.5.3.2Elmendorf Tear Tester

To measure the tearing strength of yarn, Digital Elmendorf Tearing Tester, Model M008E (from SDL Atlas) was used (*Figure 2.16*). Test procedure was followed according to the ASTM D1424-09 (ASTM, 2009).

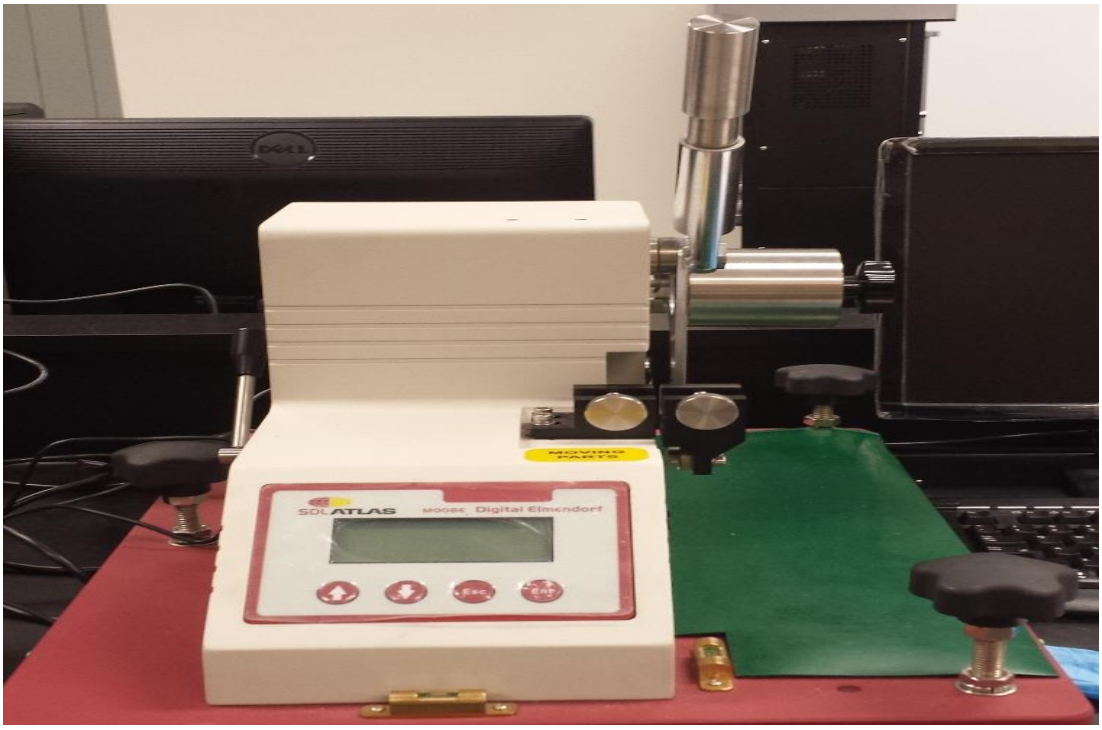

Figure 2.16. Digital Elmendorf tearing tester, Model M008E.

Samples were pre-conditioned according to the procedure of ASTM D1776 (Practice for Conditioning and Testing Textiles) before starting the test. Sample size was selected as 7cm in length and 4.5cm in width due to variation in construction between apparel grade and medical grade fabric. Four (4) untreated samples were tested using the load cell 'C' (15.7N - 16.05N) shown in Table 4.5.

2.4.6 Scanning Electron Microscopy (SEM)

The samples for SEM testing were cut into pieces approximately 1 cm^2 and placed onto a specimen stub mount. Since the samples were non-conducting, they were exposed to a plasma (60% gold and 40% palladium) using the Sputter Etch Unit to prevent scanning faults and improve image quality. The specimen mounts were transferred to the microscope for analysis of cracks, degradation, and deformations.

2.5 Conclusions

In this chapter, textile materials (apparel grade polyester yarn and medical grade polyester knitted fabric-***DVPVGKF***) as well as the testing machines (Instron universal tester, Bio bath heating device, fabric thickness tester, Bioquant life science system and digital Elmendorf tearing machine) were introduced. Several test procedures and relevant test methods for example, determining breaking and holding loads of apparel grade polyester yarn in both water and alkali, measuring diameter of yarn and filament with Bioquant, measuring thickness of ***DVPVGKF,*** determining breaking and holding loads, tearing strength of ***DVPVGKF*** and preparing samples for taking SEM images were also described.

Chapter 3 Variation in Apparel Grade Polyester Fabric

3.0 Introduction

As reported in the literature, failures of prosthetic grafts can occur right after the implantation or many years after implantation. It was suspected that this variation in failure might have come from non-uniformity in the textile materials and structure. Accordingly, for the preliminary study, yarn mechanical properties, yarn irregularity and fracture mechanisms were measured and discussed.

3.1 Results and Discussion

In this chapter, results of apparel grade polyester woven fabric irregularities are reported. The guidelines and results from the preliminary results are used to test the ***DVPVGKF***, which is given in Chapter 4

3.2 Mechanical Properties

3.2.1 Load and Extension and Time to Break

The mechanical properties of load (N) and extension (mm) and time to break the virgin and treated polyester yarns are given in Tables 3.1 – 3.4. Table 3.1 shows the breaking load for seven control samples without any holding load and water/alkali (samples: A1-1, A2-1, A3-1, A3-3, A4-1, A4-3 and A5-1). Breaking load with 80% holding load, but no water/alkali (A1-2, A5-3, blank), and with 80% holding in water (A1-3, A2-6, A3-2, A3-4) and in alkali (A2-5) are shown in Table 3.2; with 70% holding load in water (A2-3) and in alkali (A2-4), with 60% holding load in water (A2-2) in Table 3.3; with 90% holding load without any liquid (A4-4, A5-2, blank), and 98% holding load without any liquid (A4-2) in Table 3.4. The test sample

attachment for breaking load without any water/alkali is similar to *Figure 2.13(a)* and the test attachments for strength test in liquid can be seen in *Figures 2.7-2.9.*

For control samples without any holding loads and liquid, the breaking load results vary between 10.04 N for A1-1 to 6.26 N for sample A2-1. From this breaking load data, it can be stated that the variability in the yarns (weft yarns) is very high, as the standard deviation was ±1.20 (mean: 8.28 N). From the average breaking load datum and standard deviation from the first approximation, it can be stated that the variability in the yarns (weft yarns) is very high.

The extension at break of seven control samples (A1-1, A2-1, A3-1, A3-3, A4-1, A4-3 and A5-1) is given in Table 3.1. The extension at break ranges from 16.83 (A2-1) mm to 24.1 (A3-3) mm with a standard deviation of ±2.58 (mean value:20.0 mm). Since both breaking load and breaking extension vary widely, and the work of rupture is the product of these values, it is expected that the variation in work of rupture of the yarn is very high.

The time to break the seven control samples was between 50.50 seconds and 72.3 seconds. However, it is worthwhile noting that no linear relationship can be observed between breaking load and breaking time. For example, the sample with the breaking load of 10.04 broke after 59.2 seconds (A1-1); whereas, the sample with the breaking load of 7.53 N broke after 72.3 seconds (A3-3). Also, samples with almost similar breaking loads broke at different times; for example, sample: A3-1 (breaking load: 8.85 N, breaking time: 62.7 seconds), sample A4-1 (8.57 N, 66.6 seconds) and sample: A5-1 (8.79 N, 53.9 seconds).

It was thought that this irregular relationship between breaking load and time to break might have come from the extension at break. Analysis of extension at break and time to break reveals that the relationship between extension at break and time to break is linear. For example, the sample that has the largest extension at break (A3-3, extension at break: 24.1 mm) took longest time to break (72.3 seconds); and the sample that has the lowest extension at break (A2-1, extension at break: 16.83 mm) took shortest time to break (50.50 seconds). The implication of this finding for graft application is that, there may be a difference in the polyester micro structure, for example, different size in crystalline regions that may contribute to differential breaking both in vivo (Table 1.3) and in vitro (Table 3.1).

Variations in textiles are usually very high due to the presence of thin (-d<40%-200%) and thick (+d>35% - 200%) places, which lead to unevenness of yarn (Sinha & Kumar, 2013). This variation occurs due to unevenness in such production aspects as drafting zone pressure and sliver variation (carded and combed slivers) in the yarn manufacturing processes (Korkmaz & Behery, 2004; Lin, Oxenham, & Yu, 2011). A variation in strength was also found in the polyester vascular graft during the clinical investigation as the durabilty of these grafts was found to be between 2 to 10 years *in vivo* (Table 1.3).

It can be seen from Table 3.3 that at 60% (Sample A2-2, holding load: 3.75 N, *Figure 3.5*) and 70% (Sample A2-3, holding load: 4.38 N, *Figure 3.6*) holding loads, no yarn was broken after 1 hour in water at 37°C. Similarly, no yarn was broken at 70% holding load in alkali (Sample A2-4, *Figure 3.7*) for 1 hour at 37°C.

Table 3.1

Mechanical properties data of load, extension and time to break of control samples

Sample ID	Load (N)		Extension at Break (mm)	Time (second)	Fig. No/*L-E curve
	Holding Load	Load at Break			
A1-1	N/A	10.04	19.73	59.2	3.1
A2-1	N/A	6.26	16.83	50.5	3.4
A3-1	N/A	8.85	20.90	62.7	3.10
A3-3	N/A	7.53	24.1	72.3	3.12
A4-1	N/A	8.57	22.2	66.6	3.14
A4-3	N/A	7.90	18.56	55.7	3.16
A5-1	N/A	8.79	17.79	53.9	3.18

L-E curve: Load-Elongation Curve

Table 3.2 shows the breaking load data for 80% holding load at different holding time. At 80% holding load (8.03 N), yarn samples A1-2 (blank, 21°C, *Figure 3.2*), A1-3 (water, 37°C, *Figure 3.3*) and A3-2 (water, 37°C. *Figure 3.11*) broke in 3.06 minutes (holding time: 5 minutes), 0.68 minutes (holding time: 5 minutes) and 1.08 minutes (holding time: 72 hrs) respectively. It was also noted that sample A1-3 broke at 6.3 N load which is well below the holding load of 8.03 N. However, at 80% holding load (7.03 N), another yarn sample A5-3 (blank, 21°C, *Figure 3.20*) did not break even after 1 hour holding at 7.03 N load. Further, yarn samples A2-5, holding load: 5.01 N (NaOH, 37°C, *Figure 3.8*), A2-6, holding load: 5.01N (water, 37°C, *Figure 3.9*), A3-4, holding load: 6.02 N (water, 37°C, *Figure 3.13*) and A5-3, holding load: 7.03 N (blank, 21°C, *Figure 3.20*) did not break within the pre-set holding time of 1 hour, 24 hours, 72 hours and 1 hour respectively. Finally, when holding loads were 90% (A4-4, holding load: 7.12 N & A5-2;

Figures 3.17 and *3.19*) and 98% (A4-2, holding load: 8.39 N *Figure 3.15*) the samples broke between 1 and 3 minutes (Table 3.4).

Table 3.2

Mechanical properties data of load, extension and time to break of 80% holding load sample

Sample	Load (N)		Extension at Break (mm)	Time	Yarn Breakage	[a]Fig. No
	Holding Load	Load at Break				
A1-1 Control Sample	N/A	10.04	19.73	59.20 sec	Yes	3.1
A1-2 (80% load - blank)	8.03	8.0	23.0	3.06 min	Yes	3.2
A1-3 (80% load - water)	8.03	*6.3	16.5	0.68 min	Yes	3.3
A2-1 Control Sample	N/A	6.26	16.83	50.50 sec	Yes	3.4
A2-5(80% load - alkali)	5.01	N/A	16.45	60.71 min	No	3.8
A2-6 (80% load - water)	5.01	N/A	15.95	1440.6 min	No	3.9
A3-1 (control sample)	N/A	8.85	20.90	62.7 sec	Yes	3.10
A3-2(80% load - water)	7.08	*5.23	23.5	1.08 min	Yes	3.11
A3-3 (control sample)	N/A	7.53	24.1	72.3 sec	Yes	3.12
A3-4(80% load - water, 72hrs)	6.02	**4.96	24.10	4321.1 min	No	3.13
A5-1 (control)	N/A	8.79	17.79	53.9 sec	Yes	3.18
A5-3 (80% load - blank)	7.03	N/A	13.63	60.57 min	No	3.20

*sample was broken before reaching hold load; **(computer froze), [a]Load-Elongation curve

Table 3.3

Mechanical properties data of load, extension and time to break of 70% and 60% holding load sample

Sample	Load (N)		Extension at Break (mm)	Time	Yarn Breakage	[a]Fig. No
	Holding Load	Load at Break				
A2-1 Control Sample	N/A	6.26	16.83	50.50 sec	Yes	3.4
A2-2 (60% load-water)	3.75	N/A	16.5	60.66 min	No	3.5
A2-3(70% load -water)	4.38	N/A	12.30	60.48 min	No	3.6
A2-4(70% load -alkali)	4.38	N/A	12.25	60.48 min	No	3.7

[a]Load-Elongation curve

Table 3.4

Mechanical properties data of load, extension and time to break of 90% and 98% holding load sample

Sample	Load (N)		Extension at Break (mm)	Time	Yarn Breakage	[a]Fig. No
	Holding Load	Load at Break				
A4-1 (control)	N/A	8.57	22.2	66.6 sec	Yes	3.14
A4-2 (98% load - blank)	8.39	8.49	14.1	0.84 min	Yes	3.15
A4-3 (control)	N/A	7.90	18.56	55.7 sec	Yes	3.16
A4-4 (90% load - blank)	7.12	7.24	15.0	2.62 min	Yes	3.17
A5-1 (control)	N/A	8.79	17.79	53.9 sec	Yes	3.18
A5-2 (90% load - blank)	7.91	8.0	17.5	1.92 min	Yes	3.19

[a]Load-Elongation curve

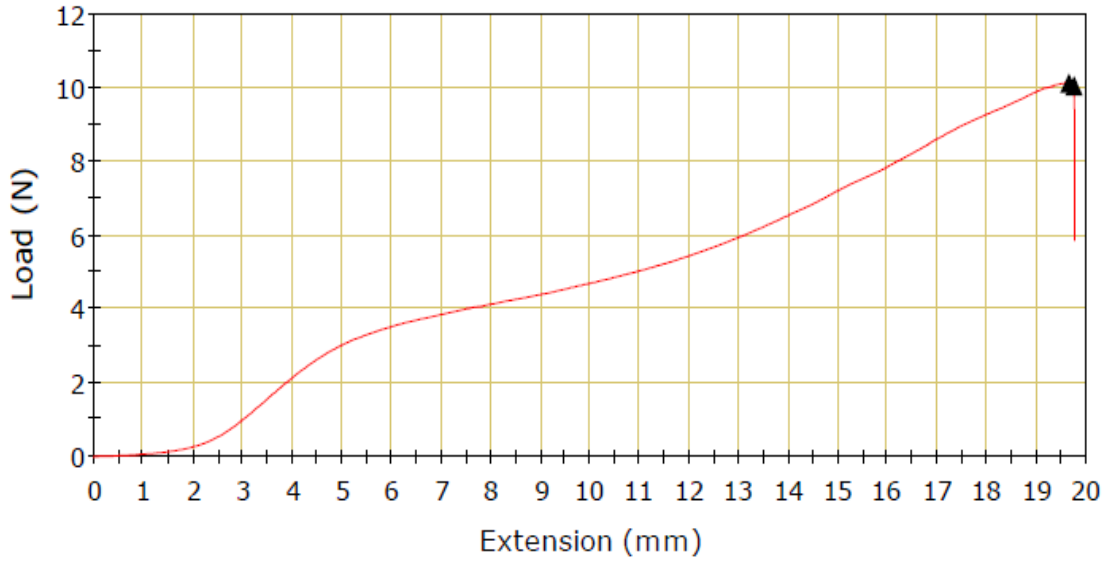

Figure 3.1. Sample A1-1 (control sample).

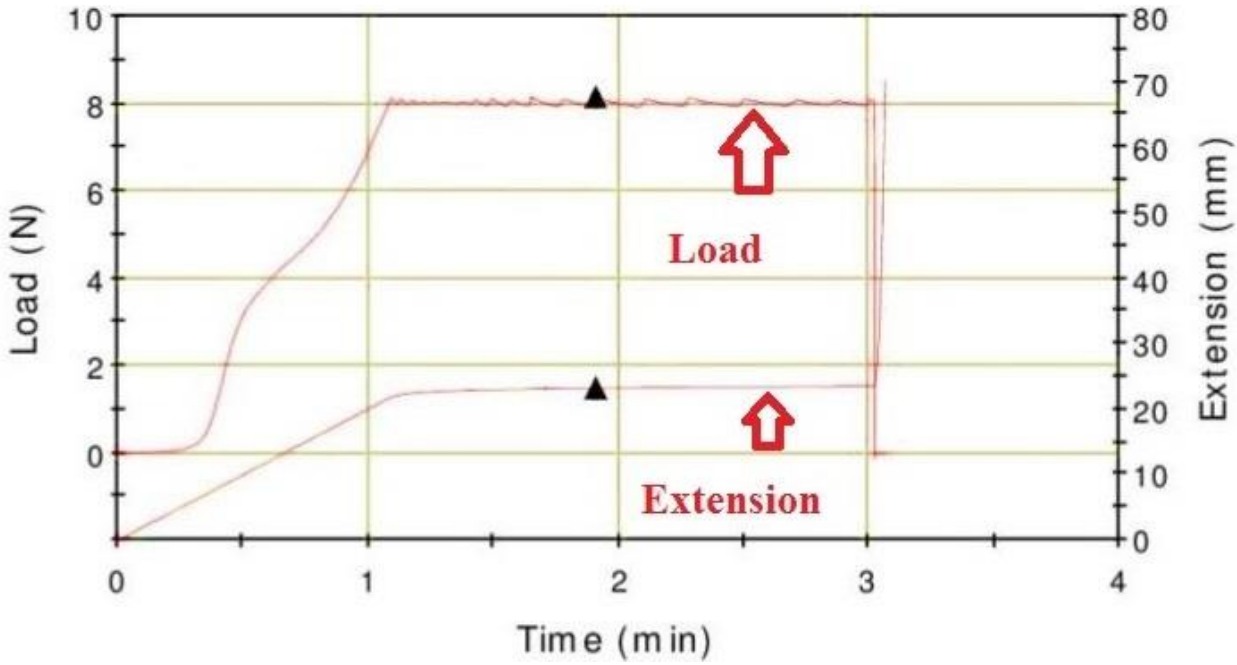

Figure 3.2. Sample A1-2 (blank, 80% fractional load, preset holding time 5 minutes, sample broke after 3.06 minutes).

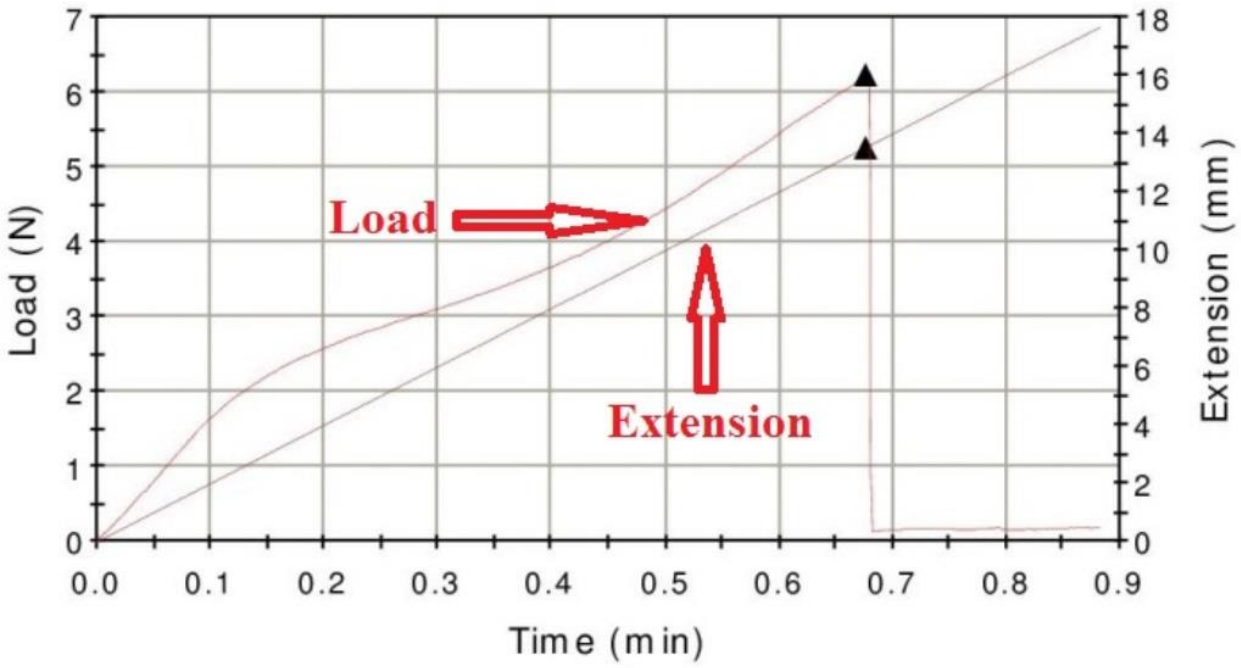

Figure 3.3. Sample A1-3 (medium-water, 80% fractional load, preset holding time 5 minutes, sample broke after 0.68 minute).

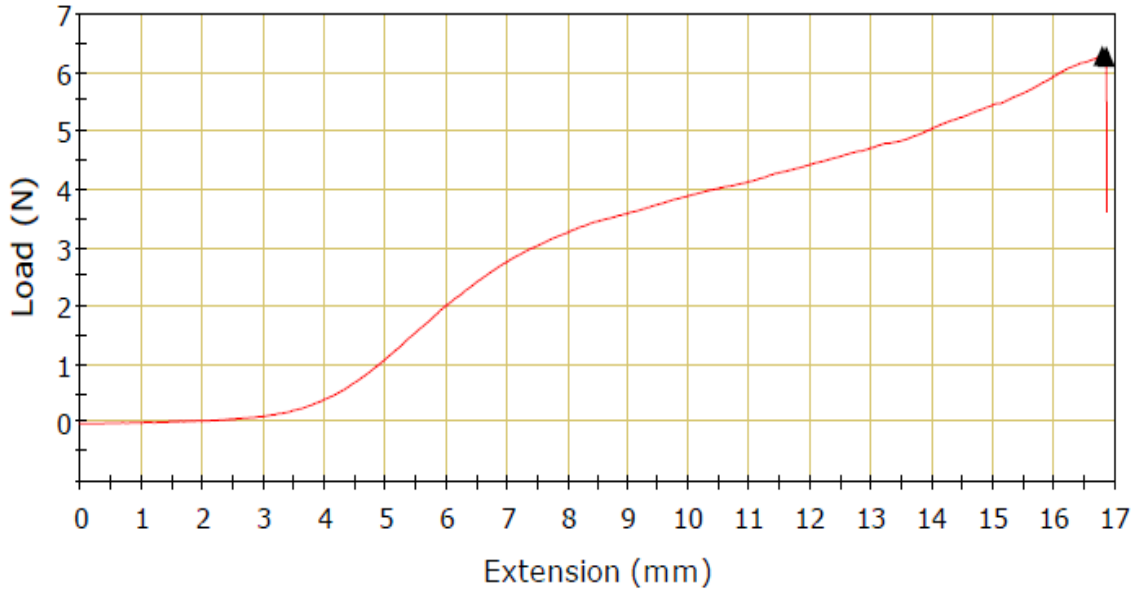

Figure 3.4. Sample A2-1 (control sample).

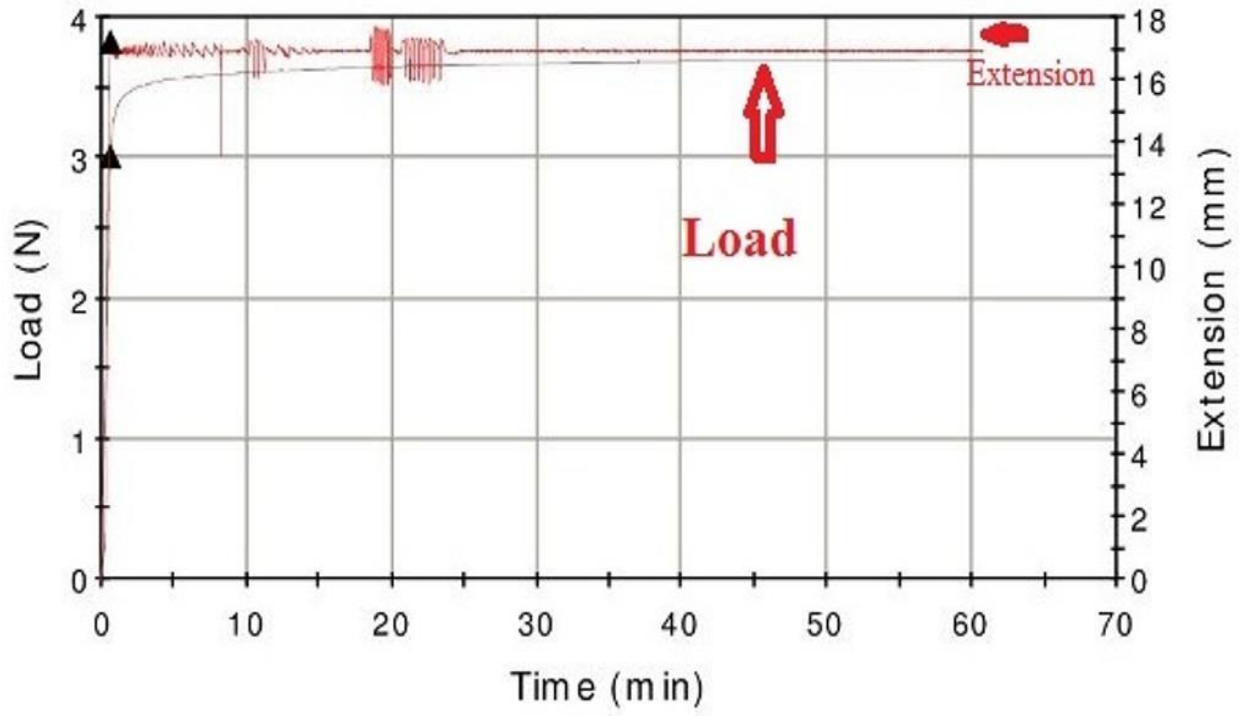

Figure 3.5. Sample A2-2 (medium-water, 60% fractional load, pre-set holding time 1hr, no breakage).

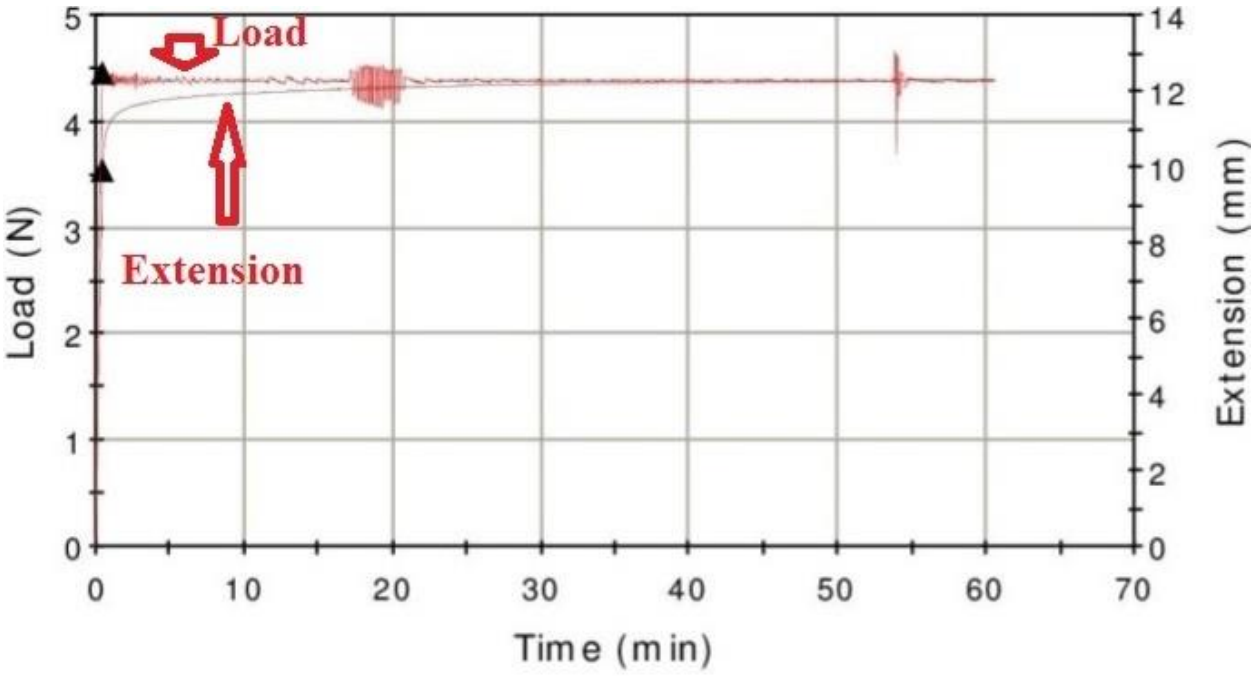

Figure 3.6. Sample A2-3 (medium-water, 70% fractional load, pre-set holding time1hr, no breakage).

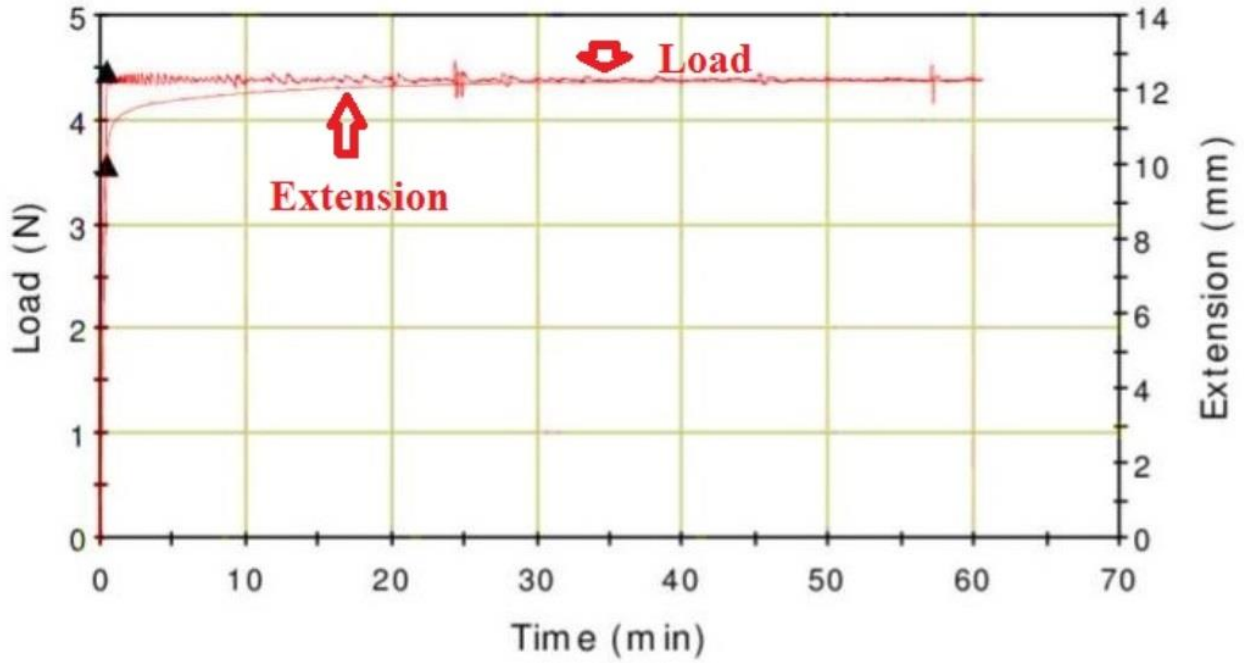

Figure 3.7. Sample A2-4 (medium- alkali, 70% fractional load, pre-set holding time 1hr, no breakage).

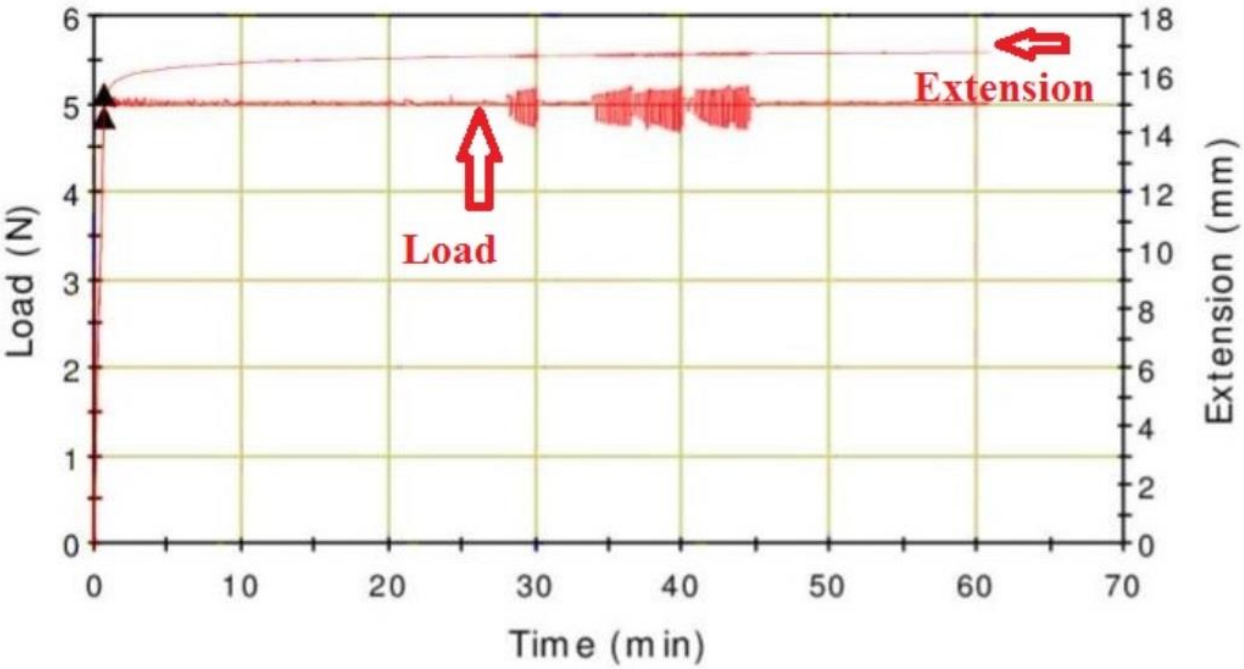

Figure 3.8. Sample A2-5 (medium-alkali, 80% fractional load, pre-set holding time 1hr, no breakage).

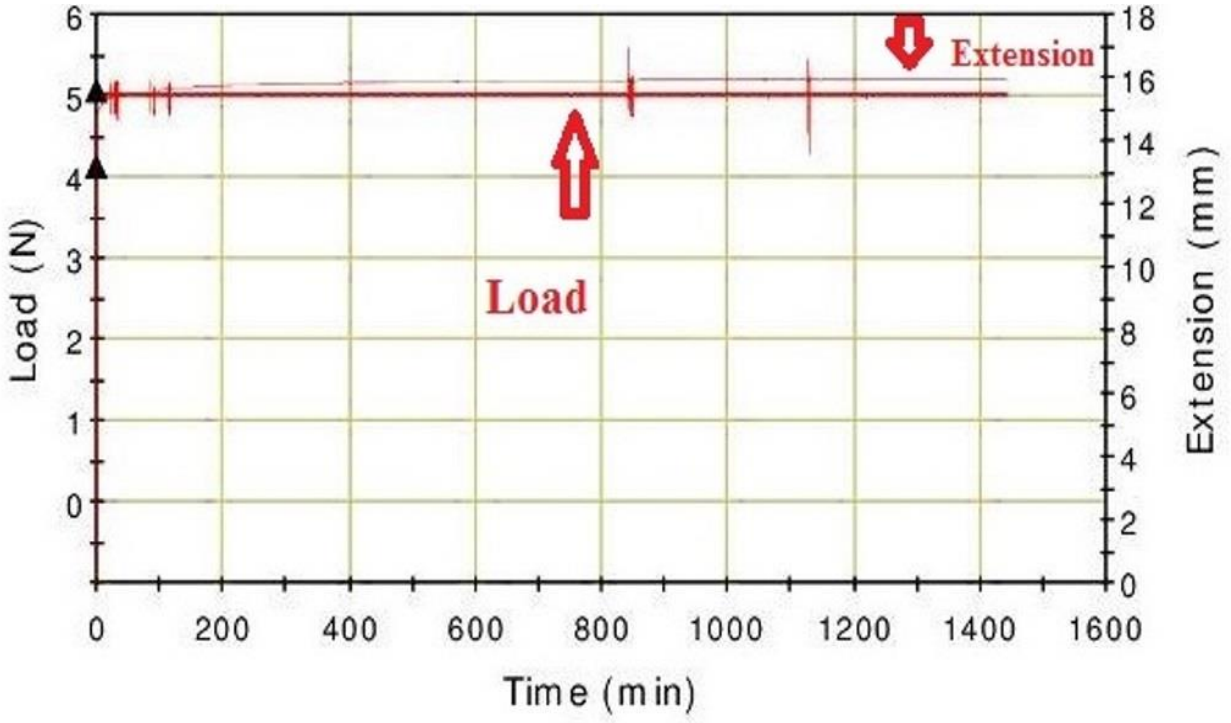

Figure 3.9. Sample A2-6 (medium-water, 80% fractional load, pre-set holding time 24hrs, no breakage).

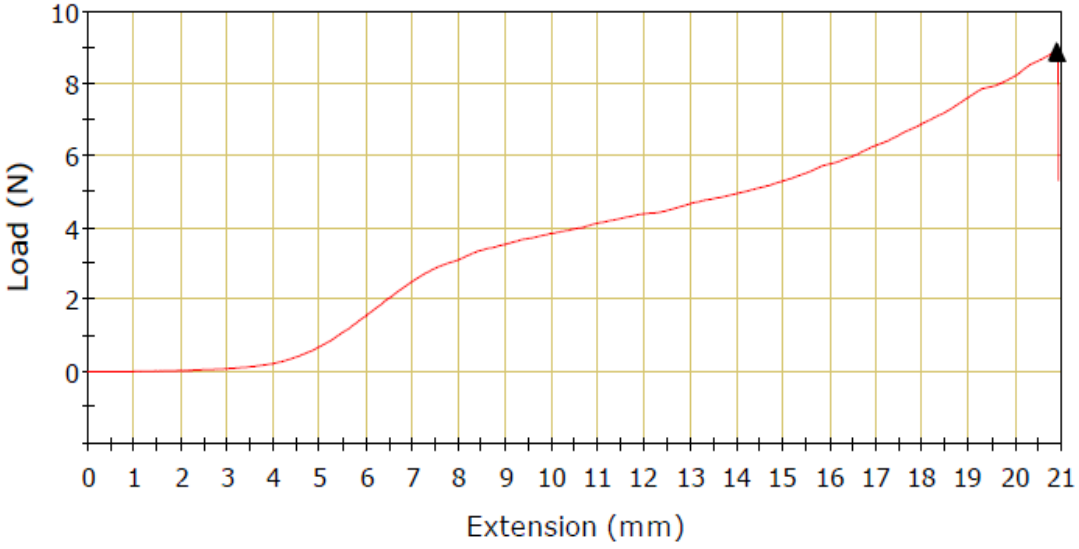

Figure 3.10. Sample A3-1 (control sample).

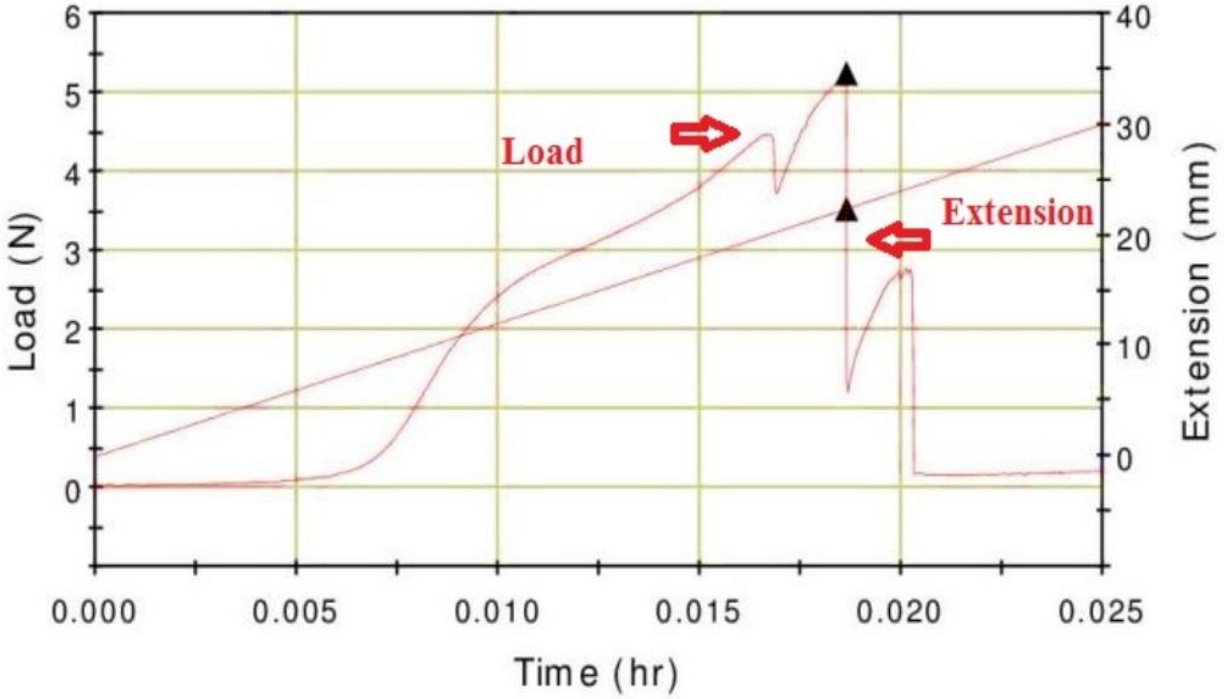

Figure 3.11. Sample A3-2 (medium-water, 80% fractional load, pre-set holding time 72 hrs, sample broke after 1.08 minutes).

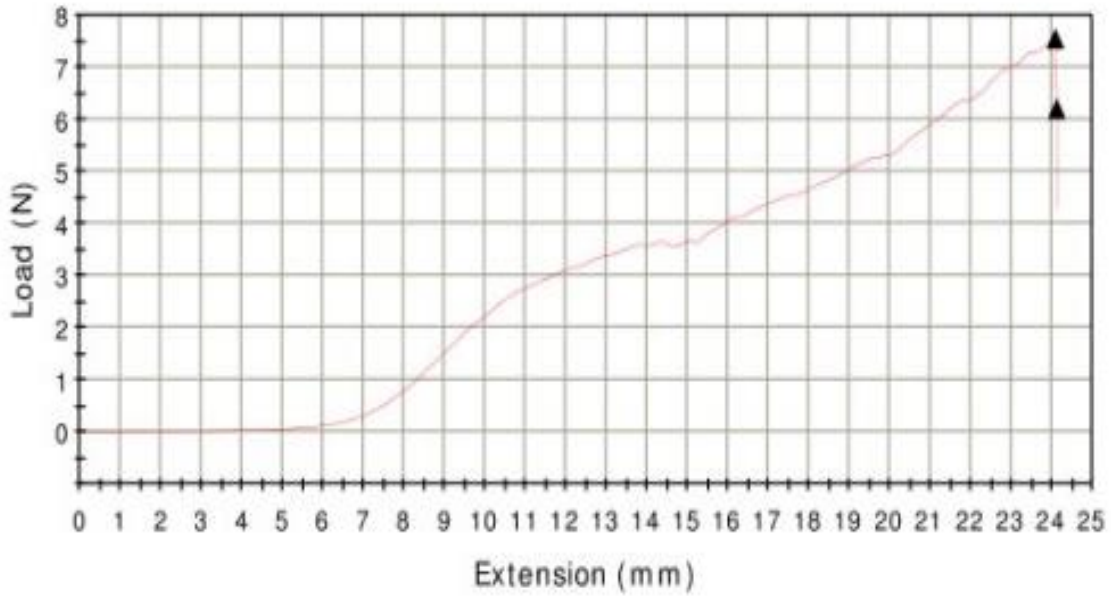

Figure 3.12. Sample A3-3 (control sample).

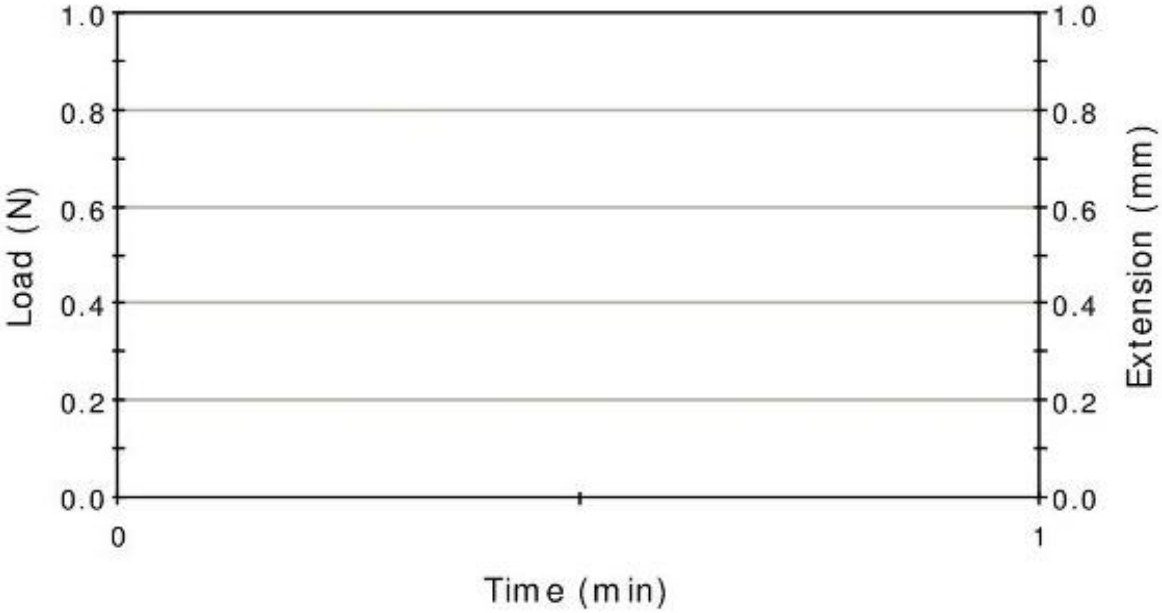

Figure 3.13. Sample A3-4 (medium- water, 80% fractional load, pre-set holding time 72 hrs, no breakage -computer froze).

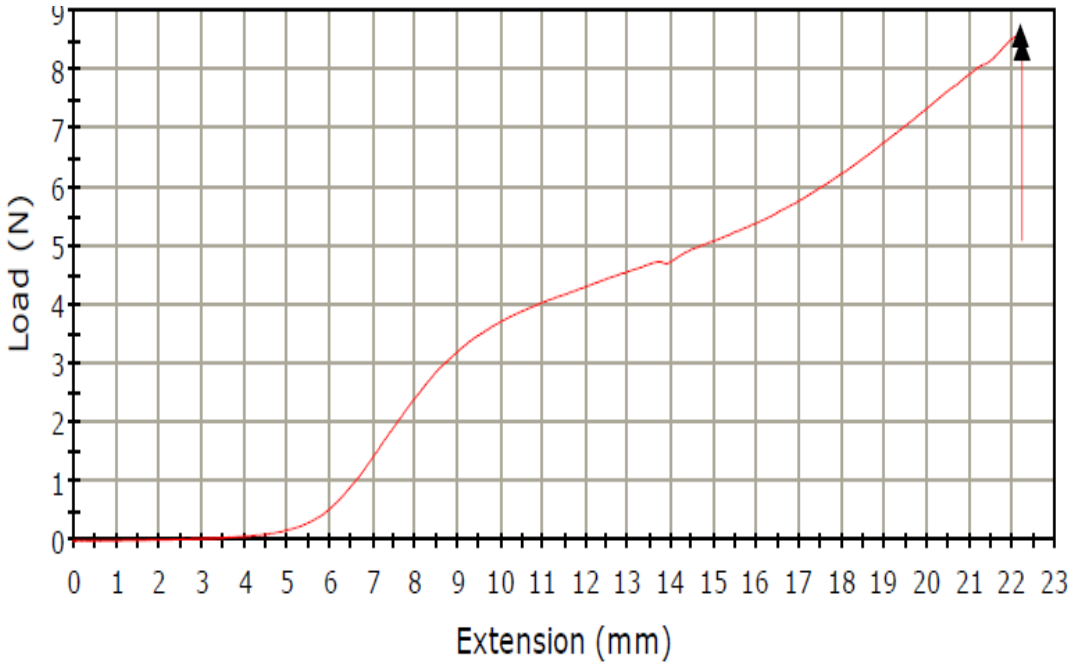

Figure 3.14. Sample A4-1 (control sample).

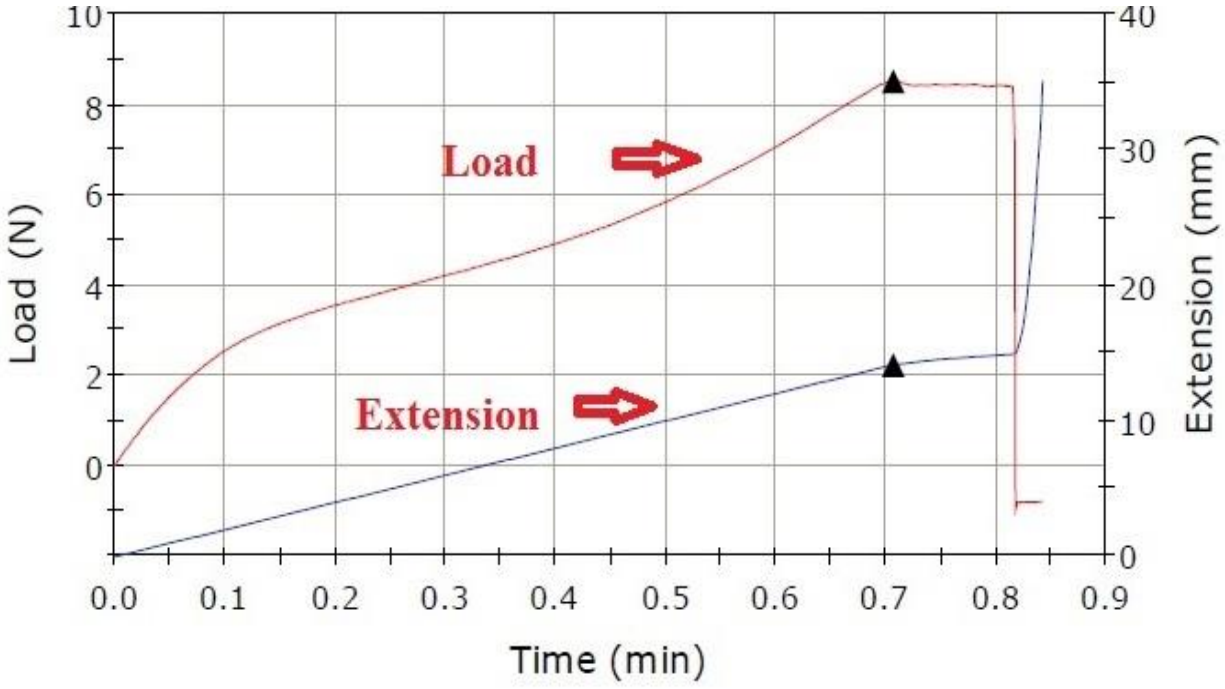

Figure 3.15. Sample A4-2 (blank, 98% fractional load, pre-set holding time 1hr, sample broke after 0.84 minute).

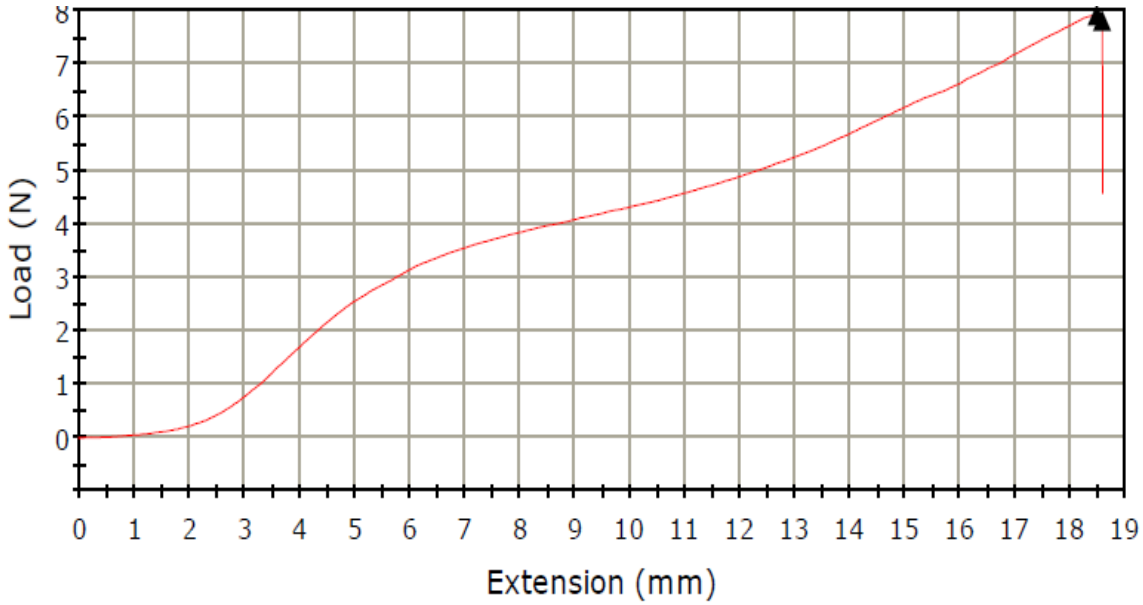

Figure 3.16. Sample A4-3 (control sample).

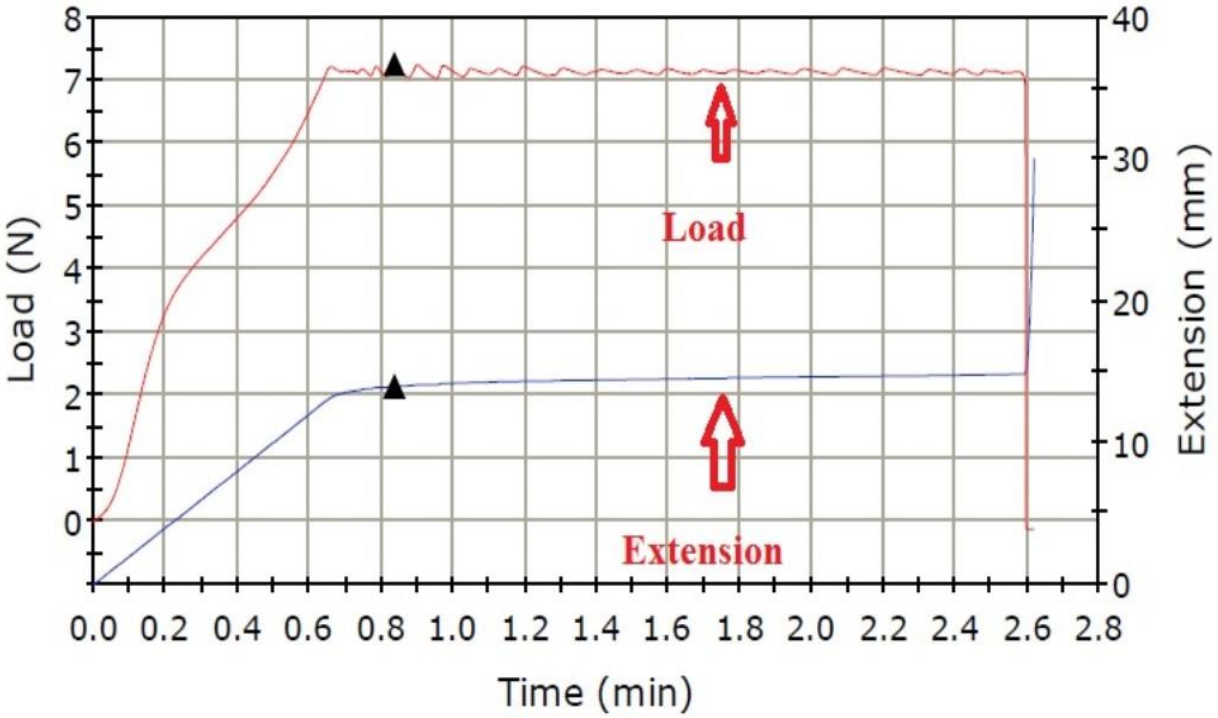

Figure 3.17. Sample A4-4 (blank, 90% fractional load, pre-set holding time 1 hr but sample broke after 2.62 minute).

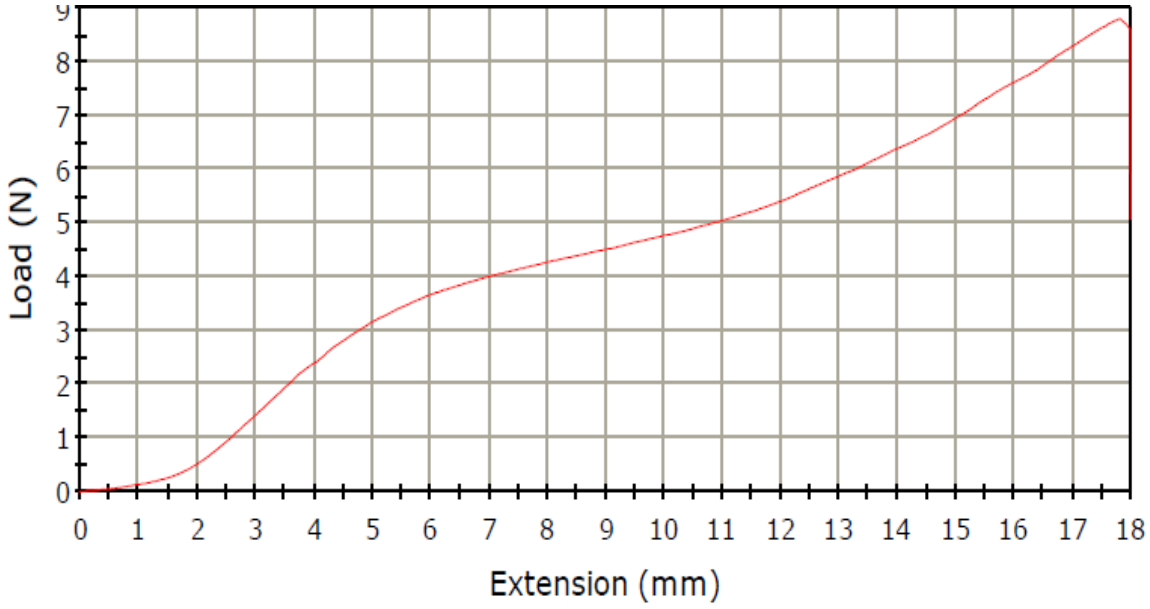

Figure 3.18. Sample A5-1 (control sample).

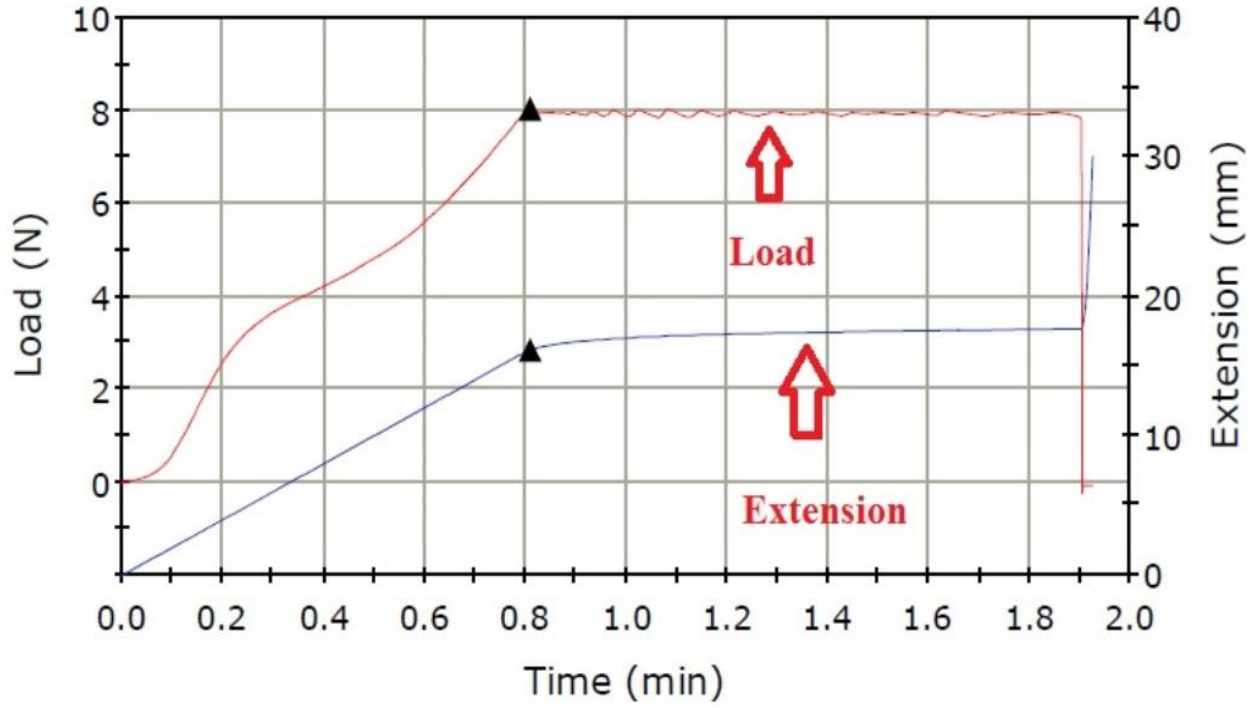

Figure 3.19. Sample A5-2 (blank, 90% fractional load, pre-set holding time 1 hr, sample broke after 1.92 minute).

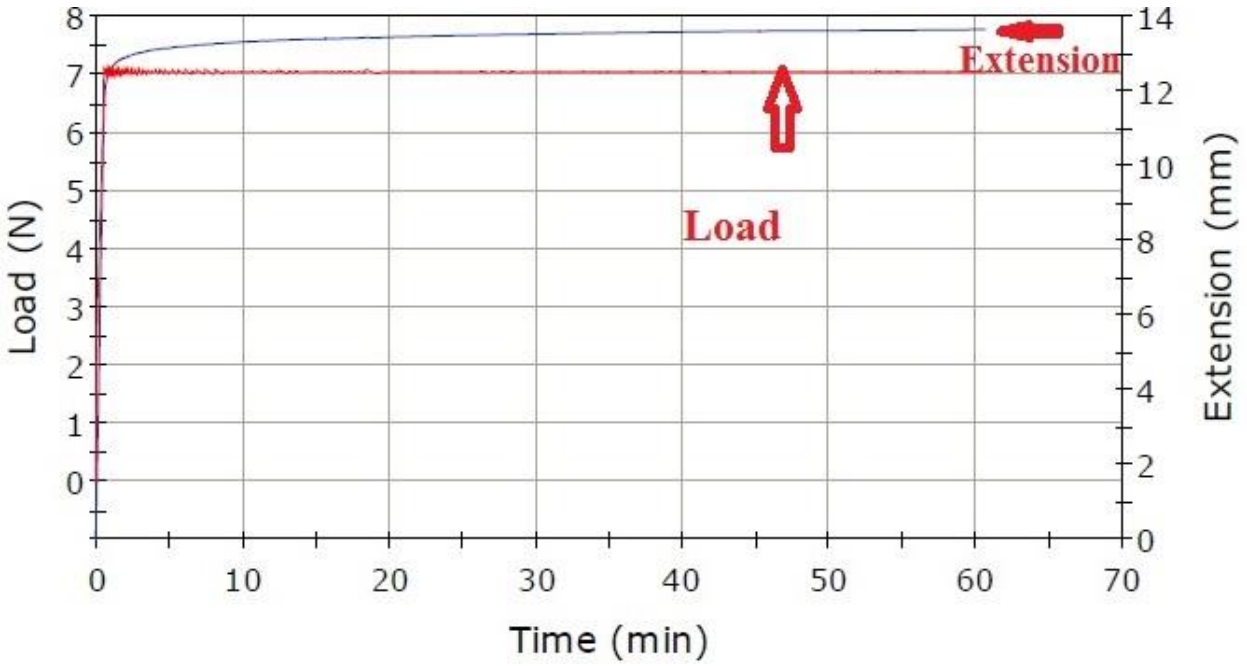

Figure 3.20. Sample A5-3 (blank, 80% fractional load, pre-set holding time 1hr, no breakage).

3.2.2 Irregularities in Load-Extension Curve

The load-extension curves of the control polyester yarn samples (with no holding load and time) is the gradual increase in extension (X-axis) under a gradually increase load [Y-axis] (*Figures 3.1, 3.4, 3.10, 3.12, 3.14, 3.16 and 3.18*). It can be seen from the load-extension curves of the control samples that all yarn samples broke sharply and no multiple breakage points can be seen. The shapes of these load-elongation curves are similar to standard curves for staple polyester fibre as reported by Adanur (1995). The initial 'flat line' in the load-extension curves between zero to ≈5 mm extension is due to the yarn slippage.

Two components of the load-extension curve are shown for samples with holding and time. One component is load-time curve and another one is extension-time curve. For samples that did not break during the holding time under different holding holds (60%, 70% and 80% holding loads), both load-time and extension-time curves are steady until the completion of the holding time after reaching the holding load and corresponding extension *(Figures 3.5, 3.6, 3.7, 3.8, 3.9 and 3.20*). No load-extension graph was obtained for the test when the computer 'froze'.

For samples that broke at different fractional loads *(Figures 3.2, 3.3, 3.11, 3.15, 3.17 and 3.19*), both load-time and extension-time curves behave differently. Further, the shapes of the curves are different. These different behaviours are: wider gap between these two graphs (*Figures 3.2, 3.15, 3.17 and 3.19*), multiple breaking points (*Figure 3.11*), multiple cross-over between load-time and extension-time curve (*Figure 3.11*), and wavy load-time curves (*Figures 3.2 and 3.17*).

3.3 Yarn Irregularity

Since the yarn breakage occurred at different breaking loads both for virgin samples and those with pre-set holding loads (for example, 80% holding load samples) as well as polyester grafts in vivo, it was suspected that the variation in breaking loads might have originated from the virgin polyester samples. Accordingly, the variation in yarn diameter was calculated (shown in *Figures 3.21 and 3.22)*. These two figures were taken from two different places along the same single yarn using Bioquant Life Science Image Analysis System (Section 2.5). Along the length of the yarn, the largest diameter measured was 572.14 µm and the minimum diameter 319.3 µm (*Figure 3.21*). In another location of this yarn, the maximum and minimum diameters were found to be 584.24 µm and 426.46 µm respectively (*Figure 3.22*). The average variation was 56.73% and 31.2%, calculated using the mean value for thick and thin places.

.

Figure 3.21. Bioquant picture of virgin polyester (maximum diameter: 572.14 µm, minimum: 319.3 µm).

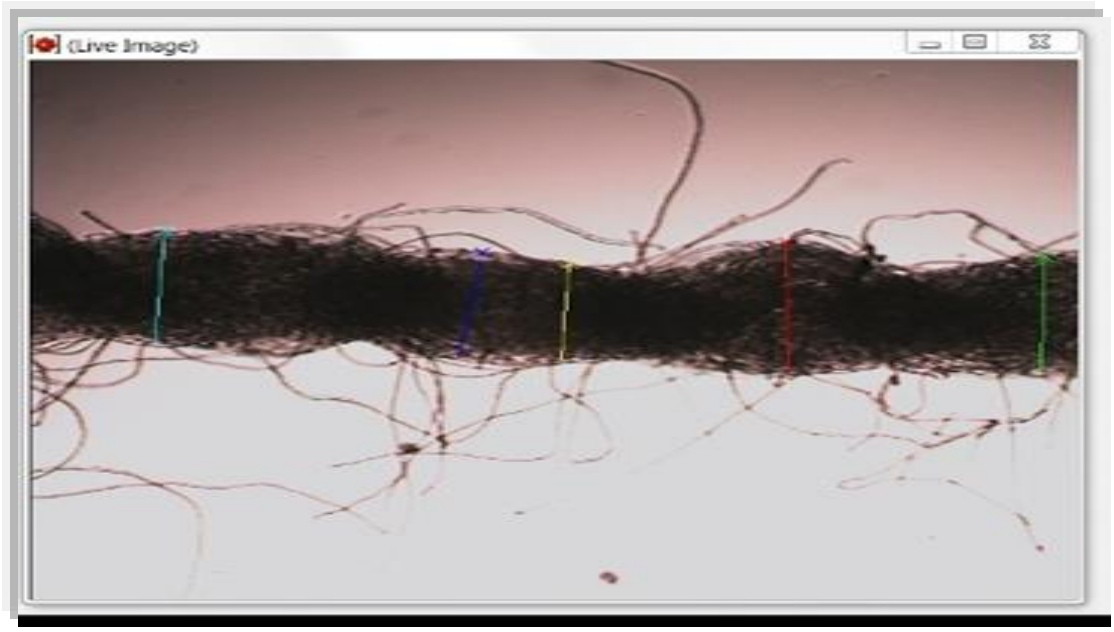

Figure 3.22. Bioquant picture of virgin polyester (maximum diameter: 584.24 µm, minimum: 426.46 µm).

3.4 Fracture Mechanisms

The fracture behaviour of the yarn is shown in *Figures 3.23 - 3.26*. During yarn breakage, it was found that no fibre breakage occurred. The fibres within the yarn, which are bound by twisting, pulled out from the yarn core as a result of tension load and split into two separate yarns (*Figure 3.26*). During the break, the yarn lost twists per inch and the fibres lost cohesion (*Figure 3.25*). This loss of cohesive force among the fibres was responsible for yarn breakage.

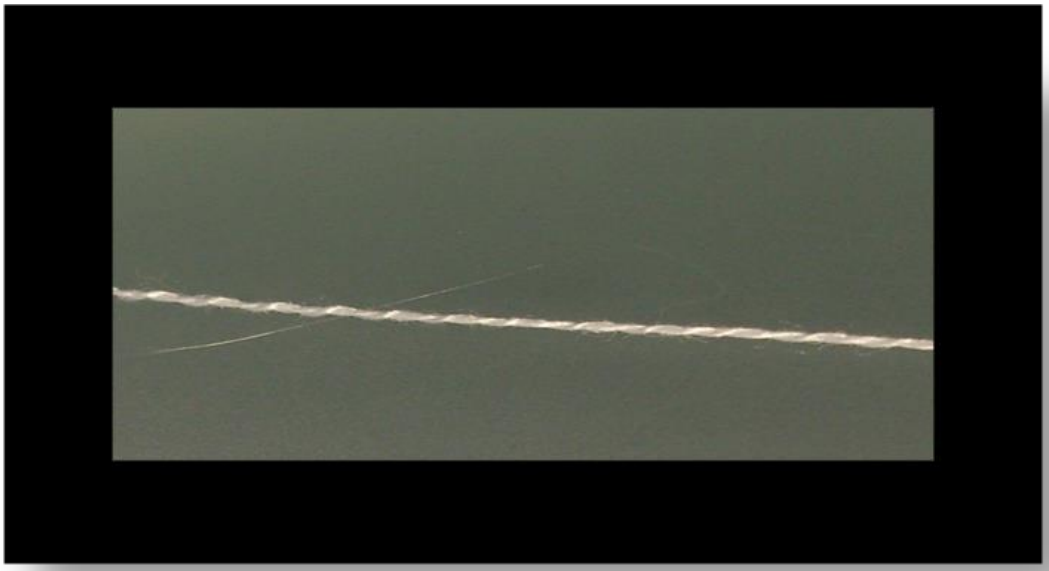

Figure 3.23. Original yarn (without broken ends).

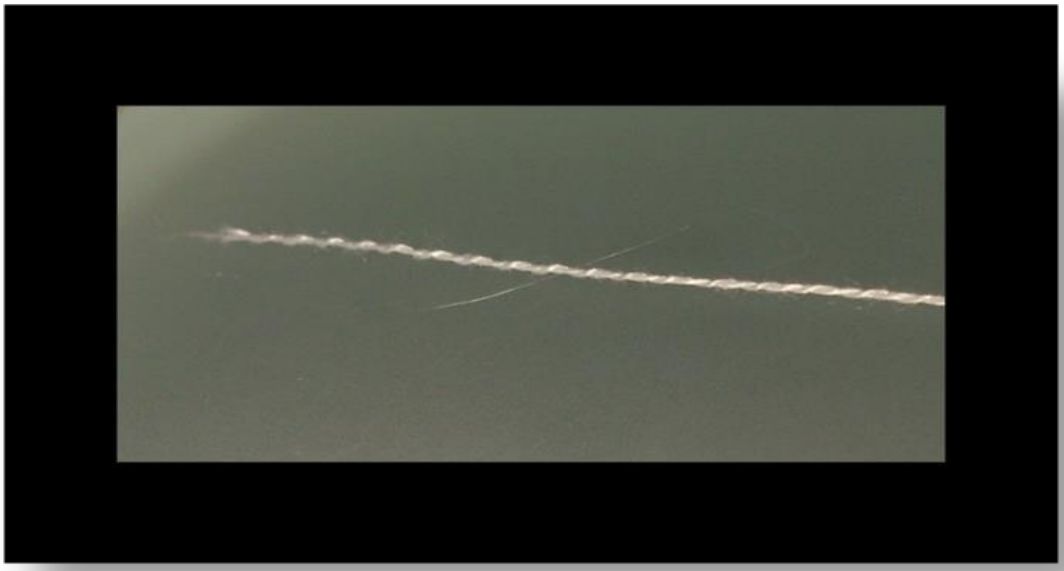

Figure 3.24. Dacron sample A2-1 (after breakage).

Figure 3.25. Dacron sample A2-1 (twist appearance - after breakage).

Figure 3.26. Dacron sample A2-1 (end point of break).

3.5 Conclusions

The current study shows that the variation in breaking load for the virgin polyester was very high. No fibre breakage occurred within the holding period when the holding load was 60% and 70% of the original breaking load. However, variation in breaking time was observed when the holding load was 80%. When the holding load was above 90% of original breaking load, fibre breakage occurred within 3 minutes. The extension at break also varies widely. It was found that the variations in mechanical properties were due to the thick and thin places in the virgin polyester yarns.

No fibre breakage occurred during yarn break. The yarn breakage occurred due to the fibres slipping away from each other within the yarn core due to the loss of the cohesive forces which exerted using binding force. Since *in vivo* polyester grafts have failed at different times resulting in numerous human deaths, the preliminary study concluded that these failures occurred due to the differential work of rupture (breaking load and extension at break) of polyester.

The preliminary study was conducted in water and alkali (pH=12.6) at 37°C at different pre-set holding loads. The experimental temperature was similar to physiological temperature; however, the pre-set load was much higher than the physiological load. Further, the fabric used was apparel grade which may not behave similar to the actual vascular graft material.

Chapter 4 Variation in Vascular Graft Polyester Fabric

4.0 Introduction

In this chapter, Double Velour Polyester Vascular Graft Knitted Fabric (***DVPVGKF***) is used to understand the fabric irregularity. This fabric is used to make vascular graft in tubular form as shown in *Figure 1.1* (Chapter 1, Section 1.1).

4.1 Results and Discussion

To understand the variability in polyester materials, a regular grade polyester was used first (Chapter 3), and vascular graft fabric (Virgin Double Velour Polyester Knitted Fabric – ***DVPVGKF*** -size-6″x6″, lot- HUWJ1970 from Bard group) was used in the second stage. Yarn diameter, filament count (tex), filament diameter, fabric thickness, fabric breaking load and breaking extension at different holding loads and times, tearing strength of virgin and hydrolyzed samples were measured to determine the irregularity in the vascular graft fabric. Probability analysis was conducted to determine the percentage of samples lying outside of the mean strength value.

Ideally, vascular graft polyester fabric should be regular as it is produced using improved process parameters (heat setting, intrinsic viscosity, godet rollers) compared to regular grade polyester (Falkai, 1996). It should have greater flexibility and ability to resist physiological pressure, sufficient amount of tensile and shear strength (to resist fraying), and sufficient circumferential strength to withstand arterial pressure for a longer period of time than the regular grade polyesters (Zeronian & Collins, 1988; Hearle, 1970; Ward, Cansfield, & Carr, 1993).

A few works that investigated failure of PET grafts, both in vivo and in vitro, found surface cracks or rupture (*Figure 1.8 and 1.9*) due to physiological stress and fluids (Wilson, Krug,

Muller, & Wilson, 1997). However, no work could be found that studied the textile fundamentals including yarn irregularities and unevenness that might contribute to the premature rupture of prosthetic grafts. Therefore, the root causes of surface cracks that resulted in graft failures are unknown. For a textile yarn, the diameter should be even throughout the yarn length. Further, twist is inserted to increase the yarn strength and twists tend to migrate to thinner sections of yarn leaving thicker sections with less twist per unit length. In general, low twist yarn will be weaker than high twisted yarn. Therefore, yarn irregularities in both thin and thick places contribute to lower strength and hence strength variation. This area of lower strength yarn will make the graft weak, and as a result the yarn will likely break or degrade faster than at other areas. In the following sections, yarn and fabric irregularities and their causes will be discussed.

4.2 Thickness variation

Thickness is an important physical property that influences the performance of fabric. Thickness is directly related to the yarn diameter that is used to make fabric. Vascular graft yarns should have a minimum variation in thickness to ensure uniform strength throughout the graft. Thickness was measured from 10 different randomly chosen spots in two different double velour polyester fabric samples according to the method described in Section 2.4.2. The thickness value for each of the 10 locations and average thickness values with standard deviation for Virgin Double Velour Polyester Knitted Fabric (***DVPVGKF***) 1 and 2 is given in Table 4.1. It can be seen from this table that the thickness value for ***DVPVGKF* # 1** lies between 1.12 mm and 1.37 mm with an average of 1.24± 0.09. For ***DVPVGKF* # 2**, the value lies between 0.98 mm and 1.19 mm with an average thickness value of 1.11±0.07 mm. These irregularities in fabric thickness are due to the irregularities present in the yarn itself which are caused by the uneven relative

displacement of fibres along the length of yarn during manufacturing, for example in drafting operation (Sen, 1950).

Table 4.1

*Thickness of **DVPVGKF # 1** and **2**, IQR data*

# of Location (*n*)	**Thickness (mm)**			
	***DVPVGKF* # 1**	Outlier Data One-and-a-half IQR's	***DVPVGKF* # 2**	Outlier Data One-and-a-half IQR's
1	1.27	None	1.14	None
2	1.37		1.19	
3	1.37		1.12	
4	1.30		1.12	
5	1.12		1.17	
6	1.14		1.14	
7	1.17		1.02	
8	1.30		1.07	
9	1.19		1.09	
10	1.17		0.98	
Mean ($\bar{X}$)	1.24		1.11	
*S.D.	0.09		0.07	
t value	3.77			
Df	18			
$t_{0.05}$ from t-distribution table (Appendix B, Table 1)	2.10			

*Standard Deviation

4.2.1 Calculation of Outliers for Thickness Values

It seems that there may be a significant different in thickness between the vascular graft fabric samples, which was not expected since these graft fabrics were made using high tenacity medical grade yarn. It was suspected that the variations in the thickness data might have come from

experimental procedures. Therefore, before attempting a test of statistical significance, a statistical test was conducted to determine the outlier data in each data set.

In order to find the variation between the individual data within each fabric sample, lower inner fence and upper inner fence were calculated for both ***DVPVGKF* # 1** and **2** (Equations I, II, III and IV) to check if any outlier was present. The lower inner fence and upper inner fence data were 0.912 (Equation I) and 1.568 (Equation II) respectively for ***DVPVGKF*** # **1**, and 0.912 (Equation III) and 1.296 (Equation IV) for ***DVPVGKF* # 2**. It can be seen from these four equations (Equations I, II, III and IV) that no outlier data was present in either of these samples to the points that are beyond the quartiles by one-and-a-half IQR's (Interquartile range) as shown in Table 4.1.

***DVPVGKF* # 1:**

Median, Q = (1.19+1.27)/2 = 1.23

Lower Quartile, Q1 = (1.12+1.14+1.17+1.17+1.19)/5 = 1.158

Upper Quartile, Q3 = (1.27+1.30+1.30+1.37+1.37)/5 = 1.322

Interquartile Range, IQR = Q3 – Q1= 1.322- 1.158 = 0.164

Lower Inner fence = Q1-(1.5x IQR) = 1.158-(1.5 x 0.164) =0.912 …… Equation I

Upper Inner fence =Q3+ (1.5x IQR) = 1.322+ (1.5 x 0.164) = 1.568 …… Equation II

***DVPVGKF* # 2:**

Median, Q = (1.12+1.12)/2 = 1.12

Lower Quartile, Q1 = (0.98+1.02+1.07+1.09+1.12)/5 = 1.056

Upper Quartile, Q3 = (1.12+1.14+1.14+1.17+1.19)/5 = 1.152

Interquartile Range, IQR = Q3 – Q1= 1.152- 1.056 = 0.096

Lower Inner fence = Q1-(1.5x IQR) = 1.056-(1.5 x 0.096) =0.912 …… Equation III

Upper Inner fence =Q3+ (1.5x IQR) = 1.152+ (1.5 x 0.096) = 1.296 …… …. Equation IV

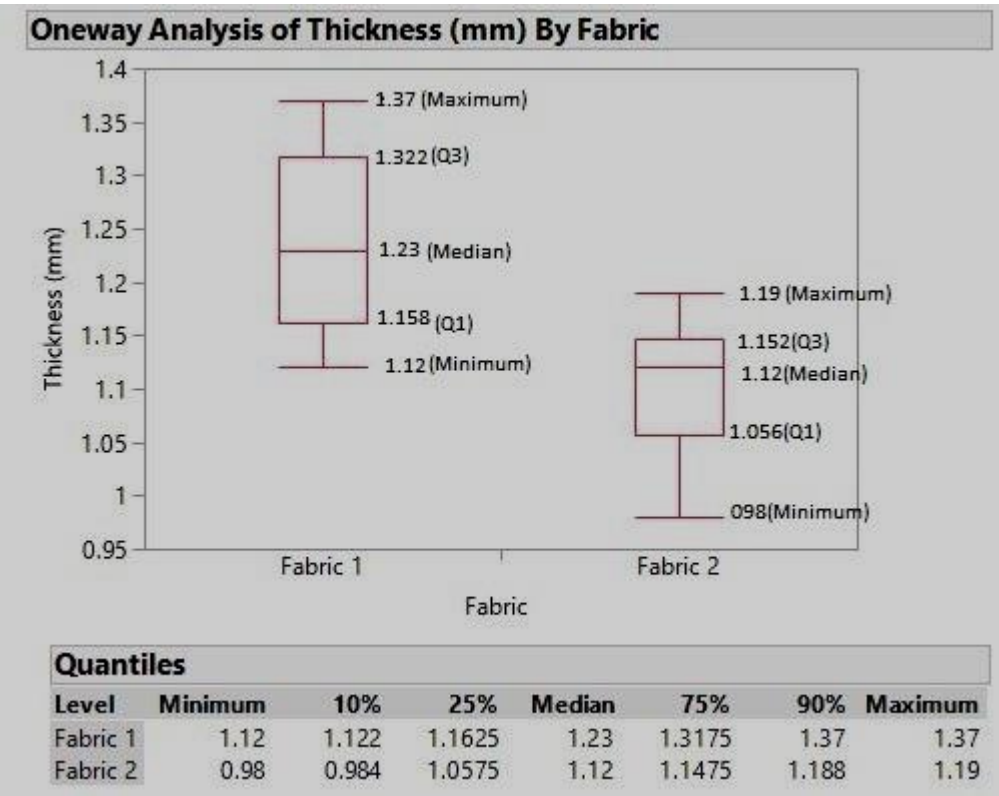

Quantiles

Level	Minimum	10%	25%	Median	75%	90%	Maximum
Fabric 1	1.12	1.122	1.1625	1.23	1.3175	1.37	1.37
Fabric 2	0.98	0.984	1.0575	1.12	1.1475	1.188	1.19

Figure 4.1. Side-by-side boxplot of thickness of ***DVPVGKF* #1** and **# 2.**

Side-by-side Box plot pictures for the thickness data set are shown in *Figure 4.1* for ***DVPVGKF* # 1** (left) and ***DVPVGKF* # 2** (right). Minimum, first quartile Q1, median, third quartile Q3 and maximum data values are 1.12, 1.158, 1.23, 1.322 and 1.37 respectively for ***DVPVGKF* # 1**. Minimum, first quartile Q1, median, third quartile Q3 and maximum data values are 0.98, 1.056, 1.12, 1.152 and 1.19 respectively for ***DVPVGKF* # 2**. It was found that the distribution of thickness data shape in Fabric 1 is slightly skewed to the right as the lower whisker (1.158-1.12=0.038) is smaller than upper whisker (1.37-1.322 = 0.048) and in ***DVPVGKF* # 2**, the distribution is skewed to the left as lower whisker (1.056-0.98=0.076) is bigger than the upper

whisker (1.19-1.152 = 0.038). The minimum thickness value of ***DVPVGKF* # 1** and median thickness data of ***DVPVGKF* # 2** is the same (1.12) which proves that most of the data in ***DVPVGKF* # 2** are smaller than ***DVPVGKF* # 1** and the thickness of the two fabrics is different.

4.2.2 Calculation of Significant Test between the Fabric Samples (*DVPVGKF* # 1 and *DVPVGKF* # 2)

In order to find out the difference between the average thicknesses of these two vascular graft fabric samples, significant test was conducted which is given below in Equations V and VI.

$$S = \sqrt{\left[\frac{(n_1 - 1)\mathrm{SD}_1{}^2 + (n_2 - 1)\mathrm{SD}_2{}^2}{n_1 + n_2 - 2}\right]}$$

…….. Equation V

$$S = \sqrt{\frac{(10 - 1) \times .09^2 + (10 - 1) \times .07^2}{10 + 10 - 2}}$$

= 0.0806

Where *S* is the pooled estimate of the population standard deviation (SD) and n_1 and n_2 are the number of locations in ***DVPVGKF* # 1** and ***DVPVGKF* # 2** respectively. SD_1^2 and SD_2^2 denote standard deviation for ***DVPVGKF* # 1** and ***DVPVGKF* # 2** respectively**.**

$$t = \frac{[\text{Mean of } \boldsymbol{DVPVGKF}\#1 - \text{Mean of } \boldsymbol{DVPVGKF}\#\ 2]}{S\sqrt{(\frac{1}{n_1} + \frac{1}{n_2})}}$$

…… .. Equation VI

$$t = \frac{[1.24 - 1.104]}{.0806\sqrt{\left(\frac{1}{10} + \frac{1}{10}\right)}}$$

= 3.77

The *t* value ($t_{0.05)}$ calculated in Equation VI was found to be $t_{0.05}$ = 3.77. The $t_{0.05}$ value at 5% significant level is 2.101 (Appendix B, Table 1), which is lower than the calculated value; therefore, it can be concluded that the difference in thickness between the two vascular graft fabric samples is significant at 5% significance level.

4.3 Variation in Yarn Linear Density (Tex)

To determine the sources of fabric thickness variation, yarn linear density (tex: defined as the weight of 1000 meter of yarn in grams), was calculated from diameter, as it is known that fabric thickness is directly related to yarn linear density and weight per unit length (Chattopadhyay, 2010). In this current study, the vascular graft fabric (***DVPVGKF***) used is manufactured from multifilament yarn, which means one yarn contains numerous single filament yarns. The number of filaments in a multifilament yarn depends on the end use of the yarn. For example, about 180 to 200 individual filament yarns are used to make a high tenacity multifilament yarn for geotextile and industrial applications (Rahman, 2006); whereas, for apparel applications, the number of filament was reported to be between 30 to 40 (Collins, Zeronian, & Semmelmeyer, 1991).

For variation in yarn linear density measurement, two yarns (multifilament) were taken from one ***DVPVGKF*** sample: identified as Multifilament #1 and Multifilament #2. The total number of filaments in each multifilament yarn (Multifilament yarn # 1 and Multifilament yarn # 2) was counted visually using the 'live' picture from the Bioquant Analyzer monitor as shown in *Figures 4.2* and *4.3*. For diameter measurement, a single filament from each multifilament (#1 and #2) yarn was removed. The diameter was measured at eight different places along the length of the single filament as shown in *Figures 4.4* and *4.5*. The yarn tex for each single filament was calculated from the average diameter using the formula given in Equations VII and VIII (Section

4.3.1). The tex for each multifilament yarn was calculated by multiplying the single filament tex with the number of filaments in each multifilament yarn. For example, for Multifilament Yarn # 1, the total number of filaments was found to be 34. Therefore, in order to obtain the tex of Multifilament yarn #1, the single filament yarn tex (0.22), was multiplied by 34 to provide the tex value of 7.48 (Equation VIII). A similar procedure was applied to obtain the tex for Multifilament Yarn # 2, and was found to be 7.8. Table 4.2 contains the individual diameter data, average diameter with standard deviation, tex for single filament, number of filament yarns in multifilament yarns, and tex for Multifilament yarn # 1 and # 2. Table 4.2 also contains data for statistical significant tests, which will be discussed in the subsequent sections.

Figure 4.2. Number of filaments (= 34) in multifilament yarn # 1.

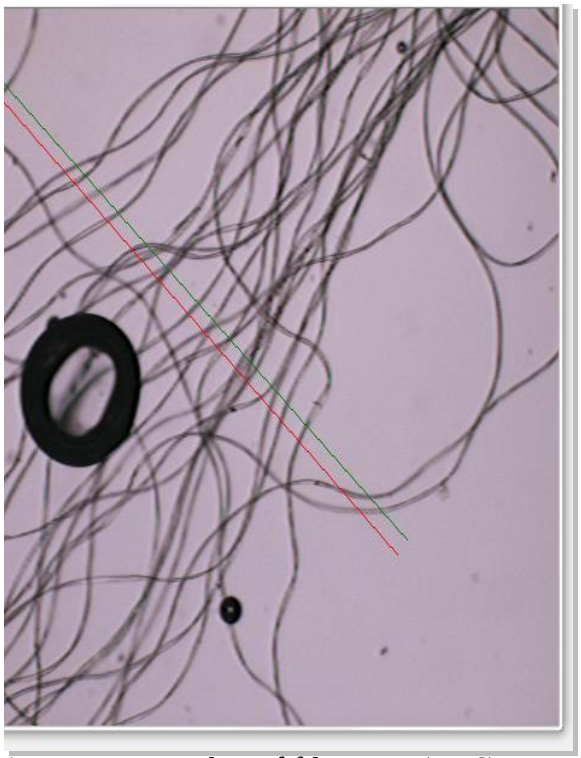

Figure 4.3. Number of filaments (= 26) in multifilament yarn# 2.

Figure 4.4. Single filament # 1 diameter measurements.

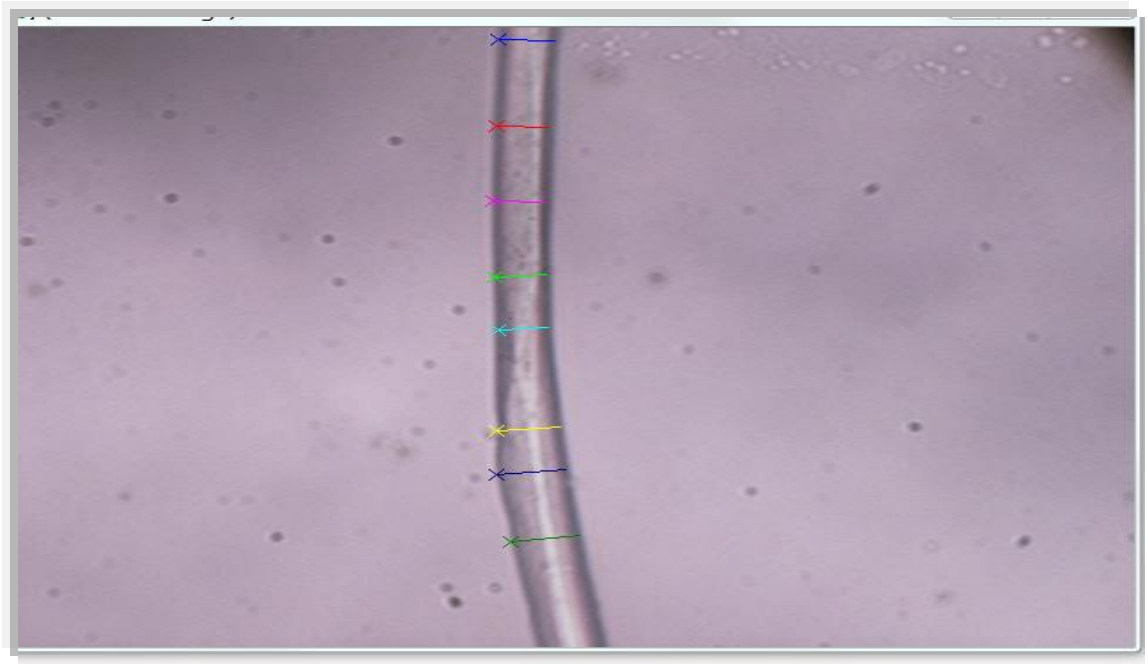

Figure 4.5. Single filament # 2 diameter measurements.

Table 4.2

Measurement of diameter of two different filament yarns (multifilament yarn #1 and # 2)

# of Location	Diameter for single Filament Yarn # 1 (µm)	Tex for single Filament Yarn # 1	Tex for Multifilament Yarn # 1	Diameter for single Filament Yarn # 2 (µm)	Tex for single Filament Yarn # 2	Tex for Multifilament Yarn # 2
1.	13.19	0.22	0.22 x [a]34 = 7.48	16.08	0.33	0.33 x [b]26 = 7.8
2.	13.85			14.62		
3.	14.53			15.11		
4.	14.94			14.64		
5.	12.97			14.16		
6.	14.32			18.08		
7.	13.58			19.58		
8.	14.90			19.63		
Mean	14.04			16.49		
Std Dev	0.75(s_1)			2.28 (s_2)		
$t_{0.05}$ value (calculated)		-2.9				
df		9				
$t_{0.05}$ from t-distribution table		2.262				

S_1 - Standard Deviation for yarn # 1, S_2– Standard Deviation for yarn # 2;
[a]# of filament = 34; [b]# of filament = 26

The diameter was measured from 8 different places using Bioquant live pictures (*Figures 4.4* and *4.5*). As seen in Table 4.2, a single filament diameter in Multifilament Yarn# 1 varies from 12.97 µm to 14.94 µm, with an average of 14.04±0.75 µm. In Multifilament Yarn# 2, the diameter varies from 14.16 µm to 19.63 µm, with an average of 16.49±2.28 µm. A statistical test was conducted (for Filament Yarn#1) to check if there were any outliers – i.e. any data outside of the

lower inner fence value of 11.83 [Lower Inner fence = Q1- (1.5 x IQR)] and upper inner fence value of 15.98 [Upper Inner fence = Q3 + (1.5 x IQR)]. It was found that all data were within the fences and no outlier was present. The detailed calculation is not shown for tex, however, a similar calculation is given for thickness data (Equations I to IV).

To check if the diameter data set of two different filament yarns (Filament Yarn #1 and #2) is significantly different, t value ($t_{0.05}$) at degree of freedom, df = 9 was calculated in Equation IX and X (Section 4.3.2) and was found to be $t_{0.05}$ = -2.9. Since $t_{0.05}$ value at 5% significant level is 2.262 (Appendix-B, Table 1) which is lower than the calculated value of -2.9 (calculation shown in equation X), it can be concluded that the difference in tex between the two vascular graft yarn samples is significant at 5% level (Table 4.2).

4.3.1 Tex Calculation of Yarn

Filament # 1:

Mean diameter (d) =14.04 μm = 0.00001404 meter = 0.001404 cm

Filament Count (tex) = 10^5 x (πd^2)/4 x ρ ……. Equation VII

= [10^5 x (3.14 x 0.001404^2)/4 x 1.39], here ρ (fibre density) = 1.39 g/cc

= 0.22

Yarn Tex for Multifilament Yarn # 1 was calculated by multiplying the count (tex) of each filament yarn by the total number of filament yarns.

Yarn Tex of Multifilament Yarn # 1 = Single Filament tex * Total Number of Filaments

…….. Equation VIII

=0.22 x 34 = 7.48 tex

Count of filament yarn # 2 was calculated as 7.8 tex using the same formula as Equations VII and VIII.

4.3.2 Calculation of Significance Test

Degree of freedom,

$$df = \frac{\left(\frac{s_1^2}{n_1} + \frac{s_2^2}{n_2}\right)^2}{\frac{1}{n_1 - 1}\left(\frac{s_1}{n_1}\right)^2 + \frac{1}{n_2 - 1}\left(\frac{s_2}{n_2}\right)^2} \quad \ldots\ldots \text{ Equation IX}$$

$$= \frac{\left(\frac{0.75^2}{8} + \frac{2.28^2}{8}\right)^2}{\frac{1}{8-1}\left(\frac{0.75^2}{8}\right)^2 + \frac{1}{8-1}\left(\frac{2.28^2}{8}\right)^2}$$

$= 9.0$

Where s_1 = standard deviation of Filament Yarn # 1 diameter, s_2 = standard deviation of Filament Yarn # 2 diameter; n_1 = number of locations in Filament Yarn # 1; n_2 = number of locations in Filament Yarn # 2; $\bar{x}_1$=mean diameter of Filament Yarn # 1 and $\bar{x}_2$ = mean diameter of Filament Yarn# 2.

$$t = \frac{\overline{x_1} - \overline{x_2}}{\sqrt{\frac{s_1^2}{n_1} + \frac{s_2^2}{n_2}}} \quad \ldots\ldots \text{ Equation X}$$

$$= \frac{14.04 - 16.49}{\sqrt{\frac{0.75^2}{8} + \frac{2.28^2}{8}}}$$

$= -2.9$

4.4 Fabric Breaking Load and Holding Load

Rupture of a fabric occurs when the applied force reaches fabric work of rupture which is approximately half of the product of breaking force and breaking extension. A good quality vascular graft should not rupture during the patient's life time. However, this has not been the case for polyester vascular grafts as shown in Table 1.3. In order to identify the premature rupture of graft fabric, breaking load and breaking extension of virgin Double Velour Polyester Vascular Graft Knitted Fabric (***DVPVGKF***) was measured using the method described in Section 2.4.3 and 2.4.4.

At first, the breaking load was determined for the virgin sample (***DVPVGKF***) and then different holding loads, for example, 80% of breaking load, were calculated based on the measured breaking load of the virgin sample. The sample was kept under holding conditions to examine if the samples could survive the pre-set duration. The breaking load data and breaking load under different holding conditions was then used to relate the material irregularities with in vivo premature rupture, which has occurred at different time intervals (Table 1.3).

Table 4.3 contains the breaking load (N), breaking extension (mm) and extension (%), ratio of breaking load to breaking extension, holding load, and holding time. Corresponding information is shown in Figures 4.6 – 4.11 for load-elongation curve, and Figures 4.12 – 4.17 for fabric swatches. The breaking pattern of fabric swatches (*Figures 4.12 – 4.17*) is discussed in Section 4.6. Table 4.3 shows that for virgin double velour polyester vascular graft knitted fabric sample (***DVPVGKF***), the breaking loads and extensions are 48.2 N, 28.84 mm or 13.545% for B1 (Load-elongation *Figure 4.6*); 49.7 N, 30.83 mm or 21.3% for B2 (Load-Elongation *Figure 4.7*); and 55.5 N, 41.69 mm or 64.13% for B3 (Load-Elongation *Figure 4.8*). The immediate

conclusion is that there is a difference in breaking load and extension (%) in virgin double velour polyester graft fabrics.

These three virgin samples also ruptured at different time periods (B1: 86.51 seconds, 92.48 seconds, and 125.17 seconds). Further, the ratio of breaking load to breaking extension of these three virgin samples are 1.67 (B1), 1.61 (B2) and 1.33 (B3) which means that the variation in breaking extension is larger than the variation in breaking load.

Since the variation in breaking load was high, it was suspected that these fabric samples might break at a lower holding load if the fabric were kept at a constant holding load for a pre-set time. The holding load was calculated based on the breaking load of the virgin samples. For example, the holding load for sample B4 (44.7 N) was 90% breaking load of sample B2, the breaking load of sample B2 was 49.7 N (Table 4.3). At this holding load of 44.7 N, the holding time was pre-set for one hour. At the 90% holding load, no breakage occurred for this sample (B4) for one hour holding time. The holding time was then increased to 24 hours for 90% holding sample (B5); however, fabric breakage occurred just after 2 hours. Since the fabric ruptured within a short period of time, the holding load was reduced to 80% (sample B6) and this sample did not break in 48 hours.

There was a problem associated with the holding load samples. Firstly, it was difficult to monitor the machine continuously, and secondly, the computer froze and no data was obtained for one holding load sample after 36 hours of holding (*Figure 4.11* and *Figure 4.17*). Therefore, holding load data was not used for further analysis. Only breaking load and breaking extension data were used for statistical analysis in the following section.

4.4.1 Probability Analysis: Calculation of Proportions of Samples Outside Range

It is very difficult to predict how long a vascular graft will last. Vascular graft manufacturers do not need to specify the expected life-time of their products, although according to Medical Device Regulations under Food and Drugs Act (Food and Drugs Act, Canada, 2017), the graft must be produced and meet quality management requirements of National Standard of Canada (CAN/CSA-ISO 13485:03: Medical devices – Quality management systems – Requirements for regulatory purposes.). It is worth mentioning here that this regulatory standard does not give any quality parameters. In literature, it is reported that graft failures have occurred right after implantation, or up to 10 years later (Edwards, 1978). Although modern vascular grafts similar to the one used in the current study are claimed to be manufactured using high quality materials and machinery (Section 1.3.4), the latest medical literature , reports that of the more than 400,000 prosthetic grafts performed in the USA each year, premature rupture accounted for almost 25% of graft implant failure in coronary bypass graft surgery within 12 to 18 months post-surgery mainly due to early thrombosis, intimal hyperplasia (IH) and compliance mismatch (Singh, Wong, and Wang, 2015). The probable causes of premature rupture were discussed in Table 1.3 (Section 1.4.1).

Table 4.3

Fractional load, holding load, breaking load, breaking time and extension of ***DVPVGKF***

Sample ID#	Holding Time (hr)	Holding Load (N)	Load at Break (N)	Extension at Yield (mm)	Extension (%)	Ratio of Breaking Load to Extension	Time to Break [d](sec)	Fabric Broken	Load-Elongation Curve Figure#	Fabric swatch Figure#
B1 (Control Sample)	N/A	N/A	48.2	28.84	13.54	1.67	86.51	[a]Yes	4.6	4.12
B2 (Control Sample)	N/A	N/A	49.7	30.83	21.3	1.61	92.48	[a]Yes	4.7	4.13
B3 (Control Sample)	N/A	N/A	55.5	41.69	64.13	1.33	125.17	[a]Yes	4.8	4.14
B4 (90% of B2)	1	44.7	N/A	27.81	9.49	N/A	61.39 min	[b]No	4.9	4.15
B5 (90% of B2)	24	44.7	45.8	33.52	31.97	1.61	129.25 min	[a]Yes	4.10	4.16
B6 (80% of B3)	48	44.4	N/A	47.34	86.38	N/A	48 hrs	[c]No	4.11	4.17

[a]:fabric broke; [b]fabric did not break; [c]fabric did not break; computer froze after 32hrs; [d]sec:second

It is noted that the tensile strength of high tenacity medical grade polyester is about 1090 MPa (Adanur, 1995). The maximum amount of force that blood puts on the wall of a blood vessel is about 16 kPa. There is a distinct disconnect between the maximum force and the tensile or rupture point of these products. Even though this maximum force is much less than the rupture point, premature rupture of these grafts still occurs. It can be implied that something in the manufacturing process (spinning, winding, warping, looming) and/or during usage (pressure, physiological fluid) creates a weak point (defect) that allows for such a low load to break a relatively strong material. This implication is also supported by the results of the significant variation in thickness (Section 4.2), significant variation in diameter/tex (Section 4.3), and variation fabric strength (Section 4.4) data in the studies.

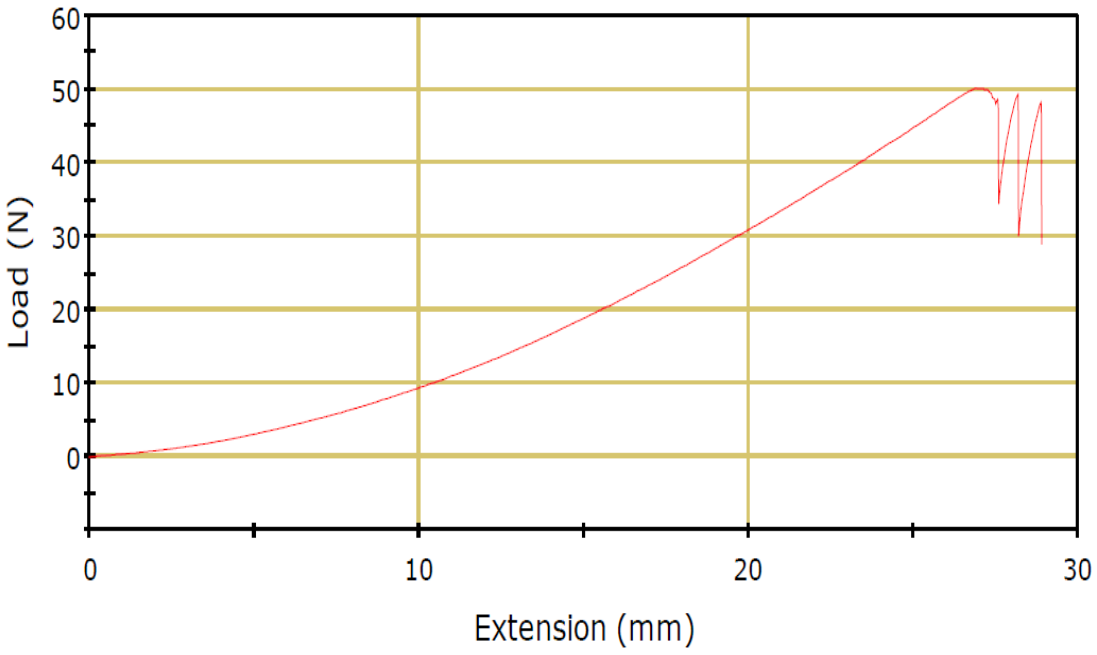

Figure 4.6. Sample# B1-control sample.

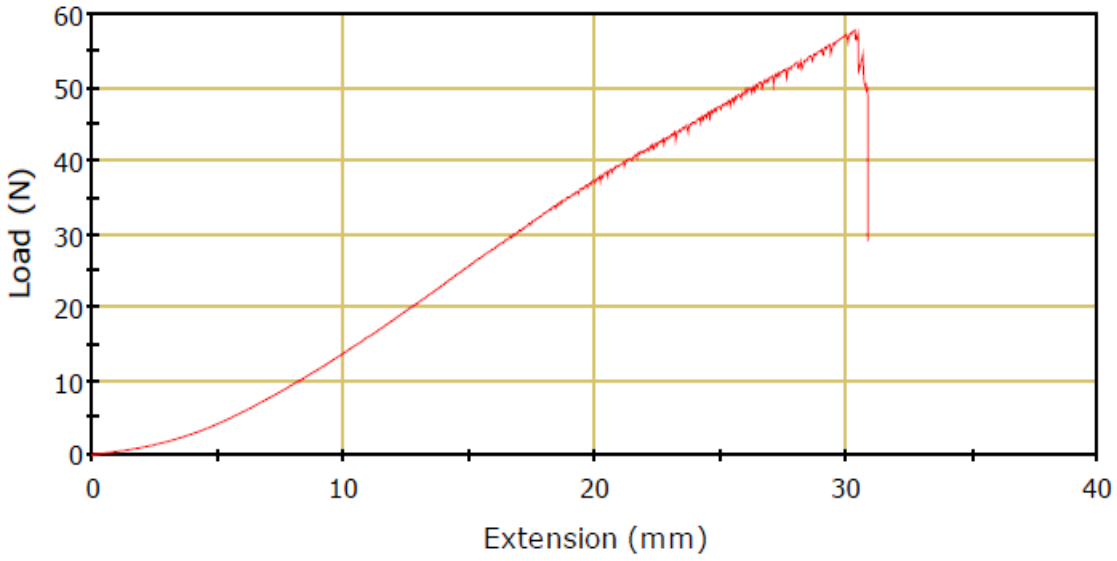

Figure 4.7. Sample# B2-control sample.

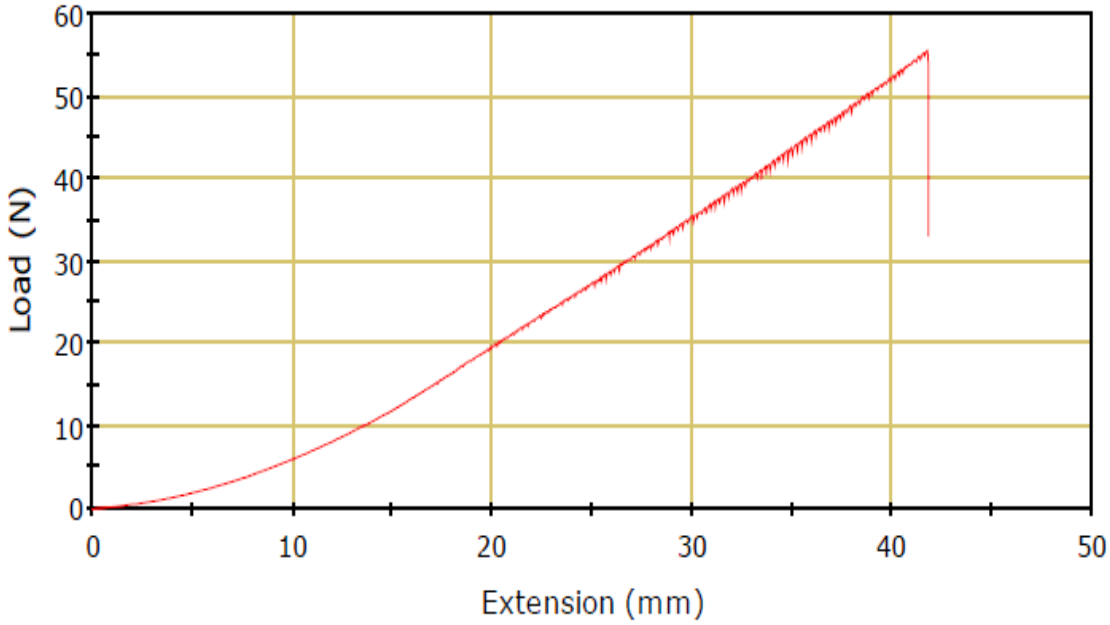

Figure 4.8. Sample# B3-control sample.

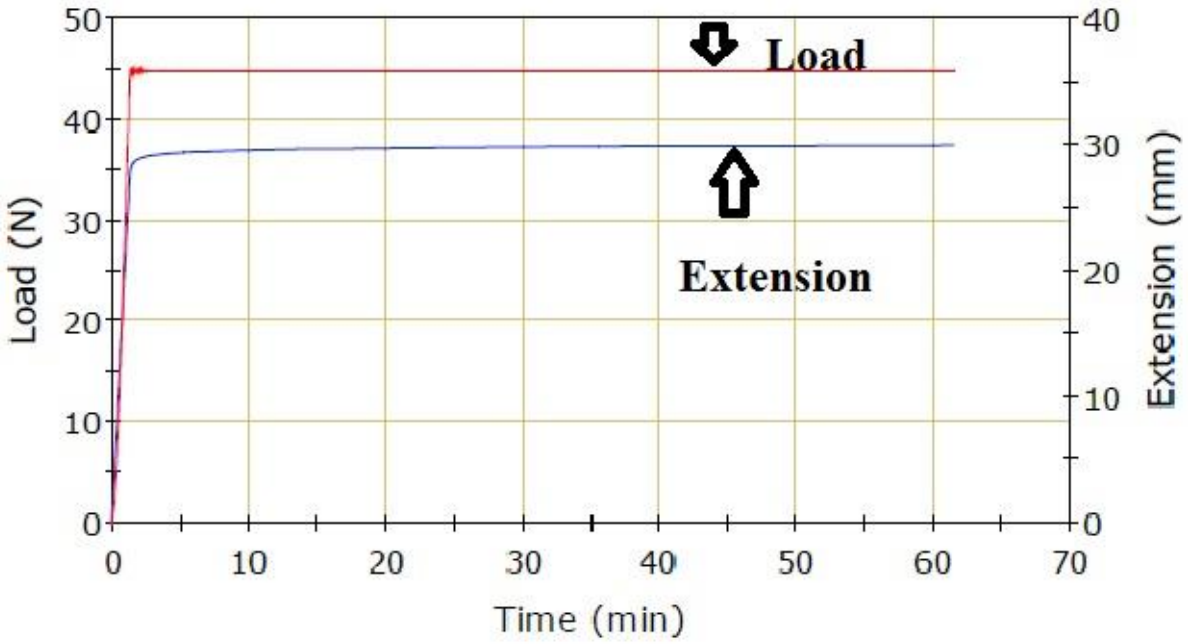

Figure 4.9. Sample# B4 (90% fractional load of sample B2, pre-set holding time 1hr, sample did not break).

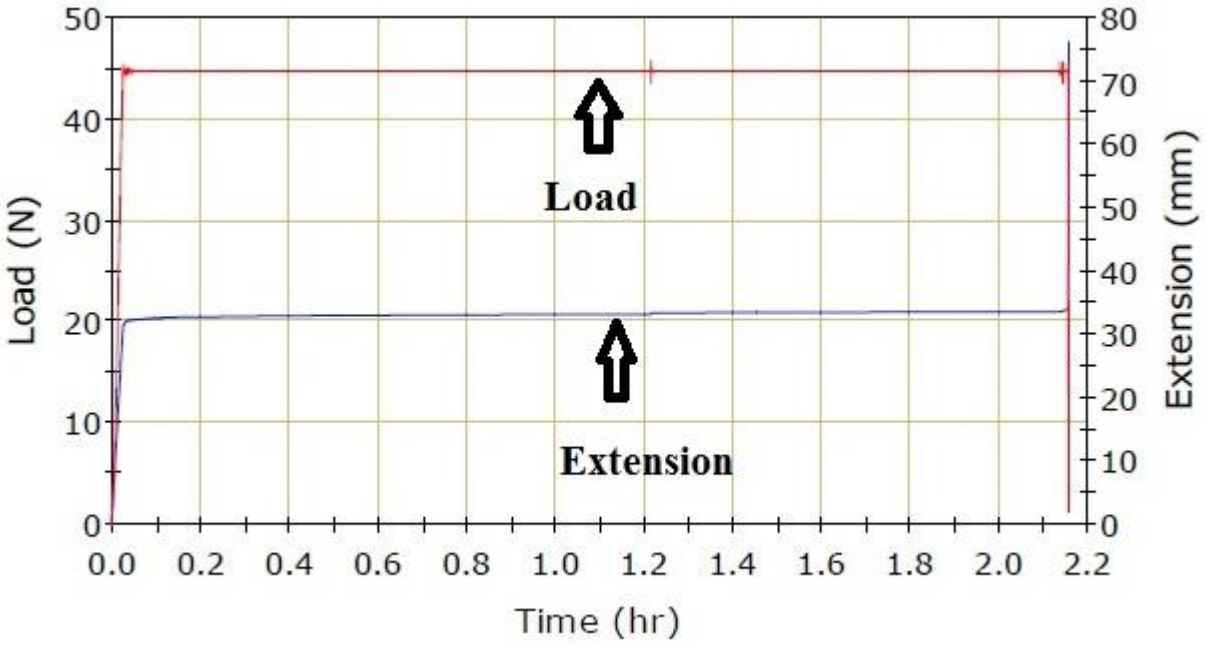

Figure 4.10. Sample # B5 (90% fractional load of sample B2, pre-set holding time 24hr, sample broke after 129.25 minutes).

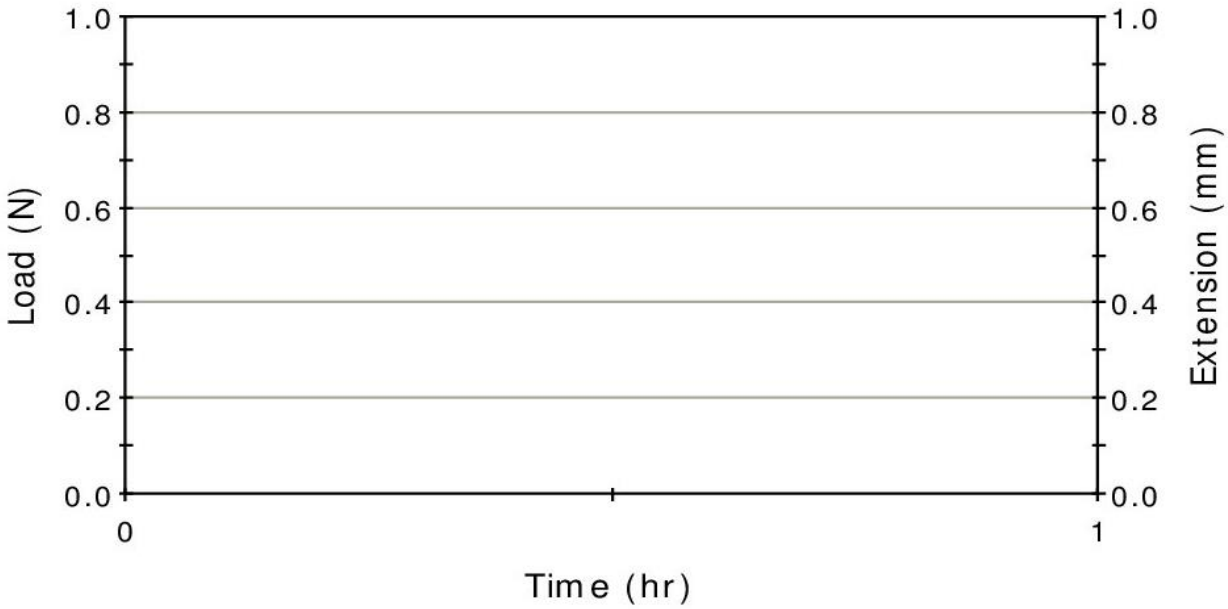

Figure 4.11. Sample # B6 (80% fractional load of sample B3, pre-set holding time 48hr, sample did not break. computer froze after 32 hr).

Figure 4.12. Sample # B1 (control sample).

Figure 4.13. Sample # B2 (control sample).

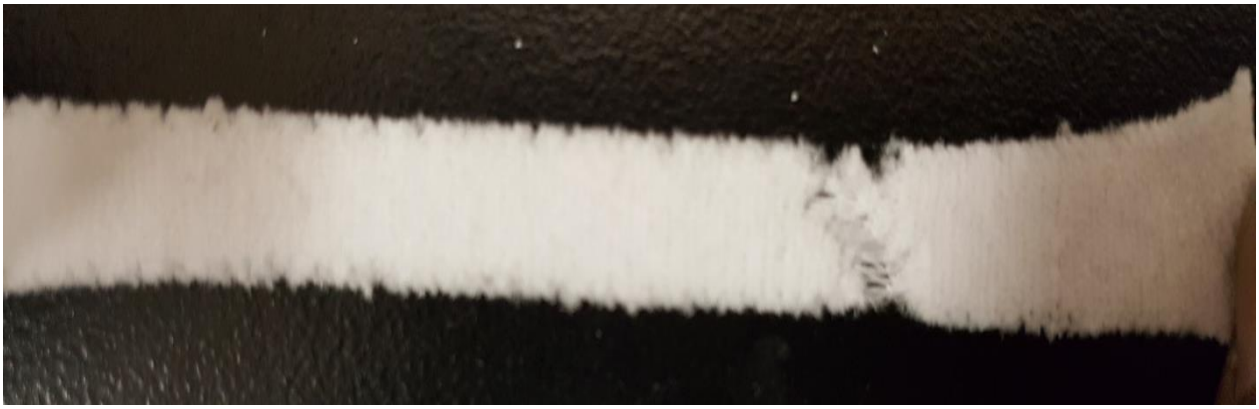

Figure 4.14. Sample # B3 (control sample).

Figure 4.15. Sample # B4 (90% of sample B2, holding time 1hr).

Figure 4.16. Sample # B5 (90% of sample B2, holding time - 24hrs, sample broke after 129 minutes).

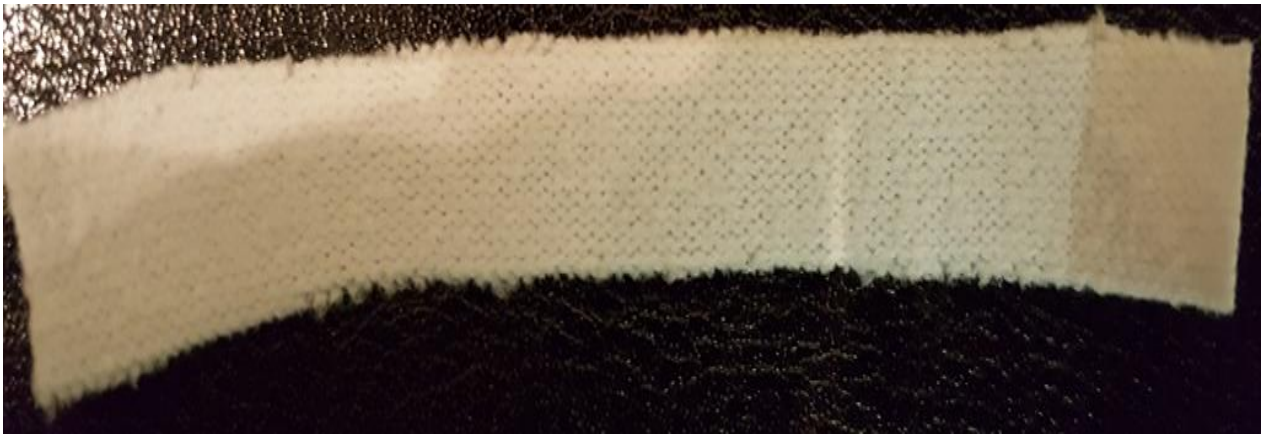

Figure 4.17. Sample # B6 (80% of sample B3, holding time - 48Hrs, did not break).

Figure 4.18. Close view of sample B2 in fabric analyzer.

4.4.2 Probability Calculation - Proportion of Virgin Double Velour Polyester Knitted Fabric (*DVPVGKF*) Breaking Load Lying Outside Mean

In order to check the significance of the mean value (49.8 N±4.09) breaking load (mean value shown in Table 4.4), analysis was conducted to determine the breaking load proportionally close to the mean. In this respect, the difference in breaking load of 15 N (Equation XI), 13 N (Equation XII), 10 N, 5 N and 2 N (calculation not shown) from the mean breaking load (49.8 N) were considered for comparison (Table 4.4) (Booth, 1968). It was found that the smaller the difference from the mean, the greater the chance of the value lying close to the mean. So for

example, in case of 15 N difference from the mean breaking load of 49.8 N, the range will be 34.8 N (49.8 N -15.0 N) to 64.8 N (49.8 N + 15.0 N) and the d/SD is 3.67 (Equation XI). According to the Normal Distribution Function table (Appendix C -Table 2), it can be noted that since 3.67>3.49 (Appendix C, Table 2), the probability of the breaking load lying at or above 34.8 N is more than 0.9998, which means all the data will lie inside the 49.8±15.0 N range. In other words, it can be stated that there is no probability of having any ***DVPVGKF*** with a breaking load of 34.8 N or less (49.8-15=34.8), or all ***DVPVGKF*** will have a breaking load of 34.8 N or more.

In the same manner, for 13 N differences from the mean breaking load of 49.8 N±4.09 means the theoretical range will be 36.8 N - 62.8 N. However, probability analysis using the standard deviation of mean shows that 0.14% (1.0 – 0.9993*2 = 0.0014*100) [Appendix C, Table 2] data for the d/SD = 3.18 value (Equation XII) would have breaking load between 36.8 N and 62.8 N. In other words it can be stated that 0.07% of data will have a breaking load value of at least 13 N differences from the mean and will lie between 34.8 N to 36.8 N. This corresponds to 280 graft failures (0.07*40,000/100) when the breaking load is 36.8 N or less. The number of ruptured prosthetic grafts (280) is far fewer than the 25% rupture of 400,000 implanted annually in the USA (Singh & Wang, 2015).

Expressing the difference d, of 15 N breaking load in terms of SD

d/SD = 15/4.09 =3.67 . …….. Equation XI

Expressing the difference d, of 13 N breaking load in terms of SD

d/SD = 13/4.09 =3.18 …… Equation XII

Table 4.4

Probability analysis of breaking load of ***DVPVGKF***

Property	Mean (N)	Range	Std Dev (SD)	Distance from Mean (d)				
				15 N	13 N	10 N	5 N	2N
[a]Breaking Load	49.8	9.62	4.09	[b]NA	0.14%	1.4%	22.2%	62.4%

[a]only those load when samples broke were considered
[b]all data lie within the mean

The question now arises is whether 36.8 N breaking load is weak enough to be ruptured *in vivo*. In order to answer this question, fabric strength in kPa is calculated from the breaking load, fabric thickness and fabric effective width as shown in Equation XIII.

$$Fabric\ strength = \frac{Breaking\ Load\ (N)}{[Fabric\ Width\ (m) x\ Fabric\ Thickness\ (m)} \quad \ldots\ldots \text{Equation XIII}$$

$$= \frac{36.8\ (N)}{0.0127\ m * 0.00117\ m}$$

$= 2476613.4\ N/m^2$

$= 2.48\ MPa = 2480\ kPa$

Where Breaking load = 49.8N, Width=0.5 inch =.0127m,

Thickness = avg. thickness of Fabric 1 and 2

= (1.24+1.104)mm/2 =1.172 mm = 0.00117 m

Fabric tenacity must be sufficient for a strong and long lasting medical grade graft as it is subjected to high arterial pressure under alkaline medium. In general, a person in good medical condition should have regular blood pressure of diastolic 80 mmHg~10.66 kPa and systolic 120 mmHg~15.99 kPa. But this blood pressure increases during physical exercise, especially running, and heavy lifting. The maximum blood pressure ever recorded was 370/360 mmHg which is equal to 49.3/47.99kPa (Narloch & Brandstater, 1995). Due to post implantation intimal

hyperplasia, arterial pressure could increase 140 fold in circumferential wall stress on the textile grafts compared to regular circumstances (Singh and Wang, 2015). So, post implantation, the pressure could be as much as 2200 kPa (16 kPa x 140 fold = 2200 kPa), which is still lower than 2480 kPa obtained for d= 13 N (Equation XIII) and 3350 kPa for d = 0. This arterial pressure of 2200 kPa is similar to the safety factor of most industrial applications i.e. 1.13 (2480 kPa/2200 kPa) and 1.5 (3350/2200=1.5). Therefore, even with the highest blood pressure due to intimal hyperplasia, the polyester graft should not rupture immediately or even between 6 to 18 months post implantation as reported in the literature. The problem might lie somewhere else. One possible source of early rupture could be hydrolysis, as polyester is susceptible to the alkaline nature of human blood (blood pH = 7.4) (Marieb, 2000) and/or irregularities (thin and thick places) and tears in the material (discussed in section 4.3) that is used to make vascular graft fabric. The effect of these two variables on yarn breaking strength is discussed in the following section 4.5.

4.4.3 Tearing Strength

Tearing strength was measured for virgin Double Velour Polyester Vascular Graft Knitted Fabric (***DVPVGKF***) (discussed in section 2.4.5.3). Tearing strength was measured using two different methods: (a) Tongue Tearing Method, and (b) Elmendorf Tearing Strength Method.

The results from tongue tearing method was analysed in details as this method seems similar to the in vivo exposure of vascular graft, while Elmendorf method was conducted to confirm the tearing results from the tongue tearing test. Further, tongue tearing was conducted for both virgin and hydrolysed samples, whereas Elmendorf test was conducted only on virgin graft sample.

4.4.3.1 Tearing Strength Virgin and Hydrolyzed Samples – Tongue Tearing Method

Hydrolysis procedure for the samples was described in section 2.4.5.1. The procedure was continued until a 25% weight loss was obtained. Theoretically, this 25% should provide a 25% loss in breaking load if no other external variables were involved (Rahman & East, 2009). Further, it is reported that up to 25% weight loss (%) was obtained at the rupture point of the polyester vascular graft (Chakfe et al., 2001).

The weight loss (%) of the hydrolyzed samples is given in Table 4.5. It can be seen from this table that the weight loss (%) increases with the increasing treatment time. Usually, if no other factors are involved, the weight loss (%) versus treatment time should be linear. However, the linear relationship has not been obtained in this study. This may be due to the presence of hydrophobic spin finishes and other finishing agents (for example, collagen) that are added during the filament manufacturing process as well as in ***DVPVGKF*** manufacturing which slowed down the reaction as the process continued (Rahman & East, 2009).

Table 4.5

Weight Loss (%) Data for Hydrolyzed ***DVPVGKF***

Sample ID	Concentration of NaOH (%)	Treatment Temperature (°C)	Treatment Time (Hour)	Weight loss (%)
Virgin Sample	N/A	NA	NA	N/A
H1 Sample	10.0	60	1	7.0
H2 Sample	10.0	60	2	16.5
H3 Sample	10.0	60	5	25.0

For the fabric tearing strength measurement, tongue tearing method ASTM D 2261 (Section 2.4.5.3) was followed (ASTM, 2013). This strength measurement method provides a breaking

strength of numerous individual multi-filament yarns while the yarns are in 'inter-looped' state instead of fabric strength as *in vivo* rupture investigation found individual broken polyester filaments in the ruptured graft fabric (Miyake, Sakagoshi, & Kitabayashi, 2016). Tongue tearing strength measurement method also produces load-elongation curves for numerous individual yarns in one curve as shown in *Figures 4.19, 4.20, 4.21, 4.22*. Each peak (upper or lower) represents one yarn breakage. The upper peak shows high breaking strength; whereas, lower peak shows lower breaking strength. The first few peaks were not considered as it takes time for the test to be stable as described in ASTM D 2261 (ASTM, 2013). The force recorded in a tear test is irregular, and as a consequence, an empirical method has been used to collect the 10 highest and 10 lowest peak data. In this study, the highest and lowest peak data was collected after 60 mm extension was obtained. For apparel application, average tearing strength is calculated using top five peaks. For the current study, analysing top 10 peaks and bottom ten peaks would enable to see the variation in the vascular graft samples since breakage of the weakest yarn would be catastrophic for the patient. In spite of the empirical nature of the reported values, since the tearing strength values were compared for all four samples (virgin, H1, H2 and H3) in a similar way, the values are considered to be reflective of actual fabric tearing strength (ASTM, 2013). The 60 mm cut off was used to avoid taking data from the initial portion of the specimens which may have some slippage point as well as extension from loop length (ASTM, 2013).

The top ten and bottom ten peaks for tearing strength (N) with maximum, minimum and averages for all four samples are given in Table 4.6. To understand the irregularities in the samples, percentage difference was calculated for all four samples. This percentage difference was calculated by subtracting minimum value from the maximum value, which was then divided

by the maximum value and multiplied by 100. For example, in virgin sample, the maximum value and minimum value was found to be 33.7 N and 8.52 N respectively, and the difference was 25.18 N (33.7 N – 8.52 N). This difference of 25.18 N was then divided by 33.7 N and multiplied by 100 to obtain the value of 74.7%. The difference for H1, H2 and H3 sample was found to be 56.1%, 64.5% and 61.7%.

Further, the difference among top ten and bottom ten peaks was found to be 5.95 N (33.7 N – 27.75 N) or 17.7% and 3.98 N (12.5 N – 8.52 N) or 31.8% respectively for virgin sample. For H1 sample, the difference is found to be 2.17 N (18.71 N – 16.54 N) or 11.6% for top ten peaks and 2.72 (10.93 N – 8.21 N) or 26.4% for bottom ten peaks; for H2 sample, the value is 2.44 N (15.03 N – 13.09 N) or 16.23% and 2.31 N (7.71 N – 5.47 N) or 32.5% ; while for H3 sample, the difference is 1.54 N (10.26 N – 8.72 N) or 15.0% and 2.15 N (6.1 N – 3.95 N) or 35.2%.

The larger percentage difference in tearing strength within each samples (virgin: 74.7%, H1: 56.1%, H2: 64.5% and H3: 61.7%) and among the bottom ten peaks for all samples (virgin: 31.8%, H1: 26.4%, H2: 32.5%, and H3: 35.2%) indicates that although hydrolyzed samples show lower tearing strength than the virgin sample, the variation in tearing strength is similar and might have originated from the manufacturing process. Scanning electron microscopy is conducted to find out defects in the samples and shown later in this chapter (Section 4.7). The effect of hydrolysis is discussed in the following section using average tearing strength.

Table 4.6

Data of 10 Highest and Lowest Tearing Strength (N) of Virgin, 7%, 16% and 25% Hydrolyzed Samples

Peak #	Virgin Sample Peaks		7% hydrolyzed Sample (H1) Peaks		16% hydrolyzed sample (H2) Peaks		25% hydrolyzed sample (H3) Peaks	
	Figure 4.19		**Figure 4.20**		**Figure 4.21**		**Figure 4.22**	
	Top 10	**Bottom 10**	**Top 10**	**Bottom 10**	**Top 10**	**Bottom 10**	**Top 10**	**Bottom 10**
1	33.70	8.52	18.71	8.21	15.53	5.47	10.26	3.95
2	33.41	9.62	18.64	8.26	14.76	6.11	9.93	4.41
3	30.68	9.78	18.48	8.33	13.96	6.19	9.66	4.53
4	30.63	10.19	18.04	8.60	13.72	7.05	9.39	4.83
5	29.30	10.41	17.64	9.36	13.60	7.32	9.27	5.61
6	29.01	10.60	17.41	9.51	13.40	7.33	9.21	5.72
7	28.81	10.77	17.31	9.73	13.32	7.45	9.09	5.80
8	28.64	10.80	17.22	9.90	13.25	7.50	8.98	6.0
9	27.97	12.02	17.07	10.27	13.10	7.65	8.74	6.03
10	27.75	12.50	16.54	10.93	13.09	7.71	8.72	6.1
Avg	29.9	10.5	17.7	9.3	13.8	6.9	9.3	5.3
Maximum	33.70		18.71		15.5		10.3	
Minimum	8.52		8.21		5.5		3.95	
Range	25.2		10.5		10.0		6.4	
Standard Deviation	2.11	1.15	0.73	0.94	0.79	0.77	0.51	0.79

Table 4.7

Average Tearing Strength (kPa) from Top Ten and Bottom Ten Tearing Strength Values

Virgin Sample (kPa)		7% Hydrolyzed Sample (H1) (kPa)		16% Hydrolyzed Sample (H2) (kPa)		25% Hydrolyzed Sample (H3) (kPa)	
Top 10	**Bottom 10**	**Top 10**	**Bottom 10**	**Top 10**	**Bottom 10**	**Top 10**	**Bottom 10**
2012.2	706.60	1191.2	625.9	928.7	464.4	625.9	356.7

The average tearing strength of the top 10 and bottom 10 peaks for virgin sample were found to be 2012.2 kPa (29.9 N) and 706.6 kPa (10.5 N) respectively, (Tables 4.6 and 4.7; calculation not shown here). However, the tearing strength values were decreased to 1191.2 kPa (17.7 N) and 625.9 kPa (9.3 N) for 7% hydrolyzed sample (H1), 928.7 kPa (13.8 N) and 464.4 kPa (6.9 N) for 16% hydrolyzed sample (H2), and 625.9 kPa (9.3 N) and 356.7 kPa (5.3 N) for 25% hydrolyzed sample (H3) (Tables 4.6 and 4.7). This gradual decrease in tearing strength of H1, H2 and H3 samples was due to the weight reduction during hydrolysis as shown in Table 4.5. The differences in the highest and lowest tearing strength values prove the irregularity and weaker yarns in vascular grafts as discussed in Sections 4.2 (Fabric Thickness) and 4.3 (Yarn Linear Density), that might play a significant role in rupture or breakage in human body after implantation.

Probability analysis of tearing data was not conducted because the average tearing strength of top 10 data for ***DVPVGKF,*** 2012.2 kPa, is lower than the highest post implantation pulsatile pressure of 2200 kPa. Even the highest tearing strength value of 2267.9 kPa (33.7 N, Table 4.6) for ***DVPVGKF*** is close to the highest post implantation pressure. The tearing data from this

study reveals that a combination of factors is responsible for premature rupture of polyester vascular grafts. These factors are: post implantation pressure, irregularities in the textile materials that reduce the tearing strength, and degradation due to hydrolysis. The irregularities in the materials are further discussed in the Scanning Electron Micrograph (SEM) Section (Section 4.6). In order to support the findings of the current study, an extensive literature review was conducted to detect the causes of *in vivo* premature polyester vascular graft ruptures and is shown in Table 1.3. Data from the premature ruptures show a majority of suture tears, cracks, holes, and dilation. Further, recent data show that the 'tear' is the major reason for premature rupture of vascular grafts (Shingaki et al., 2016).

To confirm the 'tongue tear test' results on ***DVPVGKF***, another tearing method, the Elmendorf tearing method following ASTM D 1424 (ASTM, 2013), was used. Tearing strength results from the Elmendorf tearing method are given in Table 4.8. The results showed that the average tearing strength from Elmendorf method is 20.9 N or 234.4 kPa. The general trend for tearing data from both these tests is similar, which means that both sets of tearing strengths are much lower than the tensile (breaking) strength data as shown in Table 4.3. Also, the tongue tearing strength is much higher than the Elmendorf tearing strength. This is due to the different test principle (Impact versus Constant Rate Elongation or CRE), applied load, sample dimension and sample orientation (vertical versus horizontal). Further, the tearing data from the Elmendorf test should be interpreted with caution as this method, although suitable for woven, layered blankets, napped pile, blanket, and air bag fabrics, is not suitable for course direction of warp knit fabrics, or either direction of most other knitted fabrics (ASTM, 2013). The vascular graft fabric used for the current study is a knitted structure.

Table 4.8

*Tearing strength of virgin Double Velour Polyester Vascular Graft Knitted Fabric (**DVPVGKF**)*

Sample No	Tear Strength (N)	Comments
1	23.09	Sample broke all the way
2	22.5	Sample broke all the way
3	17.69	Sample broke all the way but in an angle
4	20.61	Sample broke all the way but in an angle
Average	20.9 N or 234.4 kPa	
Standard Deviation	±2.4	

4.5 Breaking Pattern

4.5.1 Breaking Load Sample

Breaking pattern of the samples with figures and in vivo breaking pattern with references are given in Table 4.9. For breaking load tested samples, figures of 2 unbroken samples (*Figures 4.15* and *4.17*) and 4 broken samples (*Figures 4.12, 4.13, 4.14, 4.16*) are illustrated. Analysis of the first broken sample B1 (*Figure 4.12*), showed that the sample broke into two pieces which means both single filament and yarn (multifilament) broke completely. For samples B2 and B3, it was observed that the filament started breaking which resulted yarn breakage starting from the left side, at an angle of about 45°. This angular direction can be clearly seen in all broken samples. In sample B4, no fibres/yarns were broken (*Figure 4.15*). For sample B5, the fibres also started breaking from the side. Some unbroken fibres still can be seen in this sample (*Figure 4.16*). A closer look at the broken section of the sample reveals the combination of broken and intact filaments *(Figure 4.18)*.

4.5.2 Tearing Load Sample

Tearing test filament breakage can be seen and all samples broke in a diagonal way from centre towards side (*Figures 4.23-4.26*). These in vitro broken behaviours are similar to the in vivo broken pattern of polyester vascular grafts (Rahman, 2012; Riepe et al., 1997). The broken behaviour of polyester is discussed in the Scanning Electron Micrograph section (Section 4.6).

Table 4.9

Relationship between breaking pattern and load elongation curve

Sample ID # and Strength Test	Breaking Pattern and Figure #	Load-Elongation Curve and Graph #	*In Vivo* Breaking	
			Pattern	Reference
B1 (Tensile Test)	All fibres/ yarns broke and sample completely divided into two pieces, *Figure 4.12*	Multiple peaks at breaking point, *Figure 4.6*	Broken, ruptured thinned out filament	(Rahman, 2012)
B2 (Tensile Test)	Fibres started breaking from the side in an angular manner, did not break completely, *Figure 4.13*	Sharp breaking point, *Figure 4.7*	Fracture in the center and relatively smooth surface of the filament on the right side	(Riepe et al., 1997)
B3 (Tensile Test)	Fibres started breaking from the side in an angular manner, did not break completely, *Figure 4.14*	Sharp breaking point, *Figure 4.8*	Fracture in the centre and the relatively smooth surface of the filament on the right side	(Riepe et al., 1997)
B4 (Tensile Test)	Fibres did not break, *Figure 4.15*	No change in curve, *Figure 4.9*		
B5 (Tensile Test)	Fibres started breaking from the side, but still some fibres left attached, *Figure 4.16*	Sharp breaking point, *Figure 4.10*	Cracks and holes in the explanted graft	(Rahman, 2012)
B6 (Tensile Test)	Fibres did not break, *Figure 4.17*	No change in curve, *Figure 4.11*		
Control Sample (Tearing Test)	Fibres/Yarn started breaking from the side in an angle, *Figure 4.23*	Multiple peaks at the breaking point, *Figure 4.19*		
H1 (Tearing Test)	Fibres/Yarn started breaking from the centre to side and almost divided into 2 pieces, *Figure 4.24*	Multiple peaks at the breaking point, *Figure 4.20*		
H2 (Tearing Test)	Fibres/Yarn started breaking from the centre to side and almost divided into 2 pieces, Fig*ure 4.25*	Multiple peaks at the breaking point, *Figure 4.21*		
H3 (tear test)	Fibres/Yarn started breaking from the centre to side and almost divided into 2 pieces, *Figure 4.26*	Multiple peaks at the breaking point, *Figure 4.22*		

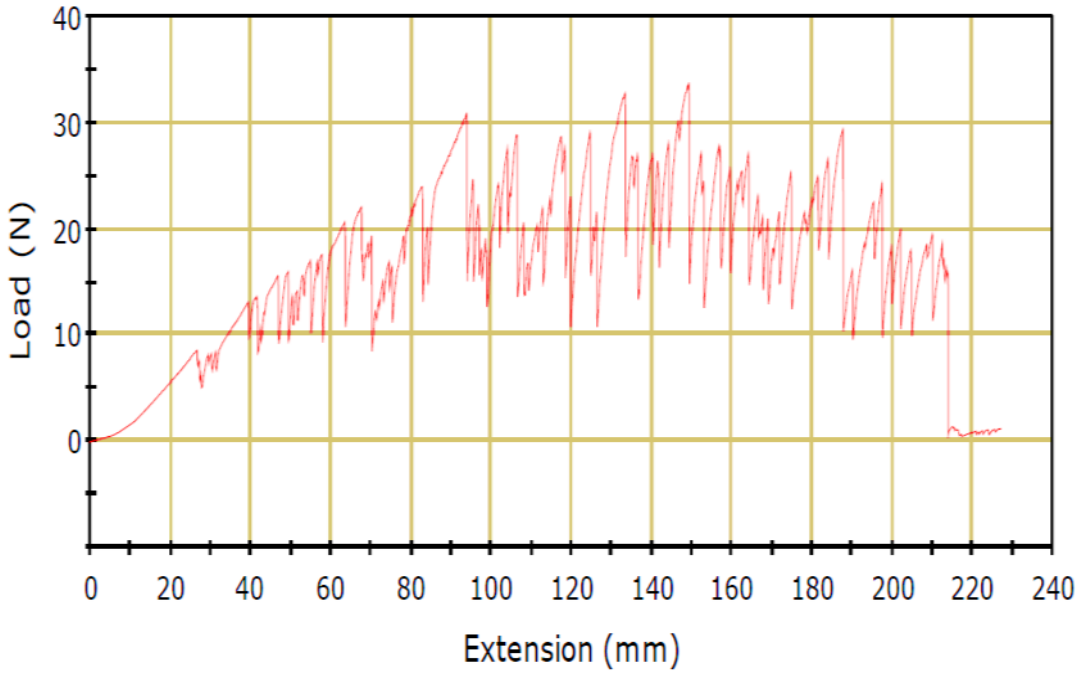

Figure 4.19. Tearing strength of virgin sample.

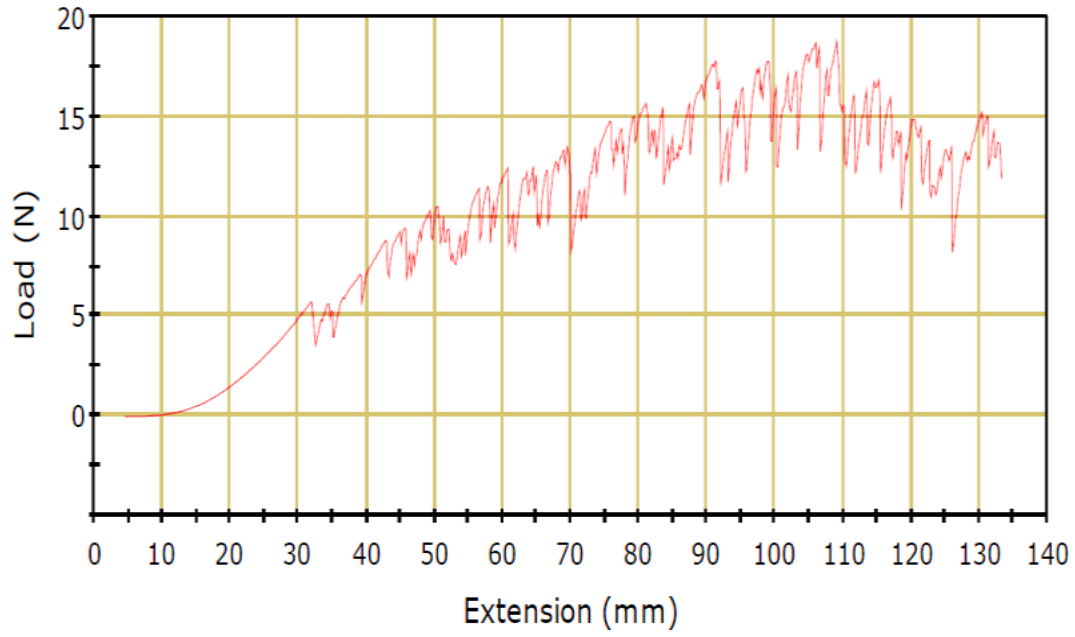

Figure 4.20. Tearing strength of hydrolyzed sample H1.

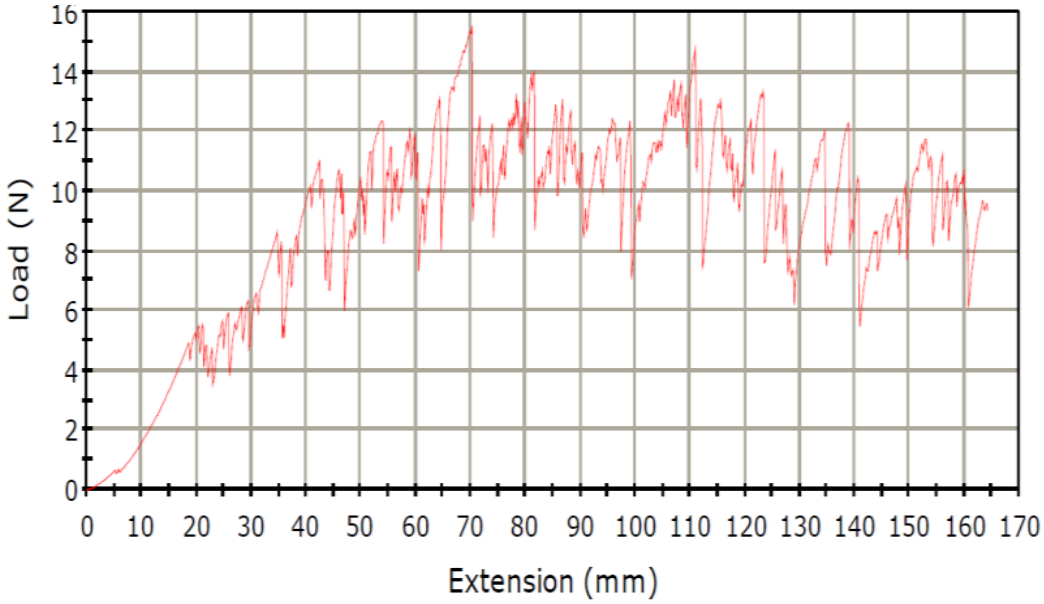

Figure 4.21. Tearing strength of hydrolyzed sample H2.

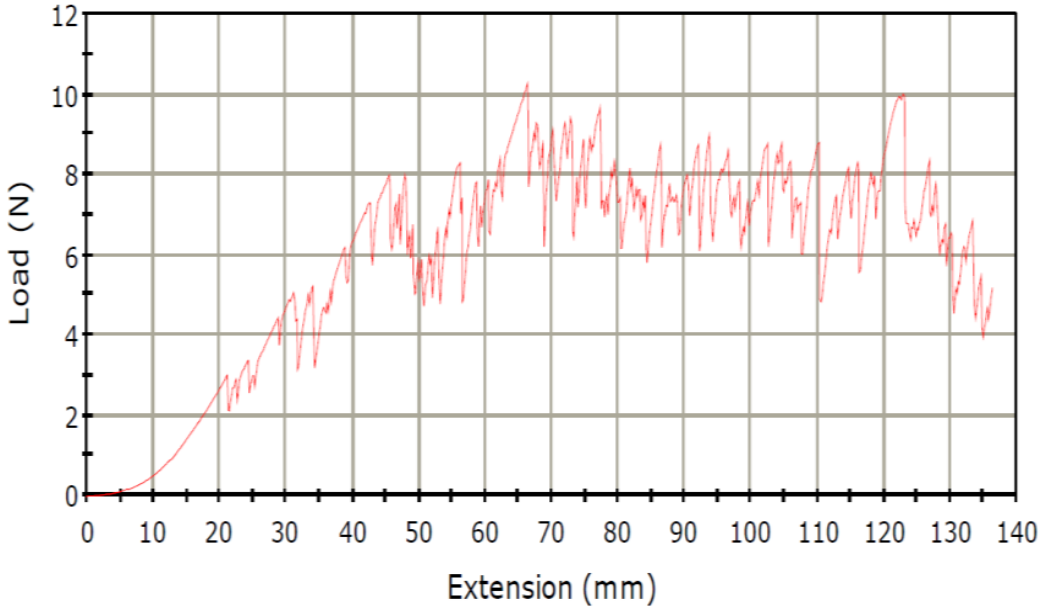

Figure 4.22. Tearing strength of hydrolyzed sample H3.

Figure 4.23. Control sample tearing.

Figure 4.24. Hydrolyzed sample H1 tearing.

Figure 4.25. Hydrolyzed sample H2 tearing.

Figure 4.26. Hydrolyzed sample H3 tearing .

4.6 Scanning Electron Microscopy (SEM)

Scanning electron microscopy (SEM) was conducted using a magnification of up to 5000x to check the diameter variation discussed in Section 4.3, to observe the fibre surface and inside layers for any manufacturing defects (tears, holes) that might be responsible for variation in tearing strength and to investigate the diagonal nature of the breakage during tensile and tear tests. For SEM analysis, three different types of graft samples were used:

(a) Virgin ***DVPVGKF***

(b) Aqueous NaOH Hydrolyzed ***DVPVGKF***

(c) Alcoholic NaOH Hydrolyzed ***DVPVGKF***

SEM micrographs of virgin sample will provide any surface defects, while hydrolysed samples will provide the defects underneath the surface as hydrolysis remove the successive surface layers of polyester fibres. For SEM analysis, samples were hydrolysed using physiological temperature (40°C), and moderate pH (molarity = 1.0).

Figures 4.27-4.29 show the SEM micrographs of virgin vascular graft fabric. Two phenomena can be observed from these three micrographs:

(a) Diameter variation, and

(b) Surface defects

Diameter variation between the two virgin individual filaments can be seen in the SEM micrograph *Figure 4.27*. The diameter of the filament on the left in *Figure 4.27* is found to be ≈13.3 μm while the value for the filament on the right is ≈19.8 μm. This diameter variation is consistent with the previous findings discussed in Section 4.3. Surface defects can be seen in SEM micrographs *Figures 4.28 and 4.29*. The defects appear on multiple individual filaments as shown in *Figure 4.28*. Further, in the SEM *Figure 4.29*, an enlarged view (1000x), shows that

most of the defects run in the direction of the filament axis. However, defects can also be seen in an angle (*Figure 4.29*).

The diameter variation is known to have occurred due to the variation in drawing speed, the inhomogeneity of the polymer solution in the spinning bath and the lack of uniformity of the spinneret hole (Abbas, 2007). One plausible explanation for the axial defect on the virgin (untreated) filament is the presence of air bubbles in the polymer solution. These air bubbles create tiny holes in the filament surface that increase in size due to the applied 'draw ratio' during filament yarn spinning. Draw ratio is the ratio of speed between collecting roller and feed roller, which is about 5 (Xi et al., 2010).

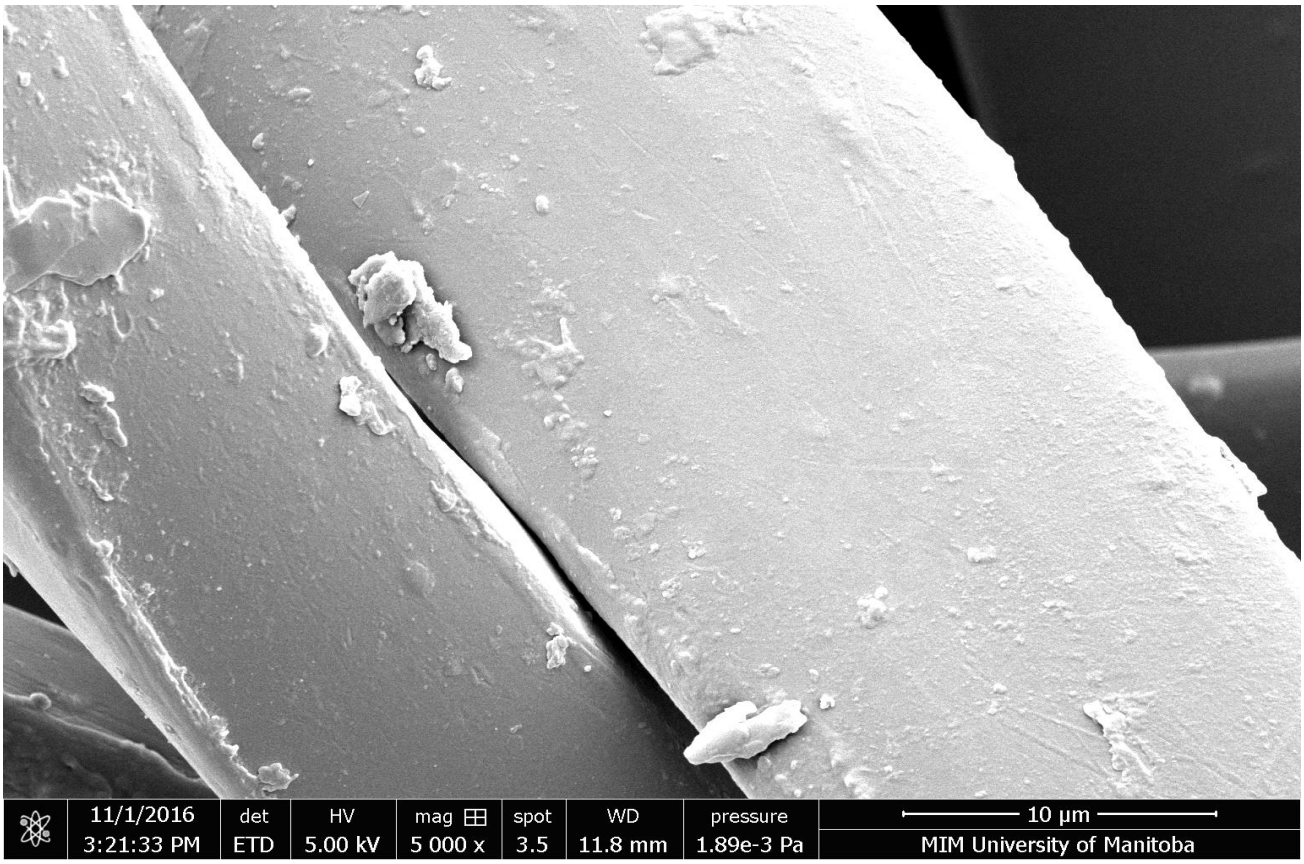

Figure 4.27. Virgin ***DVPVGKF*** sample.

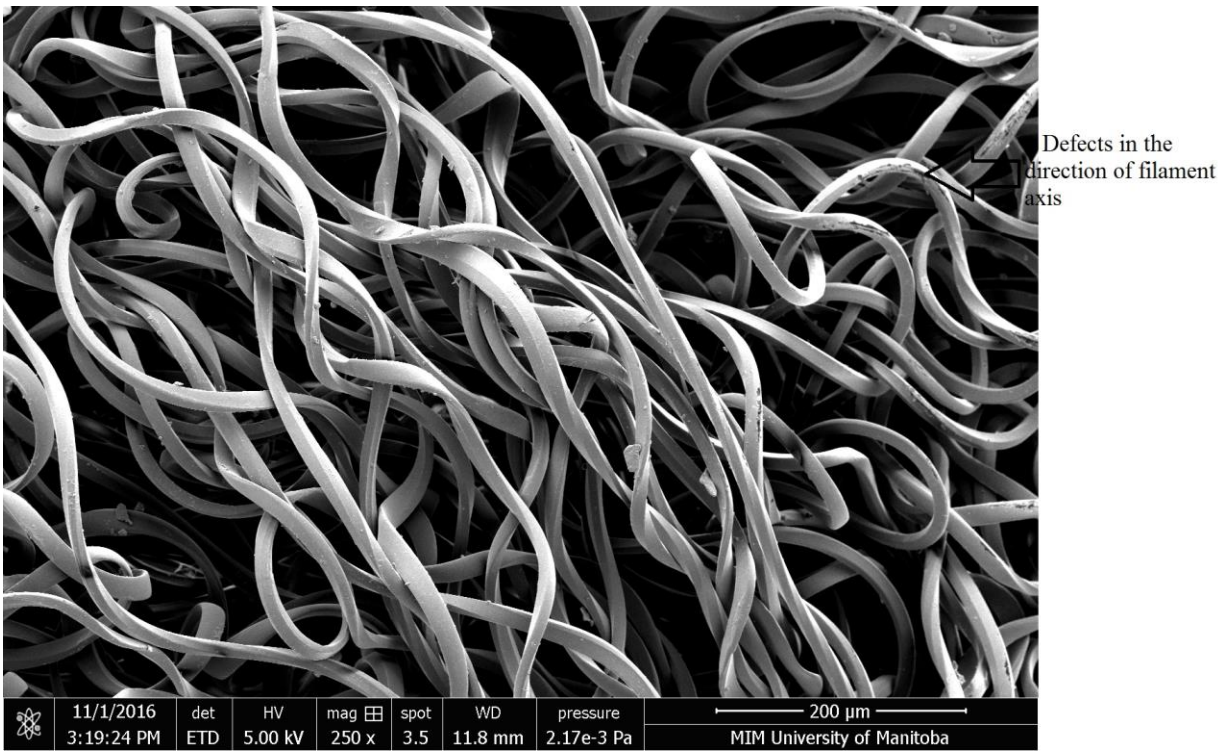

Figure 4.28. Virgin ***DVPVGKF*** sample.

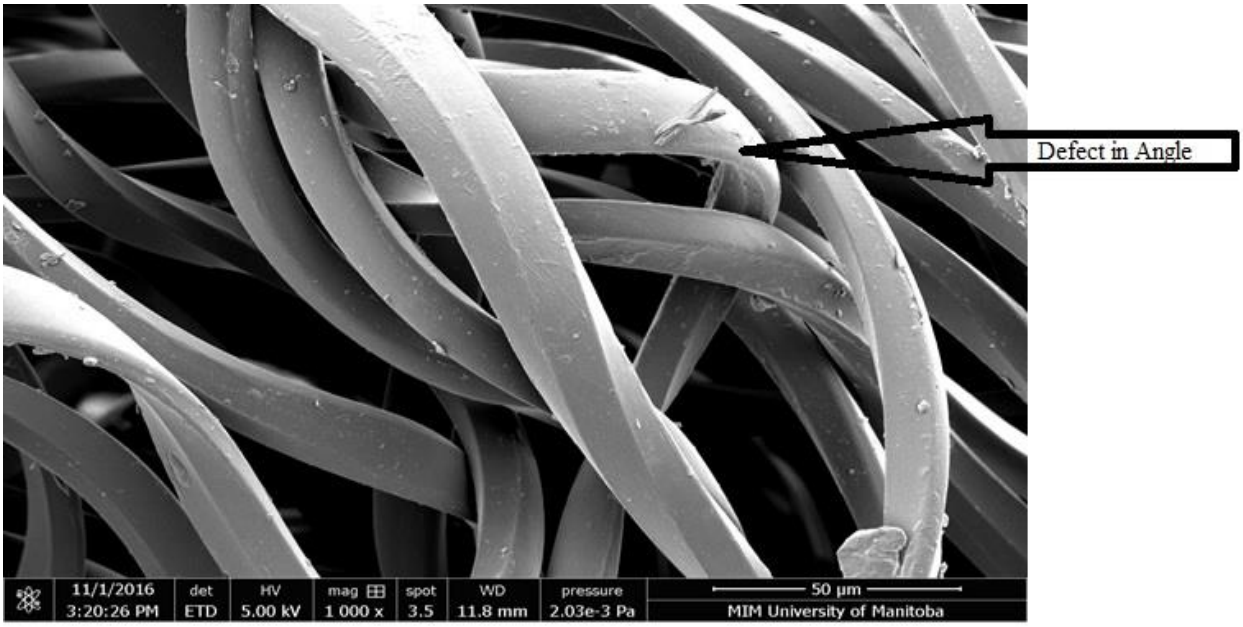

Figure 4.29. Virgin ***DVPVGKF*** sample.

In order to find out the propagation of the surface cracks, samples were etched using aqueous and alcoholic alkaline solutions. The cracks appeared to be larger and more severe in the aqueous alkaline treated samples (*Figures 4.30-4.32*) than the virgin samples (*Figures 4.27-4.29*). In the SEM micrograph *Figure 4.30*, the cracks appear to run transversely at a slight angle. However, in SEM micrographs *Figure 4.31 and 4.32*, the transverse cracks are formed at an angle and the axial cracks are longer and running on the filament edges. The formation of long running axial cracks may be due to the degradation of weak extended non-crystalline regions (long period) as shown in *Figure 4.42*.

When etched with alcoholic alkaline solution, the direction of cracks and the severity depend on the treatment time. After 10 minutes of treatment, cracks appeared in the longitudinal direction (*Figure 4.33*). Also, in this sample, some of the cracks are deeper and more circular in shape (*Figure 4.34*). Samples treated with alcoholic alkali for 20 minutes contain cracks in both longitudinal and transverse directions (*Figure 4.35*). The transverse cracks are at angle, which ranges between 30° and 45°. In other SEM micrographs [*Figures 4.36 – 4.41 (b)]*, the fibres etched with alcoholic alkaline solutions, show both axial and longitudinal cracks can be seen with the longer longitudinal cracks (*Figures 4.37, 4.39-4.40*) and angular axial cracks (*Figures 4.36, 4.38*).

While the axial cracks may have formed due to the weaker 'long period' as discussed earlier, the diagonal cracks observed in the transverse direction may be due to the hydrolysis of the amorphous fiber regions, while the crystalline fiber regions maintain resilient to degradation. As shown in *Figure 4.42*, the crystalline and amorphous regions are aligned in a checkerboard like

pattern. The degradation of the amorphous regions would create a diagonal gash in the longitudinal direction. This probably explains the angular breakage of ***DVPVGKF*** sample during tensile and tear tests.

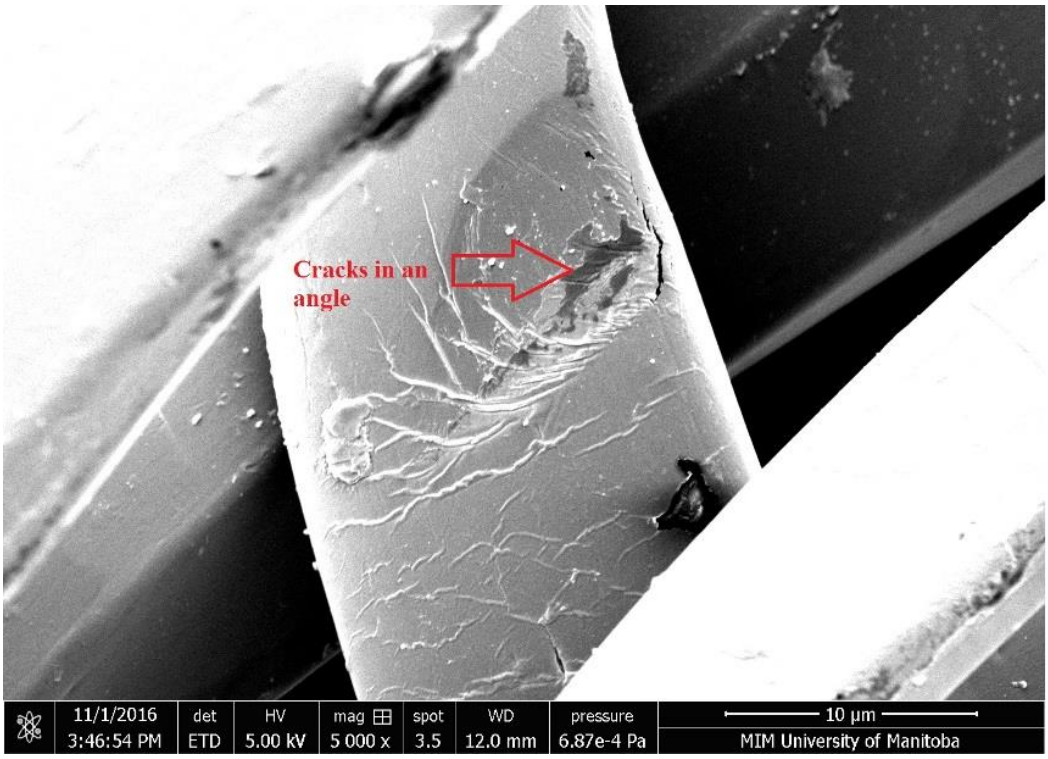

Figure 4.30. ***DVPVGKF*** sample treated with 4% NaOH in water at 40°C for 30 minutes.

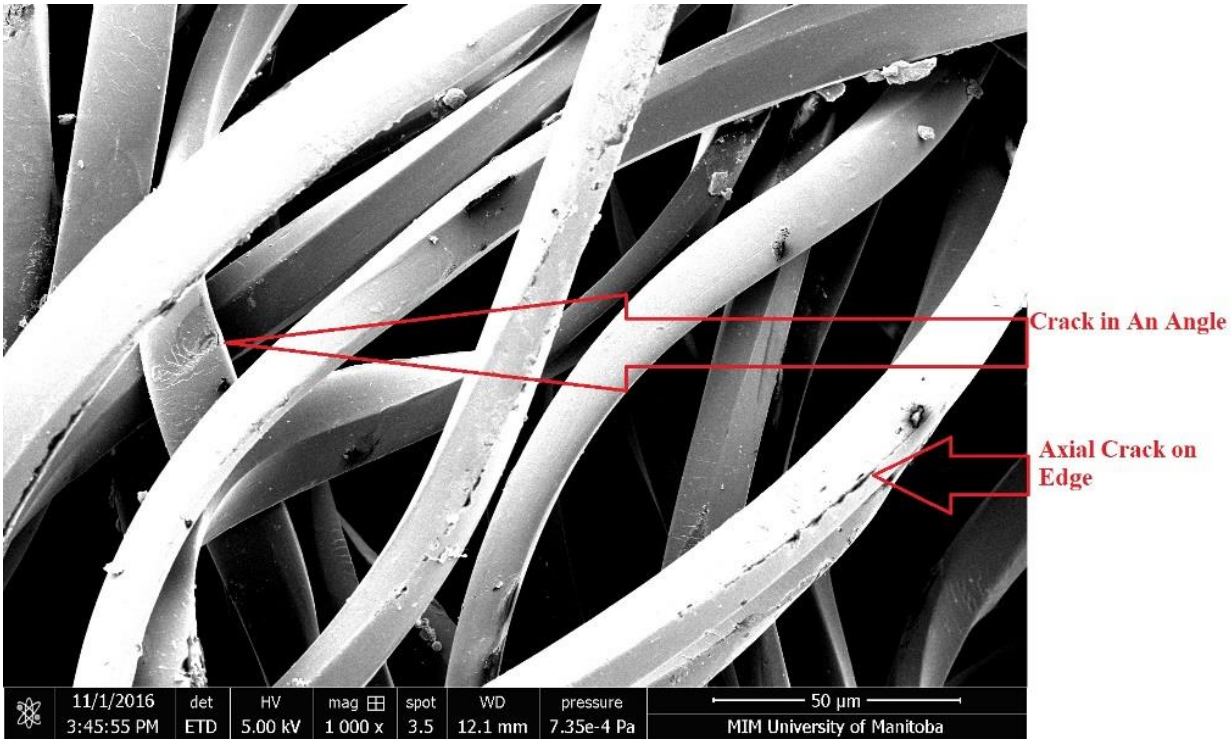

Figure 4.31. ***DVPVGKF*** sample treated with 4% NaOH in water at 40°C for 30 minutes.

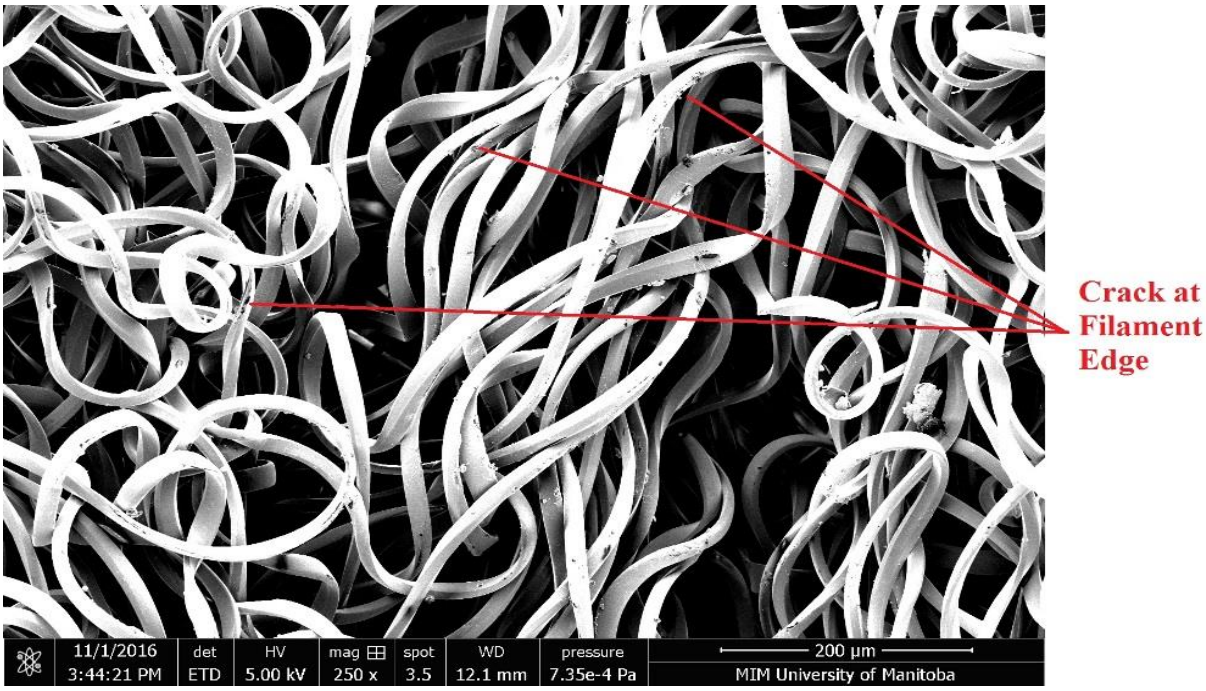

Figure 4.32. ***DVPVGKF*** sample treated with 4% NaOH in water at 40°C for 30 minutes.

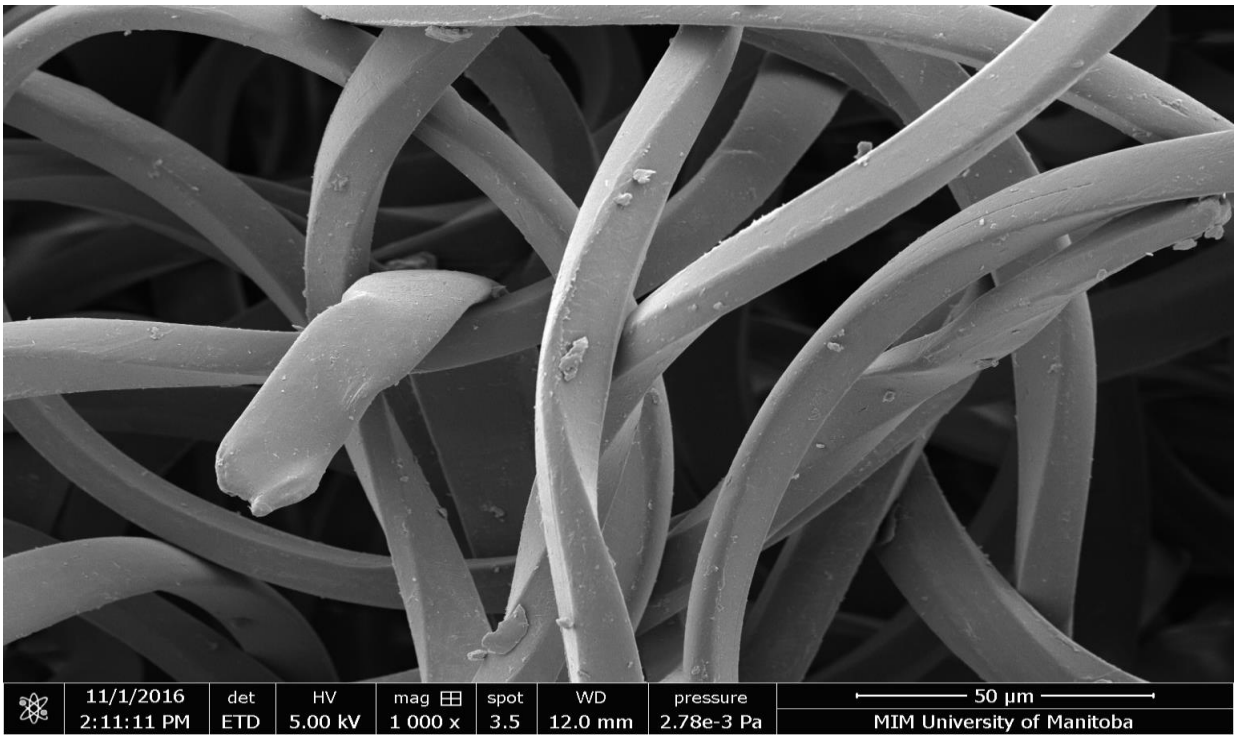

Figure 4.33. ***DVPVGKF*** sample treated with methanol in 4% NaOH at 40°C for 10 minutes.

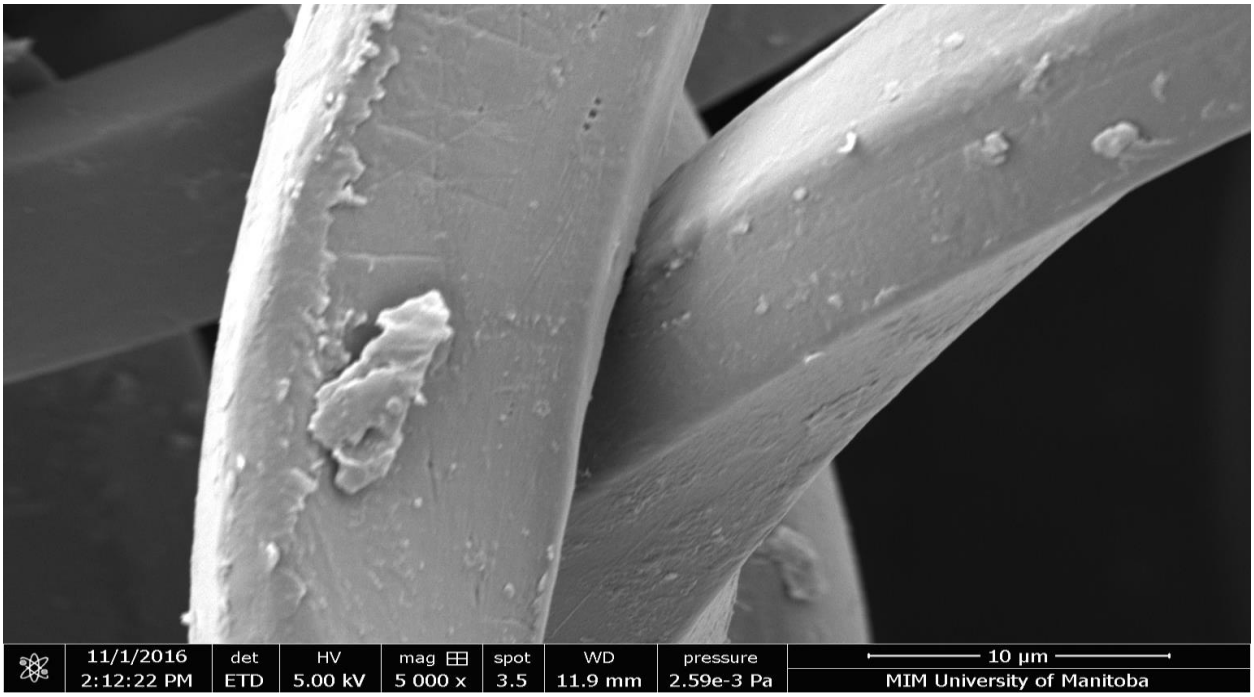

Figure 4.34. ***DVPVGKF*** sample treated with methanol in 4% NaOH at 40°C for 10 minutes.

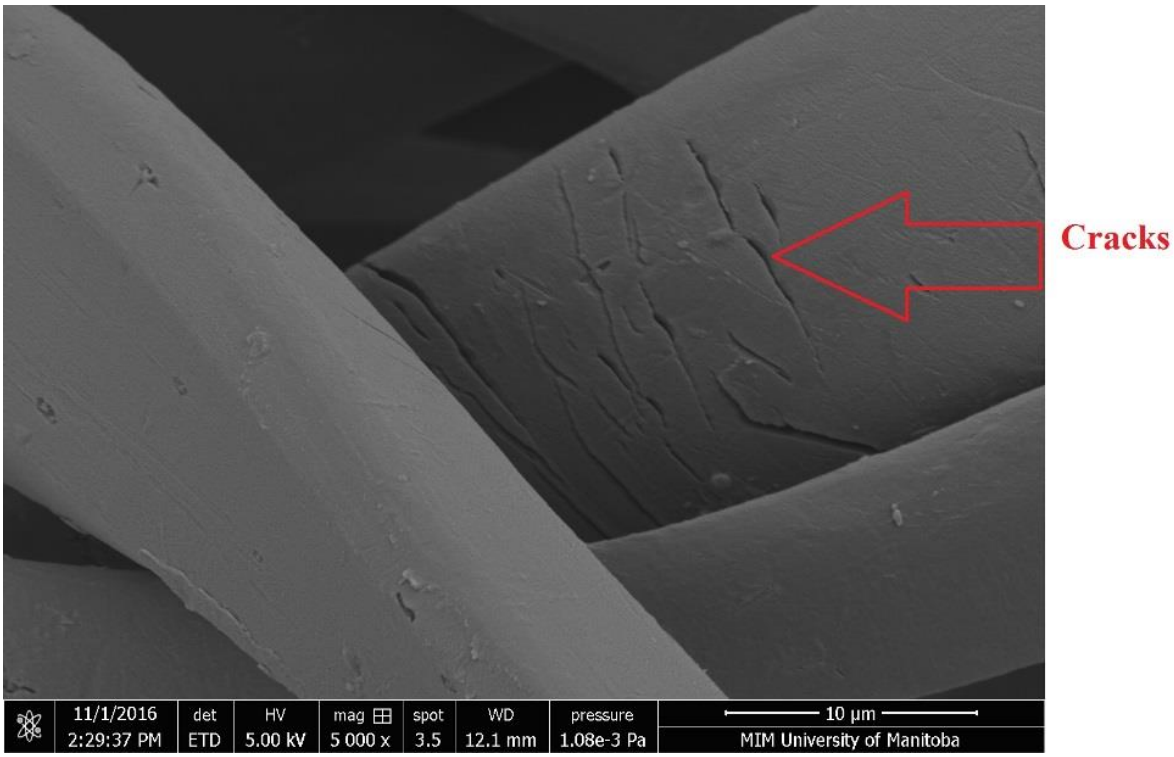

Figure 4.35. ***DVPVGKF*** sample treated with methanol in 4% NaOH at 40°C for 20 minutes.

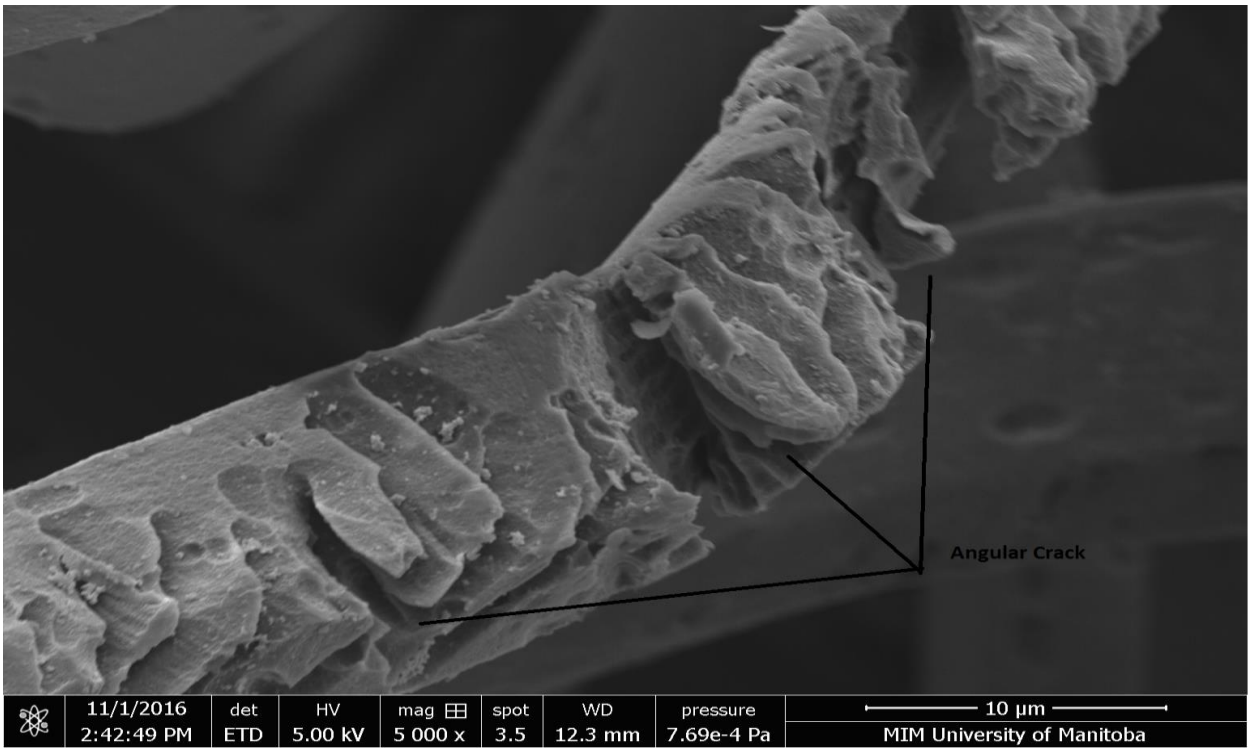

Figure 4.36. ***DVPVGKF*** sample treated with methanol in 4% NaOH at 40°C for 30 minutes.

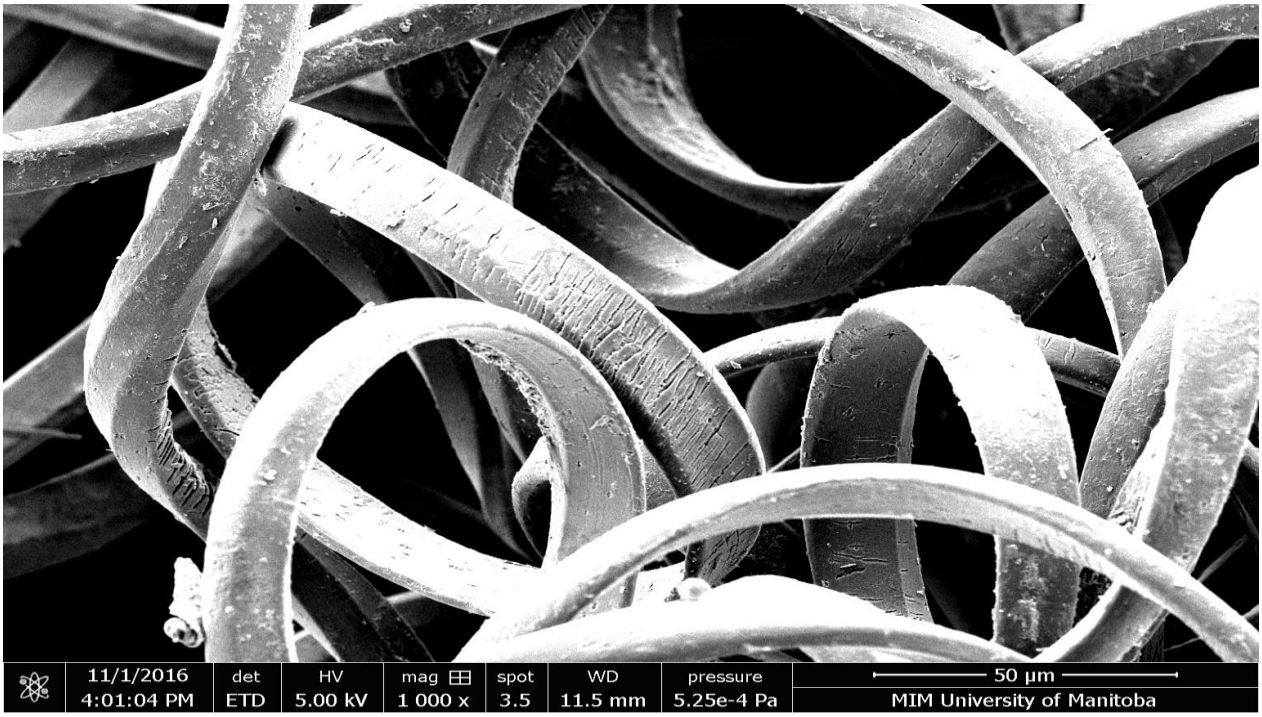

Figure 4.37. ***DVPVGKF*** sample treated with methanol in 2% NaOH at 40°C for 20 minutes.

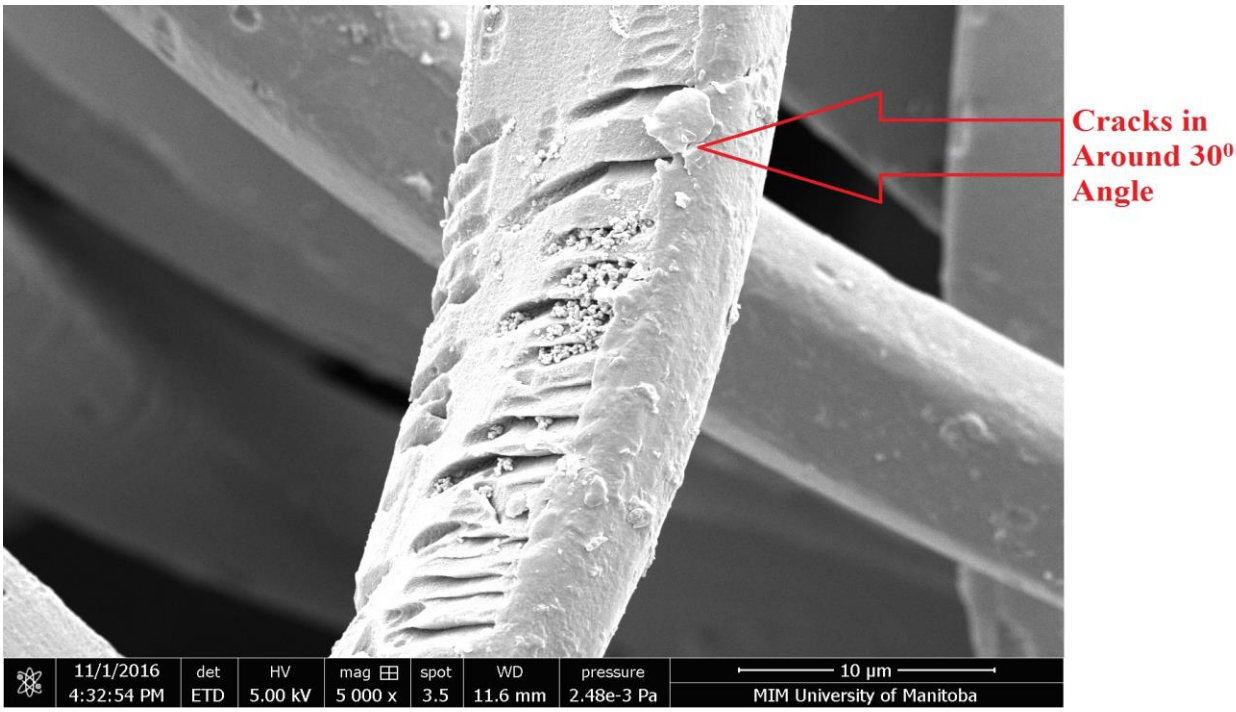

Figure 4.38. ***DVPVGKF*** sample treated with ethanol in 2% NaOH at 40°C for 30 minutes.

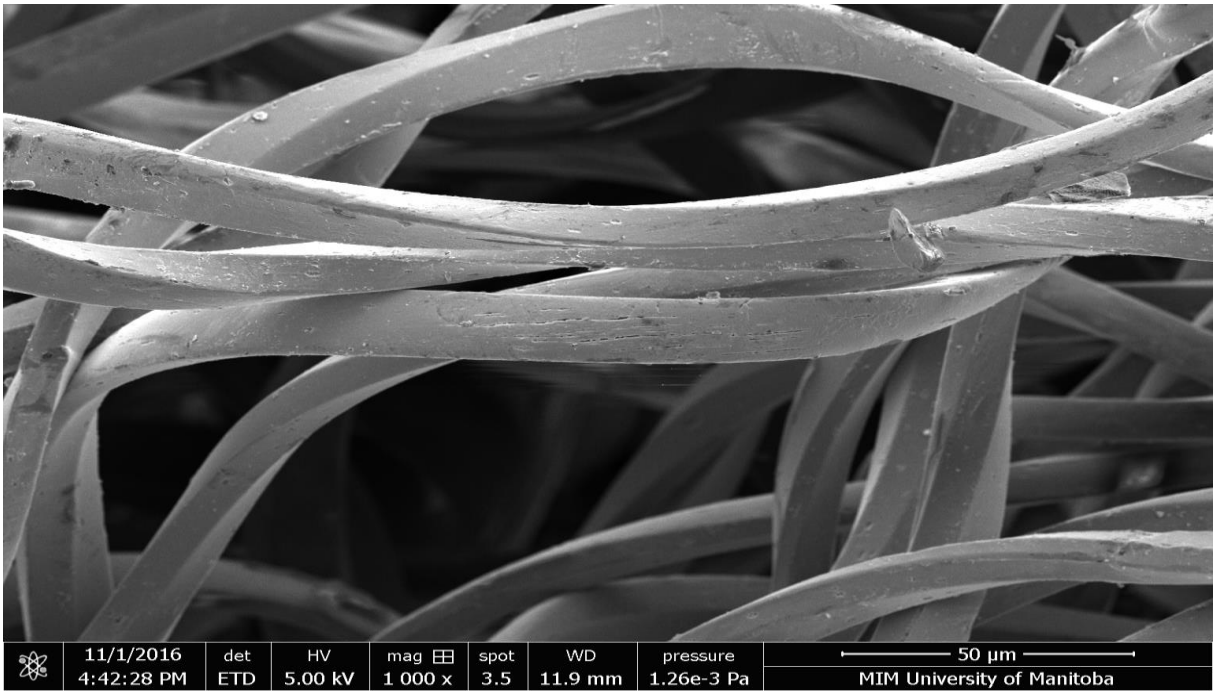

Figure 4.39. ***DVPVGKF*** sample treated with ethanol in 4% NaOH at 40°C for 10 minutes.

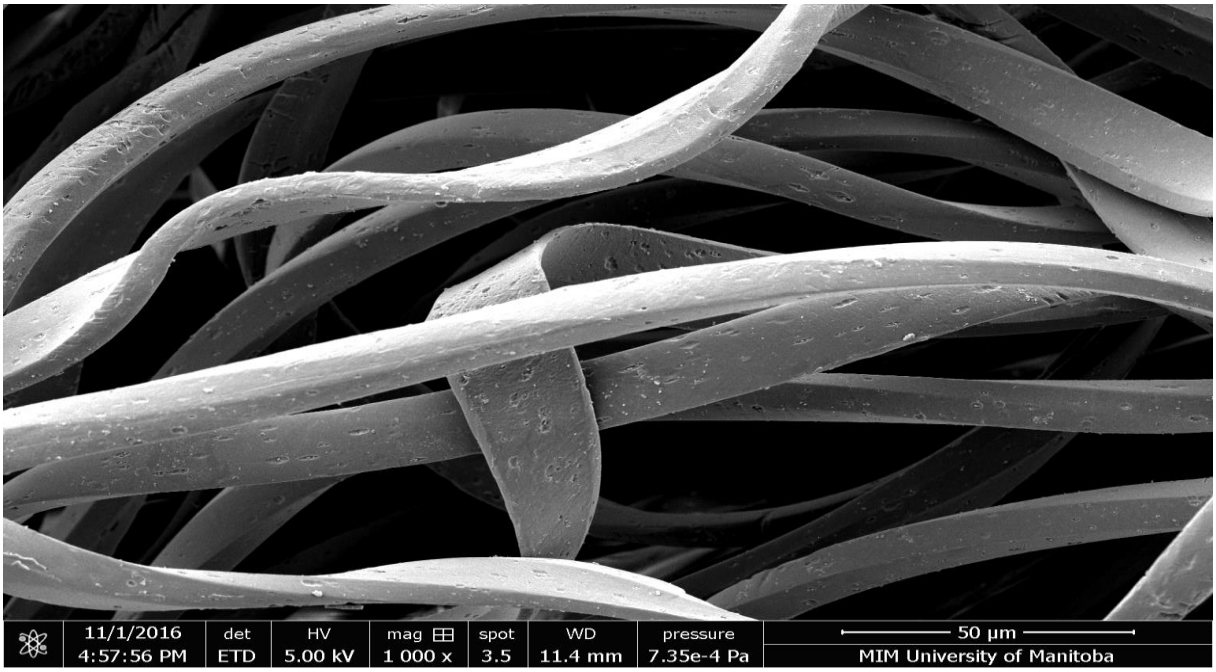

Figure 4.40. ***DVPVGKF*** sample treated with ethanol in 4% NaOH at 40°C for 20 minutes.

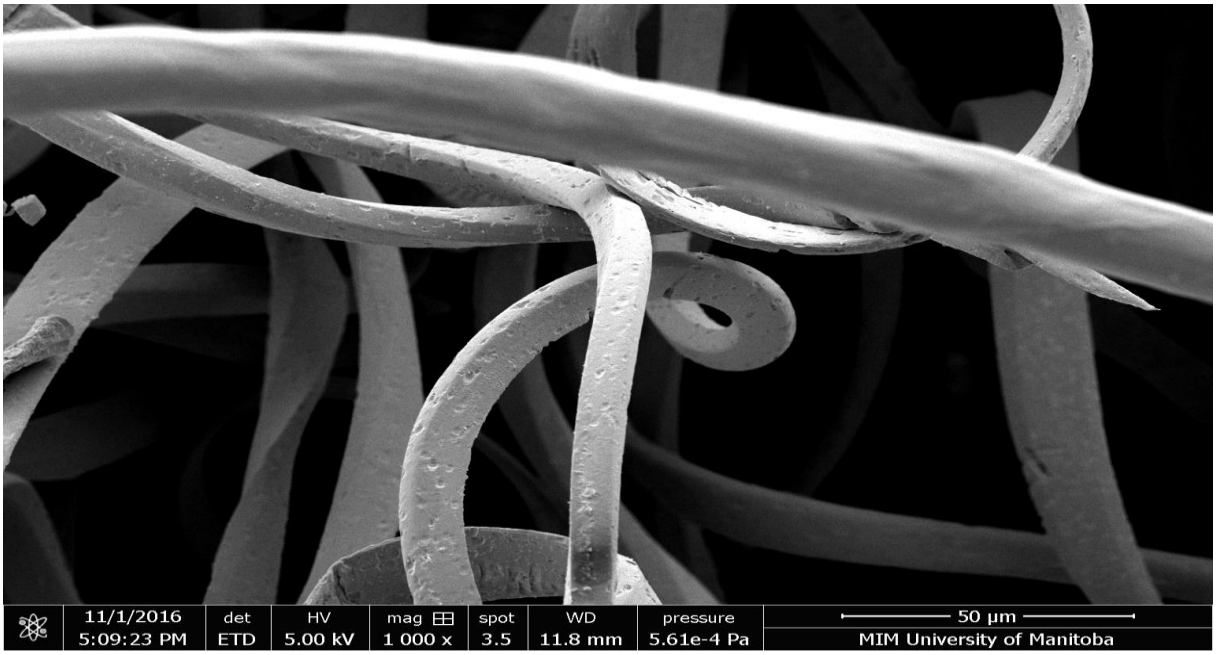

Figure 4.41 (a). ***DVPVGKF*** sample treated with methanol in 4% NaOH at 40°C for 30 minutes.

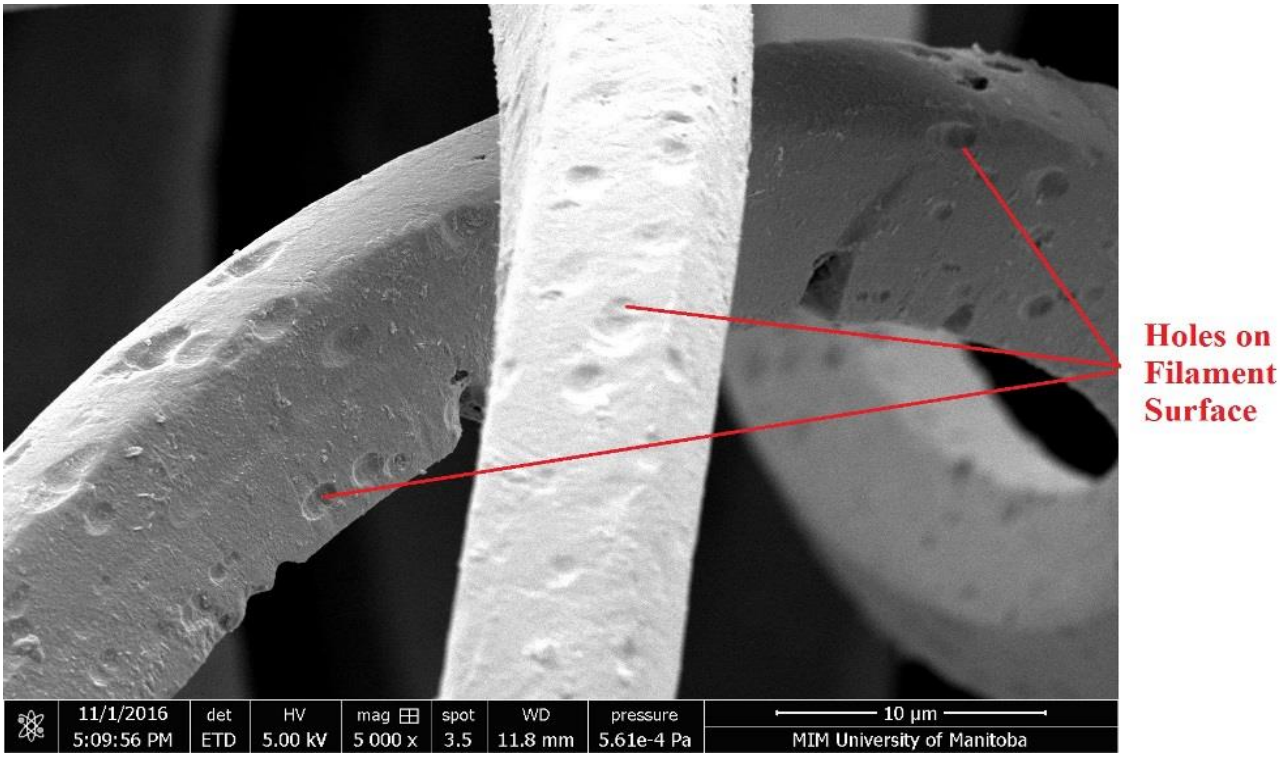

Figure 4.41 (b). ***DVPVGKF*** sample treated with ethanol in 4% NaOH at 40°C for 30 minutes.

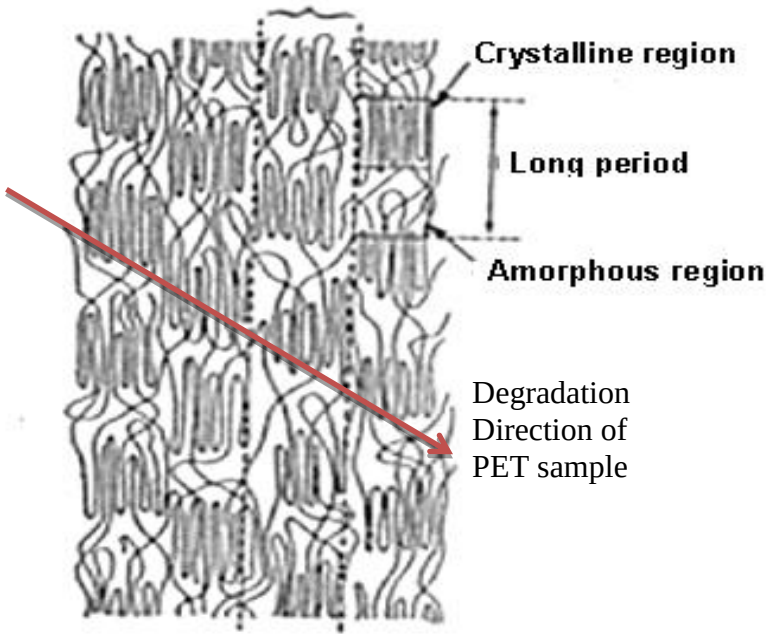

Figure 4.42. Schematic Structure of PET Fibres (Prevorsek et al., 1974, p.373). [Used with permission]

4.7 Conclusions

Material irregularities are present in the vascular graft samples. These irregularities include differences in fabric thickness, yarn linear density and diameter, breaking strength and tearing strength. Scanning electron microscopy showed that defects (cracks and holes) present in virgin sample and these defects were enhanced in alkaline media.

Chapter 5 Conclusions and Future Work

5.1 Conclusions

Based on the results of the preliminary studies, it was decided to use polyester vascular graft fabric to examine whether similar variations exist that might be responsible for the premature polyester graft failures. Thickness values of two ***DVPVGKF*** samples were compared and found to be significantly different at 5% level ($t_{0.05}$ = 3.77>2.10). Diameter and yarn tex of two filament yarns (Filament #1 and #2) were also measured and found to be significantly different at 5% level ($t_{0.05}$ = 2.9>2.262). It was logical to believe that a variation in fabric thickness and diameter in a single filament or multifilament yarn would influence the other mechanical properties for example, fabric breaking strength, tearing strength and bursting strength.

The ***DVPVGKF*** sample showed a variation in breaking strength (49.8±4.1 N, Tables 4.3 & 4.4). However, probability analysis revealed that only 0.07% of the polyester graft's breaking strength (d =13 N) could fall below the maximum post implantation pulsatile pressure (PIPP) of 2200 kPa (Table 4.4) and therefore, couldn't be responsible for the reported 25% polyester vascular graft failure. The in vivo tearing problem in the vascular graft is responsible for the majority of the graft failures (Table 1.3). The tearing strength result of the ***DVPVGKF*** shows that only two data (33.7 N & 33.4 N) from the top ten peaks lie above the maximum PIPP (Table 4.6). All other tearing strength data for the ***DVPVGKF*** sample, as well as for the hydrolysed samples (H1, H2 & H3), fall below the PIPP (Table 4.6). Therefore, this study concludes that lower tearing strength is responsible for the premature rupture of polyester vascular grafts.

Further, the present study concludes that the main cause of lower tearing strength is the presence of manufacturing defects such as tears and cracks. While investigation on the causes of from

other sources, such as suture line/dilation tears is beyond the scope of this research, scanning electron microscopy (*Figures 4.30 – 4.41b*) was conducted to find the tears due to manufacturing defects. It appears that tears in the virgin materials begin in the defect location (*Figures 4.28-4.29*) of 'long period' and amorphous regions (Figure 4.42) of the polyester fibre. Since 25% of the polyester graft failures occur between 6 to 18 months, it is reasonable to state that due to the *in vivo* hydrolysis in alkaline media (aqueous and alcoholic), the cracks that start in these two weak regions merge and produce larger cracks. This larger crack, which has lower tearing strength, is unable to resist the dilation force from the pulsatile pressure and thus causes the tearing and the inevitable failure of vascular grafts.

5.2 Limitation of Tearing Strength

Due to the complex knitting structure and not enough technical information available from the producer, it was hard to find out the exact knitting structure of ***DVPVGKF***. Tearing starts from a previously cut area and it slowly propagates as the applied load increases the extension. It was not possible to obtain how many yarns were broken in within 'one interloop' during tear. Further, it appears that the ratio of breaking strength to tearing strength for ***DVPVGKF*** is low compared to other standard fabric.

During tearing strength calculation, the width of the sample was used 0.0127 meter (original width: 0.02 meter) to make allowance for necking.

5.3 Future Work

The journey started for this research with a question in mind: can we have quality specifications (for example, tearing strength, imperfection data and so forth) for vascular grafts? During the course of this research, numerous contacts have been made with the vascular graft fabric supplier to obtain quality data. However, the company was reluctant to share the quality data due to confidentiality reasons. Health Canada also does not have any quality data of vascular graft material and when contacted, referred the current researcher to Medical Device Regulations under Food and Drug Act. The Medical Device Regulations (SOR/98-282, updated February 13, 2017) does not provide any quality specifications other than mentioning the following items:

Medical Device Regulations, Section 10: A medical device shall be designed and manufactured to be safe, and to this end the manufacturer shall, in particular, take reasonable measures to

(a) identify the risks inherent in the device,

(b) eliminate the risks, if they can be eliminated, or if the risks can be eliminated, eliminate them or

(c) if the risks cannot be eliminated:

(i) reduce the risks to the extent possible;

(ii) provide protection appropriate to the risks, including the provision of alarms; and

(iii) provide with the device, information relative to the risks that remain; and

(iv) minimize the hazard from potential failures during the projected useful life of the device.

Therefore, from the findings of the current research, it is recommended that the tearing strength requirement and irregularities of the polyester vascular graft should be investigated further to

confirm the findings of the current study and the data be included in the regulations. This will be a first step to prepare ‘quality specifications’ for polyester prosthetic grafts.

References

Abbas, M., Mojtahedi, M., Khosroshani, A. (2007). Effect of spinning speed on the structure and physical properties of filament yarns produced from used PET bottles. *Journal of Applied Polymer Science,* 103 (6), 3972-3975.

Adanur, S. (1995). Fibre properties and technology. *Wellington sears handbook of industrial textiles* (pp. 555-606).Pennsylvania, USA: Technomic Publishing Company, Inc.

Amorim, P., Sousa, G., Vieira, J., CE, S. L., Ribeiro, K., Sobrinho, G., ... & Albino, P. (2014). Endovascular management of an infectious and ruptured abdominal aortic aneurysm. Clinical report. *Revista portuguesa de cirurgia cardio-toracica e vascular: orgao oficial da Sociedade Portuguesa de Cirurgia Cardio-Toracica e Vascular, 21*(1), 65-68.

ASTM International (2008). *ASTM D1776: Standard practice for conditioning and testing textiles.* ASTM International, West Conshohocken, PA.

ASTM International (2013). *ASTM D 2261: Standard test method for tearing strength of fabrics by the tongue (single rip) procedure (Constant-rate-of-extension tensile testing machine),* ASTM International, USA.

ASTM International (2013). *ASTM D 1424: Standard Test Method for Tearing Strength of Fabrics by Falling-Pendulum (Elmendorf-Type) Apparatus.* ASTM International, USA.

Baird, R., & Abbott, W. (1976). Pulsatile blood-flow in arterial grafts. *The Lancet* 308, (7992), 948–50.

Berger, K., & Sauvage, L. R. (1981). Late fiber deterioration in Dacron arterial grafts. *Annals of Surgery, 193*(4), 477–91.

Booth, J. E. (1968). The elements of statistics. *Principles of textile testing: An introduction to physical methods of testing textile fibres, yarns and fabrics*. London (pp 32-34): Heywood Books.

Carothers, W.H., & Hill, J. W. (1932). Studies of polymerization and ring formation XV. Artificial fibers from synthetic linear condensation super polymer. *Journal of the American Chemical Society*, 54, 1579-1587.

Chakfé, N., Dieval, F., Riepe, G., Mathieu, D., Zbali, I., Thaveau, F., … Durand, B. (2004). Influence of the textile structure on the degradation of explanted aortic endoprostheses. *European Journal of Vascular and Endovascular Surgery*, *27*(1), 33–41. https://doi.org/10.1016/S1078-5884(03)00341-1

Chakfe, N., Riepe, G., Dieval, F., Le Magnen, J.-F., Wang, L., Urban, E., … Kretz, J.-G. (2001). Longitudinal ruptures of polyester knitted vascular prostheses. *Journal of Vascular Surgery*, *33*(5), 1015–1021.

Chattopadhyay, R. (2010). Introduction: Types of technical textile yarn. *Technical Textile Yarns–Industrial and Medical Applications*, 3-55.

Collier, B. J., & Epps, H. H. (1999). *Textile testing and analysis*. Upper Saddle River, NJ: Prentice Hall

Collins, M. L., Zeronian, S. H., & Semmelmeyer, M. (1991). The use of aqueous alkaline hydrolysis to reveal the fine structure of poly (ethylene terephthalate) fibers. *Journal of Applied Polymer Science*, 42(8), 2149-2162.

Conner, C. S., Morris, R. P., Vallurupalli, S., Buford, W. L., & Ivey, F. M. (2008). Tensioning of anterior cruciate ligament hamstring grafts: Comparing equal tension versus equal stress.

Arthroscopy: The Journal of Arthroscopic & Related Surgery, *24*(12), 1323–1329. https://doi.org/10.1016/j.arthro.2008.07.006

Creech, O., Deterling, R., Edwards, S., & Al, E. (1957). Vascular prostheses.Report of the committee for the study of vascular prostheses of the society of vascular surgery. *Surgery*, *41*, 62-80.

Damme, H. V., Deprez, M., Creemers, E., & Limet, R., (2005). Intrinsic structural failure of polyester (dacron) vascular grafts. A general review. *Acta Chirurgica Belgica,* 105 (3): 249–55.

D'Sa, A. B., Berger, K., Di Benedetto, G., Parenzan, L., Rittenhouse, E. A., Mansfield, P. B., … Sauvage, L. R. (1980). A healable filamentous Dacron surgical fabric. Experimental studies and clinical experience. *Annals of Surgery*, *192*(5), 645–57.

Edwards, W. S. (1978). Arterial grafts of teflon. In *Vascular Graft* (pp. 173–176). New York: Appleton-Century-Crofts..

Falkai, B.V. (1996). Developments in the production of industrial PET filaments. *Asian Textile Journal*, *5*, 26–38.

Harris, E. J., Shumacker, H. B., Siderys, H., Moore, T. C., & Grice, P. F. (1955). Pliable plastic aortic grafts; Experimental comparison of a number of materials. *A.M.A. Archives of Surgery*, 71(3), 449–59.Retrieved from http://laws-lois.justice.gc.ca/eng/regulations/sor-98-282/FullText.html

Hearle, J. W. S., & Greer, R. (1970). Fibre Structure. *Textile Progress*, 2(4), 1-187.

Hughes, A. J., McIntyre, J. E., Clayton, G., Wright, P., Poynton, D. J., Atkinson, J., ... & Ferguson, W. J. (1976). The production of man-made fibers. *Textile Progress*, *8*(1), 1-125.

Joseph, R., Shelma, R., Rajeev, A., & Muraleedharan, C.V. 2009. Characterization of surface

modified polyester fabric. *Journal of Materials Science: Materials in Medicine* 20 (S1): 153–59. doi:10.1007/s10856-008-3502-6.

Korkmaz, Y. A., & Behery, H. M. (2004). Drafting dynamics of fine denier polyester fibers. *Textile Research Journal*, *74*(6), 497–501.

Lin, Q., Oxenham, W., & Yu, C. (2011). A study of the drafting force in roller drafting and its influence on sliver irregularity. *Journal of the Textile Institute*, *102*(11), 994–1001. https://doi.org/10.1080/00405000.2010.529284

Ludewig, H., & Roth, W. (1971). *Polyester fibres; Chemistry and technology*. London NY: Wiley-Interscience.

McIntyre, J.E. (1993). *Annual symposium, performance and failures*, The University of Leeds, U.K. 3-10.

Marieb, E. P. (2000). *Essentials of human anatomy and physiology*, 6th ed, San Francisco, USA: Addison Wesley Longman.

Miyake, K., Sakagoshi, N., & Kitabayashi, K. (2016). Transverse rupture of ring-supported dacron graft 10 years after axillobifemoral artery bypass: induced by graft deterioration and fogarty thrombectomy. *Journal of Artificial Organs*, *19*(4), 403–407.

Narloch, J. A., & Brandstater, M. E. (1995). Influence of breathing technique on arterial blood pressure during heavy weight lifting. *Archives of Physical Medicine and Rehabilitation*, *76*(5), 457–462. doi.10.1016/S0003-9993(95)80578-8

National Standard of Canada (2003), CAN/CSA-ISO 13485:03: Medical devices – Quality management systems – Requirements for regulatory purposes, Canada Centre for Occupational Health and Safety, accessed thorugh internet on October, 2011.

O'Mahony, M. (2011). Advanced Textiles for Health and Well-being. *The Textile Institute*, Manchester, U.K.

Pourdeyhimi, B., & Wagner, D. (1986). On the correlation between the failure of vascular grafts and their structural and material properties: A critical analysis. *Journal of Biomedical Materials Research*, *20*(3), 375–409. https://doi.org/10.1002/jbm.820200309

Prevorsek, D. C. (1974). Structure of semi crystalline fibers from interpretation of anelastic effects. *Journal of Polymer Science Part C: Polymer Symposia*, *32*(1), 343–375. https://doi.org/10.1002/polc.5070320119

Rahman, M. (2012). Degradation of Polyesters in Medical Applications. *INTECH Open Access Publisher*. doi:10.5772/47765.

Rahman, M., & East, G. C. (2006). Effect of applied stress on the alkaline hydrolysis of poly(ethylene terephthalate) at 40°C: Relevance to medical textiles. *Journal of Applied Polymer Science*, *102*(5), 4814–4822. https://doi.org/10.1002/app.24684

Rahman, M., & East, G. C. (2009). Titanium dioxide particle-induced alkaline degradation of poly(ethylene terephthalate): Application to medical textiles. *Textile Research Journal*, 79 (8): 728–36. doi:10.1177/0040517507081916.

Ravi, S., & Chaikof, E. L. (2010). Biomaterials for vascular tissue engineering. *Regenerative Medicine*, *5*(1), 107–20. https://doi.org/10.2217/rme.09.77

Riepe, G., Loos, J., Imig, H., Schroder, A., Schneider, E., Petermann, J., … Morlock, M. (1997). Long-term in vivo alterations of polyester vascular grafts in humans. *European Journal of Vascular and Endovascular Surgery*, *13*(6), 540–548. https://doi.org/10.1016/S1078-5884(97)80062-7.

Rigby, A. J., Anand, S. C., & Horrocks, A. R. (1997). Textile materials for medical and healthcare applications. *Journal of the Textile Institute* 88 (3): 83–93. doi:10.1080/00405009708658589.

Salacinski, H. J., Tai, N. R., Carson, R. J., Edwards, A., Hamilton, G., & Seifalian, A. M. (2002). In vitro stability of a novel compliant poly(carbonate-urea) urethane to oxidative and hydrolytic stress. *Journal of Biomedical Materials Research*, *59*(2), 207–218. https://doi.org/10.1002/jbm.1234

Samuel E, W., Richard, K., Mueller, G., & Latresia, W. (1997). Late disruption of dacron aortic grafts. *Annals of Vascular Surgery*, *11*(4), 383–386.https://doi.org/10.1007/s100169900065

Santos, I. C., Rodrigues, A., Figueiredo, L., Rocha, L. A., & Tavares, J. M. R. (2012). Mechanical properties of stent-graft materials. *Proceedings of the Institution of Mechanical Engineers, Part L: Journal of Materials: Design and Applications*, 226(4), 330–41.

Schroeder, T. V., Eldrup, N., Just, S., Hansen, M., Nyhuus, B., & Sillesen, H. (2009). Dilatation of aortic grafts over time: What to expect and when to be concerned. *Seminars in Vascular Surgery*, *22*(2), 119–124. https://doi.org/10.1053/j.semvascsurg.2009.04.002

Sen, K. R. (1950). Quantitive relation between yarn strength and fibre properties. *Current Science*, 19(4), 106-109.

Shingaki, M., Kato, M., Motoki, M., Kubo, Y., Isaji, T., & Nobukazu, O. (2016). Endovascular repair for abdominal aortic aneurysm followed by type B dissection, *Asian Cardiovascular & Thoracic Annals*, 24(8) 805–807.

Singh, C., & Wang, X. (2015). A new design concept for knitted external vein-graft support mesh. *Journal of the Mechanical Behavior of Biomedical Materials*, 48, 125–33.

Singh, C., Wong, C., & Wang, X. (2015). Medical textiles as vascular implants and their success to mimic natural arteries. *Journal of Functional Biomaterials*, 6(3), 500–525. https://doi.org/10.3390/jfb6030500

Sinha, S., & Kumar, P. (2013). An Investigation of the Behavior of Thin Places in Ring Spun Yarns. *Journal of Textile and Apparel, Technology and Management*, *8*(2).

Stollwerck, P. L., Kozlowski, B., Sandmann, W., Grabitz, K., & Pfeiffer, T. (2011). Long-term dilatation of polyester and expanded polytetrafluoroethylene tube grafts after open repair of infrarenal abdominal aortic aneurysms. *Journal of Vascular Surgery*, *53*(6), 1506–1513. https://doi.org/10.1016/j.jvs.2011.02.028

Van Damme, H., Deprez, M., Creemers, E., & Limet, R. (2005). Intrinsic structural failure of polyester (Dacron) vascular grafts. A general review. *Acta Chirurgica Belgica*, *105*(3), 249–255.

Voorhees, A.B., Jaretzki, A., & Arthur, H. B. (1952). The use of tubes constructed from vinyon 'N' cloth in bridging arterial defects. *Annals of Surgery,* 135 (3), 332–36.

Ward, I., Cansfield, D. O., & Carr, P. (1993). *Polyester 50 years of achievement.* The Textile Institute, Manchester, U.K., 192-195.

Warner, S. B. (1995). Microstructure and macrostructure of synthetic fibers, *Fiber Science* (pp. 30-63). New Jersey: Prentice Hall.

Whinfield, J.R., & Dickson, J.T., (June 1946). *London Patent No 578079*, Imperial Chemical Industries Ltd : The Patent Office, London.

White, S. R., & Hann, H. T. (1992). Process modeling of composite materials: Residual stress development during cure. Part II. Experimental validation. *Journal of Composite Materials*, *26*(16), 2423–2453. https://doi.org/10.1177/002199839202601605

Wilson, S. E., Krug, R., Mueller, G., & Wilson, L. (1997). Late disruption of dacron aortic grafts. *Annals of Vascular Surgery*, *11*(4), 383–6. https://doi.org/10.1007/s100169900065

Xie, X., Guidoin, R., Nutley, M., & Zhang, Z. (2010). Fluoropassivation and gelatin sealing of polyester arterial prostheses to skip preclotting and constrain the chronic inflammatory response. *Journal of Biomedical Materials Research Part B: Applied Biomaterials*, *93B*(2), 497–509. https://doi.org/10.1002/jbm.b.31609

Yashar, J. J., Richman, M. H., Dyckman, J., & Witoszka, M. (1978). Failure of dacron prostheses caused by structural defect. *Surgery* 84 (5): 659–63.

Yaw, P. B., Grisell, T. W., Shumacker, H. B., Glover, J. L., Riberi, A., Moore, T. C., & Siderys, H. (1974). Fate of a nylon vascular prosthesis for aortic replacement: 14 year follow-up study. *Surgery*, *75*(1), 140–4. https://doi.org/10.5555/URI:PII:0039606074901937

Zeronian, S. H., & Collins, M. J. (1989). Surface modification of polyester by alkaline treatments. *Textile Progress*, *20*(2), 1–26.

Zeronian, S. H., Collins, M. J. (1988). Improving the comfort of polyester fabrics. *Text. Chem. Color*, 20(4), 25-28.

Appendix A: Parameters Set Up for Yarn Breaking Strength Measurement

1. General:
    - Method: Test type: Tension Relax/ Creep
2. Sample Description:
3. Specimen:
4. Control: Pre Test: Auto Balance

Test: Ramp 1:

- Control Mode 1: Extension

-Rate : 20 mm/min

Hold:

-Hold Control Mode: Load

-Hold start criteria: Load

- Hold Value: 8.39 N (98% of the breaking load-8.57N)

End of Test: End of Test: 1

Criteria1: Extension

Value 1: 30mm (depends on the extension of the control)

End of Hold:

Criteria: Time

Duration: 72hrs (depends on holding time)

5. Calculations:

- Setup: Available caculations

1. Break (standard)

6. Results 1:

- Columns: Available Results

2. Break (Standard)

3. Selected Results: 1. Specimen Note 1

2. Load at Yield (Zero slope)
3. Load at Yield (Zero slope)
4. Extension at Yield (Zero Slope)
5. Extension at Break (Standard)
6. Time at Break (Standard)

7. Results 2: N/A

8. Graph 1:

- Type: Select a Graph type:-Double Y- axis
- X-data: X-axis Definition:
  - Channel: Time
  - Units: Min
- Y-data: Y1-axis definition: Y2-axis definition
  - Channel: Load - Channel: Extension
  - Units: N - Units: mm

9. Raw Data:

- Columns: Selected Channels: 1) Load 2)Extension

10. Reports

11. Test Prompts

Appendix B: *t* Table

Table 1 *t* Distribution Critical Values

Table entry for p and C is the point t^* with probability p lying above it and probability C lying between $-t^*$ and t^*.

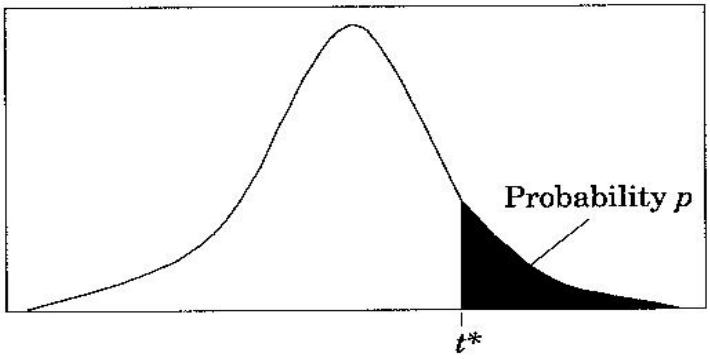

Table B t distribution critical values

	Tail probability p											
df	.25	.20	.15	.10	.05	.025	.02	.01	.005	.0025	.001	.0005
1	1.000	1.376	1.963	3.078	6.314	12.71	15.89	31.82	63.66	127.3	318.3	636.6
2	.816	1.061	1.386	1.886	2.920	4.303	4.849	6.965	9.925	14.09	22.33	31.60
3	.765	.978	1.250	1.638	2.353	3.182	3.482	4.541	5.841	7.453	10.21	12.92
4	.741	.941	1.190	1.533	2.132	2.776	2.999	3.747	4.604	5.598	7.173	8.610
5	.727	.920	1.156	1.476	2.015	2.571	2.757	3.365	4.032	4.773	5.893	6.869
6	.718	.906	1.134	1.440	1.943	2.447	2.612	3.143	3.707	4.317	5.208	5.959
7	.711	.896	1.119	1.415	1.895	2.365	2.517	2.998	3.499	4.029	4.785	5.408
8	.706	.889	1.108	1.397	1.860	2.306	2.449	2.896	3.355	3.833	4.501	5.041
9	.703	.883	1.100	1.383	1.833	2.262	2.398	2.821	3.250	3.690	4.297	4.781
10	.700	.879	1.093	1.372	1.812	2.228	2.359	2.764	3.169	3.581	4.144	4.587
11	.697	.876	1.088	1.363	1.796	2.201	2.328	2.718	3.106	3.497	4.025	4.437
12	.695	.873	1.083	1.356	1.782	2.179	2.303	2.681	3.055	3.428	3.930	4.318
13	.694	.870	1.079	1.350	1.771	2.160	2.282	2.650	3.012	3.372	3.852	4.221
14	.692	.868	1.076	1.345	1.761	2.145	2.264	2.624	2.977	3.326	3.787	4.140
15	.691	.866	1.074	1.341	1.753	2.131	2.249	2.602	2.947	3.286	3.733	4.073
16	.690	.865	1.071	1.337	1.746	2.120	2.235	2.583	2.921	3.252	3.686	4.015
17	.689	.863	1.069	1.333	1.740	2.110	2.224	2.567	2.898	3.222	3.646	3.965
18	.688	.862	1.067	1.330	1.734	2.101	2.214	2.552	2.878	3.197	3.611	3.922
19	.688	.861	1.066	1.328	1.729	2.093	2.205	2.539	2.861	3.174	3.579	3.883
20	.687	.860	1.064	1.325	1.725	2.086	2.197	2.528	2.845	3.153	3.552	3.850
21	.686	.859	1.063	1.323	1.721	2.080	2.189	2.518	2.831	3.135	3.527	3.819
22	.686	.858	1.061	1.321	1.717	2.074	2.183	2.508	2.819	3.119	3.505	3.792
23	.685	.858	1.060	1.319	1.714	2.069	2.177	2.500	2.807	3.104	3.485	3.768
24	.685	.857	1.059	1.318	1.711	2.064	2.172	2.492	2.797	3.091	3.467	3.745
25	.684	.856	1.058	1.316	1.708	2.060	2.167	2.485	2.787	3.078	3.450	3.725
26	.684	.856	1.058	1.315	1.706	2.056	2.162	2.479	2.779	3.067	3.435	3.707
27	.684	.855	1.057	1.314	1.703	2.052	2.158	2.473	2.771	3.057	3.421	3.690
28	.683	.855	1.056	1.313	1.701	2.048	2.154	2.467	2.763	3.047	3.408	3.674
29	.683	.854	1.055	1.311	1.699	2.045	2.150	2.462	2.756	3.038	3.396	3.659
30	.683	.854	1.055	1.310	1.697	2.042	2.147	2.457	2.750	3.030	3.385	3.646
40	.681	.851	1.050	1.303	1.684	2.021	2.123	2.423	2.704	2.971	3.307	3.551
50	.679	.849	1.047	1.299	1.676	2.009	2.109	2.403	2.678	2.937	3.261	3.496
60	.679	.848	1.045	1.296	1.671	2.000	2.099	2.390	2.660	2.915	3.232	3.460
80	.678	.846	1.043	1.292	1.664	1.990	2.088	2.374	2.639	2.887	3.195	3.416
100	.677	.845	1.042	1.290	1.660	1.984	2.081	2.364	2.626	2.871	3.174	3.390
1000	.675	.842	1.037	1.282	1.646	1.962	2.056	2.330	2.581	2.813	3.098	3.300
∞	.674	.841	1.036	1.282	1.645	1.960	2.054	2.326	2.576	2.807	3.091	3.291
	50%	60%	70%	80%	90%	95%	96%	98%	99%	99.5%	99.8%	99.9%
	Confidence level C											

Appendix C: Standard Normal Distribution Table

Table 2 Normal Distribution Function Table

Standard Normal Probabilities

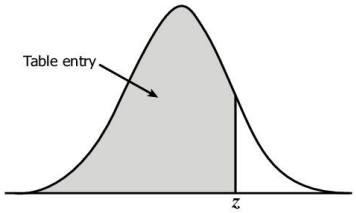

Table entry for z is the area under the standard normal curve to the left of z.

z	.00	.01	.02	.03	.04	.05	.06	.07	.08	.09
0.0	.5000	.5040	.5080	.5120	.5160	.5199	.5239	.5279	.5319	.5359
0.1	.5398	.5438	.5478	.5517	.5557	.5596	.5636	.5675	.5714	.5753
0.2	.5793	.5832	.5871	.5910	.5948	.5987	.6026	.6064	.6103	.6141
0.3	.6179	.6217	.6255	.6293	.6331	.6368	.6406	.6443	.6480	.6517
0.4	.6554	.6591	.6628	.6664	.6700	.6736	.6772	.6808	.6844	.6879
0.5	.6915	.6950	.6985	.7019	.7054	.7088	.7123	.7157	.7190	.7224
0.6	.7257	.7291	.7324	.7357	.7389	.7422	.7454	.7486	.7517	.7549
0.7	.7580	.7611	.7642	.7673	.7704	.7734	.7764	.7794	.7823	.7852
0.8	.7881	.7910	.7939	.7967	.7995	.8023	.8051	.8078	.8106	.8133
0.9	.8159	.8186	.8212	.8238	.8264	.8289	.8315	.8340	.8365	.8389
1.0	.8413	.8438	.8461	.8485	.8508	.8531	.8554	.8577	.8599	.8621
1.1	.8643	.8665	.8686	.8708	.8729	.8749	.8770	.8790	.8810	.8830
1.2	.8849	.8869	.8888	.8907	.8925	.8944	.8962	.8980	.8997	.9015
1.3	.9032	.9049	.9066	.9082	.9099	.9115	.9131	.9147	.9162	.9177
1.4	.9192	.9207	.9222	.9236	.9251	.9265	.9279	.9292	.9306	.9319
1.5	.9332	.9345	.9357	.9370	.9382	.9394	.9406	.9418	.9429	.9441
1.6	.9452	.9463	.9474	.9484	.9495	.9505	.9515	.9525	.9535	.9545
1.7	.9554	.9564	.9573	.9582	.9591	.9599	.9608	.9616	.9625	.9633
1.8	.9641	.9649	.9656	.9664	.9671	.9678	.9686	.9693	.9699	.9706
1.9	.9713	.9719	.9726	.9732	.9738	.9744	.9750	.9756	.9761	.9767
2.0	.9772	.9778	.9783	.9788	.9793	.9798	.9803	.9808	.9812	.9817
2.1	.9821	.9826	.9830	.9834	.9838	.9842	.9846	.9850	.9854	.9857
2.2	.9861	.9864	.9868	.9871	.9875	.9878	.9881	.9884	.9887	.9890
2.3	.9893	.9896	.9898	.9901	.9904	.9906	.9909	.9911	.9913	.9916
2.4	.9918	.9920	.9922	.9925	.9927	.9929	.9931	.9932	.9934	.9936
2.5	.9938	.9940	.9941	.9943	.9945	.9946	.9948	.9949	.9951	.9952
2.6	.9953	.9955	.9956	.9957	.9959	.9960	.9961	.9962	.9963	.9964
2.7	.9965	.9966	.9967	.9968	.9969	.9970	.9971	.9972	.9973	.9974
2.8	.9974	.9975	.9976	.9977	.9977	.9978	.9979	.9979	.9980	.9981
2.9	.9981	.9982	.9982	.9983	.9984	.9984	.9985	.9985	.9986	.9986
3.0	.9987	.9987	.9987	.9988	.9988	.9989	.9989	.9989	.9990	.9990
3.1	.9990	.9991	.9991	.9991	.9992	.9992	.9992	.9992	.9993	.9993
3.2	.9993	.9993	.9994	.9994	.9994	.9994	.9994	.9995	.9995	.9995
3.3	.9995	.9995	.9995	.9996	.9996	.9996	.9996	.9996	.9996	.9997
3.4	.9997	.9997	.9997	.9997	.9997	.9997	.9997	.9997	.9997	.9998

Appendix D: Parameters Set Up for Fabric Breaking Strength Measurement

1. General:
    - Method: Test type: Tension Relax/ Creep
2. Sample Description:
3. Specimen:
4. Control: Pre Test: Auto Balance

Test: Ramp 1:

- Control Mode 1: Extension

-Rate : 20 mm/min

- End of Test: End of Test: 1

Criteria1: Rate of Load

Sensitivity%- 40

- End of Test: End of Test: 2

Criteria 2: Extension

Value 2 : 35 mm

5. Calculations:

- Setup: Available caculations
    - Break (standard)

6. Results 1:

Selected Results: 1. Specimen Note 1

2. Load at Yield (Zero slope)
3. Load at Yield (Zero slope
4. Extension at Yield (Zero Slope)
5. Extension at Break (Standard)
6. Time at Break (Standard)

7. Results 2: N/A
8. Graph 1:
    - X-axis Definition:
        - Extension (mm)
    - Y1-axis definition:
        - Load (N)
9. Raw Data:
    - Columns: Selected Channels: 1) Load 2)Extension
10. Reports
11. Test Prompts